Active metal supported mesoporous materials as solid catalysts for the transesterification of triglycerides

Thesis Submitted for the Award of Degree of

Doctor of Philosophy

Submitted by
Rashi Malhotra
(Regn. No.901409011**)**

THAPAR INSTITUTE
OF ENGINEERING & TECHNOLOGY
(Deemed to be University)

Under the Supervision of
Dr. Amjad Ali
Professor and
HEAD, SCBC

SCHOOL OF CHEMISTRY AND BIOCHEMISTRY
THAPAR INSTITUTE OF ENGINEERING AND TECHNOLOGY
PATIALA-147004

September, 2019

Dedicated to

my

Beloved Parents

ACKNOWLEDGEMENTS

First and foremost, I would express my sheer thanks and gratitude to my supervisor and mentor Dr. Amjad Ali, Associate Professor and Head, School of Chemistry and Biochemistry, Thapar Institute of Engineering and Technology, for his consistent support, encouragement and perseverance all through my doctorate work. He has always been pillar of knowledge and strength. He has always been there as a great and enlightening mentor. I have learnt immensely from him and saying thanks would not be sufficient for his guidance and support.

I also thank Director, Thapar Institute of Engineering and Technology and Dean (R&SP) for giving the opportunity to take on this research work.

I would also express my thanks to my doctoral committee members, Dr. Ranjana Prakash, Dr. Manmohan Chibbar and Dr. H. Bhunia for their examining my research work time to time.

I express my acknowledgement to School of Chemistry and Biochemistry for FT-IR, SAI labs, Thapar Institute of Engineering and Technology for NMR, XRD, MP-AES, flame photometry and SEM studies, IIT, Mumbai and NIPER, Mohali for HR-TEM analysis, CSIO, Chandigarh for FE-SEM study, Sprint testing solutions for XPS. I thank Mr. Mukesh Agarwal, for always solving my querries regarding sophisticated instruments and being a kind professional. I immensely pay thanks to Dr. Soumen Basu for BET surface area analysis and helping out in problems regarding the same. I am also obliged to Mr. Chander Singh, a very fine technician and lab attendants for lending their help.

I express my utmost thanks to my very dearly loved friends, Pooja Dhawan and Pankaj Kumar for being always there for me in times of my stress and happiness and bearing with me.

This journey would not have been complete without my seniors, Dr. Navjot Kaur, Sonia Rana, Manisha Mam and my friends Jasminder Singh, Gulshan, Shagun, Surbhi and labmates. I thank Upraj Kaur for always supporting me, making me believe in myself even more and tea-time laughters.

I owe my strength of doing hardwork to my parents and brother. Thanks will fall short for them for loving me unconditionally, listening to me always, encouraging me, loving me and instilling in me the drive to work harder.

CERTIFICATE OF DECLARATION

I hereby declare that the work presented in the thesis entitled "Active metal supported mesoporous materials as solid catalysts for the transesterification of triglycerides", in fulfilment of the requirement for the award of the degree of "DOCTOR OF PHOLOSOPHY", School of Chemistry and Biochemsitry, Thapar Institute of Engineering and Technology, Patiala, is an authentic record of my own work carried out under the supervision of Dr. Amjad Ali, Associate Professor and Head, School of Chemistry and Biochemsitry, Thapar Institute of Engineering and Technology, Patiala, India. The matter embodied in this thesis has not been submitted in part or full to any other university or institute for the award of any degree in India or abroad.

(Supervisor)

Dr. Amjad Ali

Professor and Head

School of Chemistry and Biochemsitry,

Thapar Institute of Engineering and Technology,

Patiala

Rashi Malhotra

CERTIFICATE

This is to certify that thesis entitled "Active metal supported mesoporous materials as solid catalysts for the transesterification of triglycerides" being submitted by Rashi Malhotra to the School of Chemistry and Biochemistry, Thapar Institute of Engineering and Technology, Patiala for the award of degree of DOCTOR OF PHILOSOPHY is a record of bonafide work of research carried out by her. Ms. Rashi Malhotra has worked under my mentorship and supervision and has fulfilled the requirements for thesis submission which to my knowledge has reached the requisite standard.

The results represented in the present thesis have not been acquiesced in part or full to any university or institute for the award of any degree or diploma.

Dr. Amjad Ali
Professor and Head
School of Chemistry and Biochemistry
Thapar Institute of Engineering and Technology
Patiala

LIST OF PUBLICATIONS

- **R. Malhotra, A. Ali., Lithium-doped Ceria Supported SBA-15 as Mesoporous Solid Reusable and Heterogeneous Catalyst for Biodiesel Production *via* Simultaneous Esterification and Transesterification of Waste Cottonseed Oil., Renewable Energy, 2018, 119, 32-44 (I.F. 4.9) https://doi.org/10.1016/j.renene.2017.12.001**
- **R. Malhotra, A, Ali., 5-Na/ZnO Doped Mesoporous Silica as Reusable Solid Catalyst for Biodiesel Production *via* Transesterification of Virgin Cottonseed Oil., Renewable Energy, 2019, 133, 606-619 (I.F. 4.9) https://doi.org/10.1016/j.renene.2018.10.055**
- **M. Kaur, R. Malhotra, Amjad Ali., Tungsten Supported Titanosilicate Nanoflowers as Reusable Heterogeneous Catalyst for BD Production., Renewable energy, 2018, 116, 109-119. (I.F. 4.9) https://doi.org/10.1016/j.renene.2017.09.065**
- **R. Malhotra, A, Ali., K-Na Couple Imbued Mesoporous Silica as an Effective and Reusable Solid Catalyst for Biodiesel Synthesis from Cottonseed Oil (To be communicated).**
- **R. Malhotra, A, Ali., Sodium Doped Zirconia Drenched SBA-15 as a Reusable Solid Catalyst for Concurrent Esterification and Transesterification of low Quality Oils (communicated).**
- **Solid Catalysts for Biodiesel Production, a Voyage from Unsupported Catalysts to Mesoporous Silica Based Ones: a review (To be communicated).**

TABLE OF CONTENTS

LIST OF ABBREVIATIONS

Abbreviation	Description
FAME	Fatty acid methyl ester
FAEE	Fatty acid ethyl ester
BD	Biodiesel
VOs	Vegetable oils
TG	Triglyceride
FFA	Free fatty acid
MeOH	Methanol
CPP	Critical packing parameter
WCO	Waste cottonseed oil
WSO	Waste soyabean oil
VCO	Virgin cottonseed oil
JO	Jatropha oil
OA	Oleic acid
TLC	Thin layer chromatography
R_f	Retention factor
TOF	Turnover frequency
v/v	Volume by volume
$J\ K^{-1}\ mol^{-1}$	Kilojoule per lelvin per mole
min	Minute
$KJ\ mol^{-1}$	Kilojoule per mole
mL	Millilitre
wt%	Weight percentage
$mmol\ g^{-1}$	Millimole per gram
Js	Joule second
XRD	X-ray diffraction
XPS	X-ray photoelectron spectroscopy
FT-IR	Fourier Transform Infra- Red Spectroscopy
DRIFT	Diffuse reflectance Infrared Fourier Transform
FT-NMR	Fourier-Transform Nuclear Magnetic Resonance
MP-AES	Microwave Plasma-Atomic Emission Spectroscopy
BET	Brunauer–Emmett–Teller
BJH	Barrett-Joyner-Halenda
PSD	Pore size distribution
HR-TEM	High Resolution Transmission Electron Microscopy
FE-SEM	Field Emission Scanning Electron Microscopy
TMS	Tetramethylsilane
SEM-EDS	Scanning-Electron Microscopy-Energy Dispersive X-Ray
nm	Nanometer
µm	Micrometer
ppm	Parts per millon
rpm	Rotations per minute

JCPDS	Joint Committee for Powder Diffraction Standards
NR	Not reported
NF	Not found
ND	Not determined
NCC	No colour change
HC	Hydrocarbons

LIST OF SYMBOLS

Symbols	Description
Å	Angstrom
C	Celsius
$\mathbf{E_a}$	Activation Energy
$\Delta\mathbf{H}^{\ddagger}$	Enthalpy
$\Delta\mathbf{S}^{\ddagger}$	Entropy
$\Delta\mathbf{G}^{\ddagger}$	Gibbs free energy
g	Gram
h	Hour
K	Kelvin
θ	Theta
μ	Micro
k	Rate constant
m	Metre
%	Percentage
X	Conversion
T	Temperature
°	Degree
v	Volume
t	Time
R	Gas constant
$\mathbf{k_B}$	Boltzmann constant
$\mathbf{f_m}$	Active sites
$\mathbf{H_0}$	Hammett acidity or basicity

LIST OF TABLES

LIST OF FIGURES

ABSTRACT

Expenditure of energy is indispensable for the survival of mankind and the chief share of demand has been laid upon non renewable resources like fossil fuels. In this context, biodiesel has emerged as an eco-friendly green fuel substitute for the typical diesel fuel. Biodiesel is basically mono alkyl esters of fatty acids synthesised *via* transesterification of triglycerides in the attendance of either solid/ heterogeneous, homogeneous or enzyme catalysts. Customary and typical homogeneous basic catalysts (NaOH and KOH) are exceedingly effectual for mercantile scale biodiesel production. However, this process defers the products which are contaminated with catalyst simultaneously generating enormous quantity of waste matter during washing and refinement processes. Furthermore, homogeneous alkali catalyst owing to their kindliness for moisture and free fatty acids (FFA) cannot be employed for transesterification of waste oils and necessitate FFA and moisture liberated expensive refined oil. With a view to outwit the issues associated with uniphasic catalysts, development and expansion of mesoporous solid reusable and stable catalysts has attracted momentous interest in recent years. In present thesis, mesoporous silica based catalysts, Li^{+} and Ce^{4+} impregnated mesoporous silica, 10-Na/ZnO/SBA-15, 20-Na-K/SBA-15 and 30-Na/ZrO_2/SBA-15 were prepared as well as characterised by different analytical techniques such as powder XRD, BET surface area, FE-SEM, XPS, HRTEM, and Hammett indicator studies. These catalysts were triumphantly utilised for the biodiesel production from waste cottonseed oil, virgin cottonseed oil. Li^{+} and Ce^{4+} imbued SBA-15 has been prepared under normal atmospheric condition without using harsh hydrothermal method and trailing wet incipient route. The catalyst needed 4 h to give in the complete transesterification of waste cottonseed oil (> 98% FAMEs yield) with moderate requirements of alcohol and catalyst amount at 65 °C. The catalyst demonstrated good recyclability maintaining its activity for 5 successive runs.

To reduce the time and energy consumption for catalyst synthesis, Na/ZnO loaded SBA-15 was prepared by one-pot method without employing hydrothermal treatment. The catalyst was exploited for transesterification from virgin cotton seed oil. The catalyst action was found to rely more on its basic strength than on surface area. Very meagre leaching of metals < 5ppm observed in 4^{th} and 5^{th} cycle which was within ASTM specified limitations was an important feature for application of this catalyst.

In order to reduce the time of reaction, K-Na imbued SBA-15 was prepared by wet-incipient method. The prepared catalyst was exploited for BD synthesis from virgin cotton seed oil and

the activity depended on its basic strength. This catalyst could even withstand high externally added FFA content yielding upto 80% FAMEs within 8 h. In order to further develop a catalyst to execute concurrent esterification and transesterification, sodium doped zirconia impregnated SBA-15 was synthesized. It was determined that the catalyst confiscated both acidic and basic sites and hence, was victoriously exploited to carry out concurrent esterification and transesterification of VCO and high FFA holding oils. Regeneration study advocated that the catalyst may well be recycled for 5 successive cycles without significant trouncing of activity. Nevertheless, the duration of reaction entailed to achieve absolute conversion raised to 5.5 h and 8.5 h when waste soyabean oil (WSO) and jatropha oil (JO) were employed as feedstock respectively.

While partial leaching of metal ions from the catalysts was detected but seeped metal ions did not show significant homogeneous contribution, and hence, all the prepared catalysts have truly depicted the heterogeneous mode of action. The transesterification catalyzed by all the prepared catalysts has tracked (pseudo) first order kinetics and experimentally determined value of activation energy was > 25 kJ/mol to advocate that reactions were chemically controlled, not by diffusion/mass transfer limitations. The reactions were endothermic in nature.

Introduction and literature review

Abstract

Hike in the energy crisis and global warming owing to unwarranted exploitation of fossil fuels, have led to biodiesel emerge out as strongly promising eco-friendly green substitute for non-renewable fuels. Chemically biodiesel stands for alkyl esters of long chain fatty acids which is prepared *via* transesterification of vegetable oils and animal fats. Biodiesel owns many advantages over conformist diesel, as it is free of harmful hydrocarbons, causes inferior emissions of harmful green house gases, particulate matters and sulphur compounds. Despite of many benefits, biodiesel has not attracted the worth and popularity in commercial sector in India due to high production cost plus deficiency of surplus feedstock. Heterogeneous catalysts offer wide range of advantages over homogeneous counterparts, *viz*. easy removal of catalyst, regeneration of catalyst, non-tedious washing steps. In the recent past, diverse solid catalysts have expansively been explored for biodiesel production. A bunch of research activities are now centered towards synthesis and application of mesoporous silica based catalysts in biofuel synthesis. Mesoporous silica offers attractive properties such as ease of modification of surface for impregnating active catalytic species, high thermal stability, amendable pore size, lesser leaching out of active species. In this chapter, work on the expansion of various heterogeneous catalysts from the past, with a special focus on mesoporous catalysts has been reviewed.

Keywords: Biodiesel, mesoporous silica, Transesterification, Heterogeneous catalyst, Triglycerides

1.1. Introduction

The world is constantly confronting the energy and environmental crisis due to the unvarying decline in inadequate resources of fossil fuel and hike in environmental pollution as a result of fuel burning. Burning of fossil fuel causes the emission of un-brunt hydrocarbon, particulate matters, CO, CO_2, SO_3, SO_2, NO_x, etc, which are responsible for the environmental pollution as well as global warming. Such issues like global warming and continuous depletion of reserves of fossil fuel have encouraged the researches focussing on renewable energies. In this context, biodiesel (BD), fuel obtained from renewable sources, has emerged as promising and interesting choice and substitute as it is eco-friendly green fuel (Asri et al., 2013; Daud et al., 2015). Chemically, biodiesel (BD) is a mixture or combination of fatty acid methyl esters (FAMEs) which is produced *via* transesterification of triglycerides (vegetable oils or animal fat) as shown in Scheme 1.1. It is a renewable sulphur less and non toxic substitute for the conventional diesel fuel and comparatively smaller amounts of harmful chemical substances and hydrocarbons. Besides, the production processes are usually cleaner as compared to conventional fuels. Moreover, CO_2 released during its combustion is engrossed in the process of photosynthesis, ensuing in a carbon neutral route cycle (Larson, 2006). If untainted biodiesel is employed as fuel, the overall release of carbon dioxide can be reduced. Burning of 1.0 kg of biodiesel will reduce the CO_2 production by 3.2 kg (Jothiramalingam and Wang, 2009).

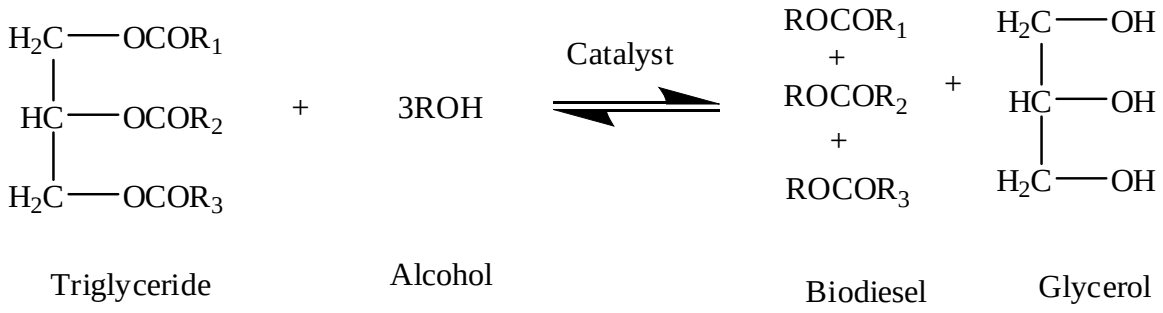

Scheme 1.1. Reaction showing transesterification of triglycerides (R_1, R_2 and R_3 are straight HC chains of fatty acids, generally having 14-20 C-atoms).

Currently, the major feedstock employed for industrial scale production of BD is edible vegetable oils (VOs). However, in India, the use of waste, ravaged or non-edible oil is encouraged for commercial BD production owing to paucity of edible VOs. The waste oils are inexpensive and thus, their use for commercial level production of biodiesel may considerably diminish the expenses of production (Teo et al., 2014).

The ancestry of what ultimately became named as "biodiesel" extends back to the breakthrough of the diesel engine which was first run by Rudolf Diesel (Songstad et al., 2009) which employed peanut oil as feedstock. It was first time-honoured in World fair in Paris in 1900. The name "biodiesel" was however first given in year 1898 (Wang, 1988). The direct utilization of VOs as fuels is generally avoided because of their sky-scraping kinematic viscosity (42cp) as compared to the diesel fuel (4-6 cp) (Goering et al., 1982). High kinematic viscosity leads to reduced flow properties of fuel plus inept integration with air. With an aim to lessen the viscosity and consequent improvement in the performance, chemical transformation of VOs into methyl esters of fatty acids *via* transesterification reaction can be carried out. FAMEs produced have less molar mass (nearly one third of VO) and viscosity than VO and have improved and superior flow properties even at low temperatures. However, it is interesting to note that many years before first diesel engine was invented, Duffy and Patrick in 1853, carried out the first transesterification reaction of vegetable oil (VO). Moreover, use of a blend of BD and fossil based diesel fuel, having up to 20 volume % of BD (v/v) doesn't require any modification in conventional diesel engine (Islam et al., 2014)

1.2. Feedstock for Biodiesel production

Any triglyceride (TG) source obtainable in geological area can be employed for BD production. However, the selection remains constrained on the basis of farming of VO in specific geographical area.

The feedstock utilised for BD production have stayed slightly altered since the time when first engine testing with VOs was performed and are usually categorised as first or second generation. The second generation feedstocks are often called as the sources for 'advanced biofuels'. Generation first BD is obtained from VOs fit for human consumption, edible oils, *viz.* soyabean, palm, rapeseed and sunflower oils. But, the meagre yields (~3000–5000 L /hectare /year) plus social and political concerns regarding the distraction of such edible and valuable crops for the synthesis of fuels has eventually resulted in their decline from support within the continents like Europe and America (Calero et al., 2014). BD which is either produced from waste cooking oil or non edible oil sources like castor oil, Jatropha oil, and neem, microalgae and animal fats (e.g. beef tallow) is called as "second generation biodiesel".

Curiosity in BD production climbed after the worldwide oil emergency of 1970s, ensuing in the U.S.A., Europe, South Africa, Brazil, China, India, assembling a UN International BD

meeting for the expansion and development of biodiesel. At present, USA, Europe, Brazil, Malaysia, stand as chief forces in biodiesel market. Presently, production at industrial level is subjugated by the use of edible VOs *viz.* palm (6.34 million), soyabean (7.08 million) and rapeseed (6.01 million). The prime expense of BD lounges in its raw material, furthermore, as the market is conquered by edible oils which are of food grade, that are radically more costly than petroleum-based diesel, economic feasibility still waits to be established (Gorji and Ghanei, 2014).

Waste cooking oil is mainly obtained from the restaurants and costs nearly 60% less than fresh vegetable oils. Waste oils by and large contain reasonably elevated free fatty acid (FFA) levels (> 2.5 wt%) and water contents (> 0.5 wt%) and diverse solid materials that have to be separated by filtration prior to the transesterification reaction. BD production cost may reduce by 50% if waste cooking oils are employed as feedstock (Escobar et al., 2009). The demand of present hour is to develop new technologies that can effectively employ low quality feedstock since the current scheme that utilises homogeneous base catalysis can only tolerate the high-quality feedstock with significantly low FFA and moisture contents.

1.2.1. Effect of composition of fatty acids in feedstock on fuel properties

The various properties of BD such as viscosity, oxidation stability, cold flow property, etc., rely upon the composition of fatty acids of triglyceride. Fats contain high amounts of saturated fatty acids and hence, are solids at room temperature whereas oils possess lofty concentration of unsaturated fatty acids and consequently, exist in liquid state at room temperature.

1.2.2. Effect of unsaturation - Double bonds are more vulnerable towards oxidation and hence, BD with high unsaturated fatty acid contents degraded/oxidized easily (Lee et al., 2014). BD produced from feedstocks that have linoleic and linolenic acids in greater amounts undergo oxidation easily. The oxidation rates of linoleates and linolineates are correspondingly 41 and 98 times elevated than monounsaturated oleates. However, the cold flow properties improve with unsaturation as BD with more number of double bonds solidifies at much lower temperatures. There occur the kinks in the structure of unsaturated fatty acids and hence, there is less efficient packing of the molecules and they tend to stay in liquid state. The unsaturation also decreases the viscosity which in turn hikes the lubricity of the resulting product (Allen et al., 1999). High lubricity BD can be used by combining it

with the low sulphur containing, conventional biodiesel which improves the overall lubricity. The Table 1.1 depicts the fatty acid %ages of different fatty acids in the feedstocks used for BD production.

Table-1.1. Composition of fatty acids of few commonly used vegetable oils for BD production and their availability.

Oil Source	Fatty acid composition (%)					
	Palmitic C16:0	**Stearic C18:0**	**Oleic C18:1**	**Linolenic C18:3**	**Linoleic C18:2**	**Availability in geographical region**
Cottonseed	20	2	35	-	42	Brazil, south America , Argentina, India
Karanja	3.7-7.9	2.4- 8.9	44.5-71.3	-	10.8-18.3	Tropical asian countries
Palm	32-45	2-7	38-52	-	5-11	Malaysia, Indonesia, other asian countries
Soyabean	7-11	2-6	22-34	5-11	43-56	USA and south America
Sunflower	3-6	1-3	14-35	-	44-75	Phillipines and south east asian countries
Jatropha	12-17	5-9.5	37-63	-	19-41	African countries and india
Mutton fat	26	14	47	1	3	-

1.2.3. Effect of chain length – With the increment in length of fatty acid chain, the viscosity of BD increases which as a consequence, again influences the fuel lubricity and flow properties of the product (Knothe and Steidley, 2005). Presence of increased chain length enhances the lubricity. Low molecular weight fats and oils result in low viscosity BD, however, such BD cannot be explored as a fuel directly owing to its reduced flow properties and problem of freezing at lower temperature. Degree of unsaturation and chain length also influences the cetane number of the resulted BD fuel. Its value reduces as the degree of unsaturation increases, the value ranges between 50-55 for the rapeseed derived BD and 48-5 for the soyabean derived product.

1.3. Alcohol employed for transesterification - Conventionally methanol is used as a co-reactant during transesterification for the large scale biodiesel production. Methanol is highly toxic and a by product of refining industry hence, resulted biodiesel will not be comprising absolutely renewable carbon atoms (Balat et al., 2008). Methanol due to its high reactivity, wide availability and cost effectiveness is preferred and used in commercial scale biodiesel production plants. Due to its lower density, fatty acid methyl esters, produced in methanolysis separate out easily from glycerol. Moreover, renewable methanol/biomethanol may be

generated from biomass, either simply by fermentation or thermal conversion (Atadashi et al., 2010).

With the intention to make the procedure more eco-friendly, application of ethanol for BD production has been accessed in recent past (Kaur and Ali, 2015). Ethanol is much less toxic than methanol and renewable as produced from biomass fermentation. However, presence of moisture in (bio) ethanol, difficulty in separation of ethyl esters from glycerol, and higher cost of ethanol, hinders its application at commercial level. In case bioethanol (ethanol derived from biomass), is employed in fatty acid ethyl ester (FAEE) production, the cost becomes almost double to that as compared to methyl ester. Thus, methanol still is a leading competitor with other alcohols for the production of BD (Brunschwig et al., 2012). In literature reactivity of ethanol remains controversial as many factors were found to influence the reactivity. Ethanol being less reactive than methanol leads to lower BD yields. Although nucleophilic power of ethoxide ion is greater than that of methoxide ion but because of longer carbon chain length, former is less mobile as well as less reactive (De Lima et al., 2016)

1.4. Catalysis

1.4.1. Homogeneous acid catalysed reactions

These catalysts (sulfonic and sulphuric acids) are employed for the transesterification in case free fatty acid (FFA) amount in feedstock are relatively higher as they can catalyze esterification as well as transesterification reactions (Ramirez-Ortiz et al., 2012). However, acid catalysts are usually less reactive than alkali catalysts and hence, demand relatively high temperature (100-120 $^{\circ}$C), high alcohol/oil molar ratio and longer reaction duration for the completion of reaction. Moreover, acid catalysts are highly corrosive and hence, acid resistance, complicated and costly reactors are required to perform the reaction. Presence of moisture also found to reduce the activity of the acid catalysts to a significant extent**.**

1.4.2. Homogeneous alkali catalysed reactions.

At industrial scale biodiesel is mainly produced through homogeneous alkali catalyzed (NaOH, KOH, alkali metal alkoxides etc.) transesterification of refined vegetable oil (Pathak, 2015). Elevated reactivity under kind reaction conditions, owing to the formation of a sole and uniform phase of reactant and catalyst, is the foremost advantage of using homogeneous catalysts commercial scale.

However, as formation of sole and uniform phase of product and catalyst occurs in case of uniphasic/homogeneous catalysts plus the product purification step for catalyst removal is cumbersome. Another limitation of homogeneous alkali catalysts is their deactivation by FFA (> 0.5 wt%), and/or moisture (> 0.3 wt%) contents *via* saponification as shown in scheme 1.2 (Sharma et al., 2018)

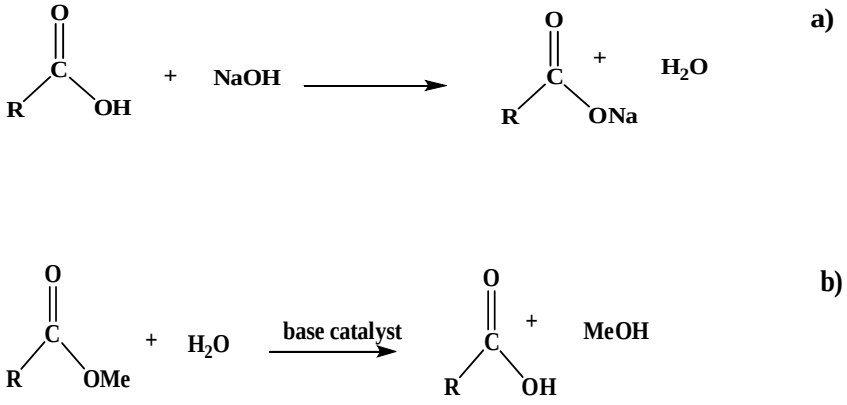

Scheme 1.2 (a). Saponification of homogeneous base by FFA, (b) Hydrolysis of biodiesel produced due to moisture.

Soap formed gets emulsified with the product to make the BD separation extremely difficult. In order to utilise the high FFA containing feedstock for BD production, FFA is in the beginning esterified with acid catalyst trailed by the later step of base catalyzed transesterification of feedstock which is loaded with ester (Kaur and Ali, 2015). The major drawbacks of the process include the utility of acerbic, strong acids requiring (i) acid resistance with intricately devised pricey reactors, (ii) obligatory acid neutralization step trailed by product rinsing to eliminate the breeded salt (iii) dumping of effluents generated during rinsing or washing step.

At an industrial level, biodiesel production is quite a lengthy procedure and involves a number of steps. A schematic flow diagram for the base catalysed production at industrial level is shown in Fig. 1.1.

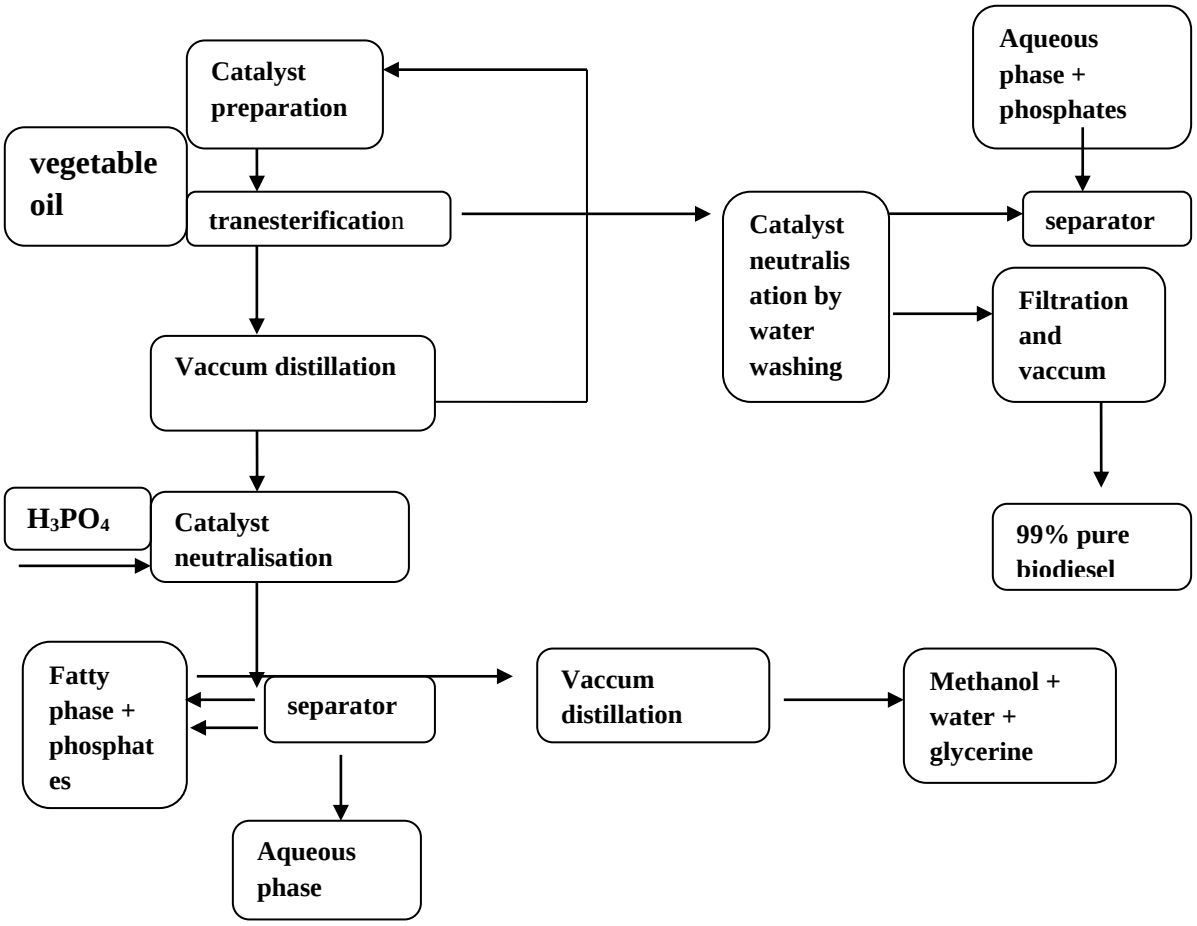

Fig. 1.1. Block diagram for BD production using alkali catalyst (Helwani et al., 2009).

1.4.3. Heterogeneous base catalysts

Solid base catalysts are by and large more dynamic and potent than acids for transesterification, and thus offer big advantage over solid acid catalysed transesterification. The other advantages offered by solid base catalysts include: a) production of sufficient FAMEs yields even when mild reaction conditions, b) consumption of lesser energy, c) simpler process of parting from the reaction mixture and hence, higher probability of regeneration making the process cost-effective (Islam et al., 2013).

Base-catalyzed conversion of oil into BD gets more attention than acid-catalyzed counterpart. The mechanistic pathway of solid-base catalysed BD synthesis has been depicted in Fig. 1.2. In a typical base catalyzed process, CH_3O^- ions play role of as active reacting species along with triglyceride molecules (Eckey, 1956). The mechanistic alleyway for heterogeneous base catalyzed transesterification appears to trail analogous pathway to that of single-phase consistent base catalyst. Initially, ion-exchange proceeds subsequent to methanol adsorption

over the facade of solid base catalyst thereby generating catalytically active species (CH_3O^-) which is stalwartly basic in nature. Secondly, occurs the nucleophilic attack of methoxide (CH_3O^-) ion on the carbonyl (-C=O) carbon of substrate (triglyceride) to produce a tetrahedral intermediate (I). Thirdly, the reorganization of the intermediate (II) formed marks the FAME formation (Lv et al., 2017).

This sequence recurs thrice to yield BD and glycerol. Literature reports a diversity of solid base catalysts employed for transesterification *viz.* pure alkali oxides, alkaline earth oxides and mixed double oxides which include metal impregnated alkali oxides and oxides of transition metals etc. which are discussed in subsequent section.

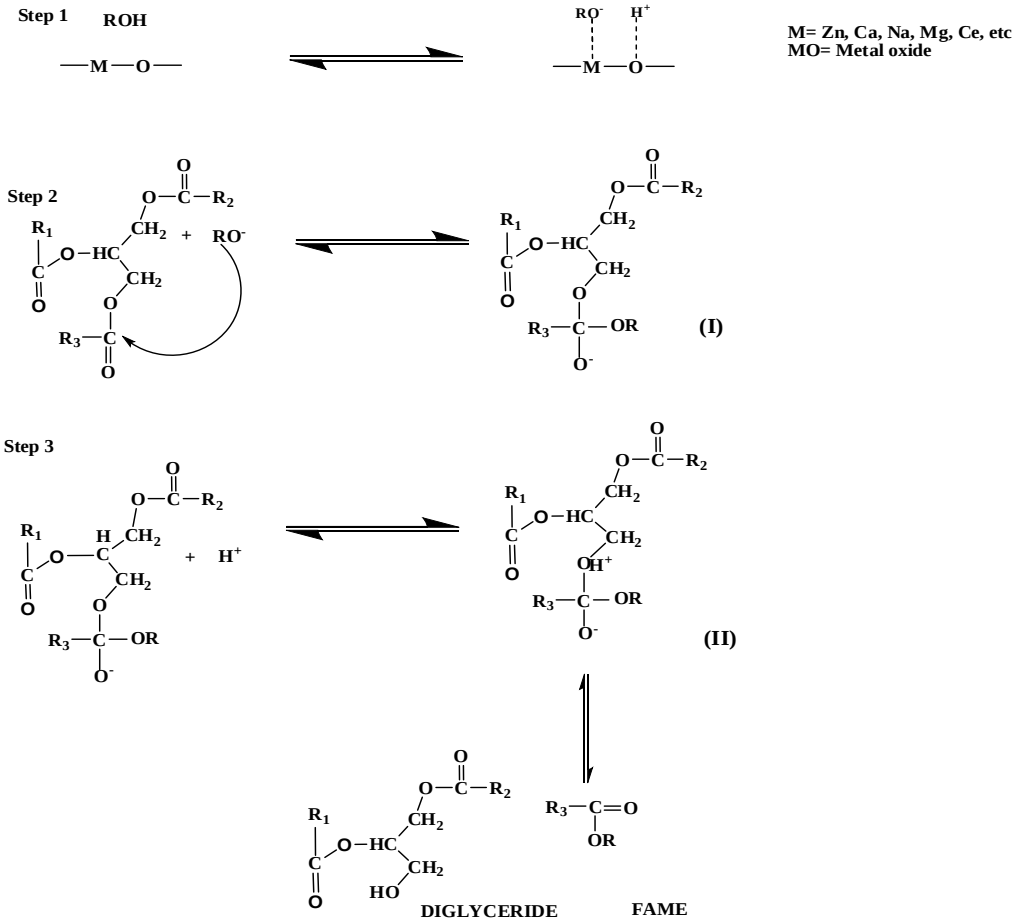

Fig. 1.2. Mechanistic pathway of solid-base catalysed transesterification (R_1, R_2, R_3 = fatty acid carbon chain of triglyceride). (Lv et al., 2017)

1.4.3.1. Industrially used heterogeneous catalysts for BD synthesis

At commercial level, various solid catalysts are in use for BD production few of which are discussed here. A heterogeneous catalytic process for the commercial BD production has been set up which finds its base in Hesterfip-H-technology originally developed and expanded by the Institute Français du Petrole. The technology utilises a catalyst consisting of mixed oxide of Zn-Al which works at 200–250 °C and 3-5 Mpa to yield FAMEs and glycerol (98% purity Moreover, it didn't require catalyst neutralization and intensive BD and glycerol purification steps (Bournay et al., 2005). Shirke Energy, is another biofuel industry in Pune and overseas which develops its own indigeneous high variety of jatropha, however, also utilising palm, animal tallow as feedstock. The company employs conventional NaOH and KOH catalysts for methanolysis. Another technology for large-scale BD production was developed by Benefuel's Ense in collaboration with NCL, Pune, utilising powdered solid acid catalyst, double-metal cyanide of Fe-Zn which can perform both esterification and transesterification (Sreeprasanth et al., 2006). Benefuel began work and toil on the scale-up of process employing fixed-bed reactors in year 2008. This durable, promoted catalyst is efficiently transforms almost all the feedstocks (*viz.* yellow grease, palm fatty acid distillate, crude palm oil and even the blend of degummed soybean oil) that have been tested in different pilot plant-scale operations (US 8,124,801 and JP 5,470,382). The large scale production and process scale up work was started in 2008. Another catalyst named T300 on undisclosed chemical identity is being used in Catalin chemical industry since 2007. The catalyst is non-toxic and could be a straight substitute for the conventional catalysts employed in BD production. In contrast to most other solid catalysts, T300 doesn't require a fixed bed, lofty temperature and pressure to work and is easily recovered by filtration with low cost inputs. Glycerin produced as coproduct during the reaction possesses purity level as high as > 98%. Another process has been developed by scientists at Chemical Engineering Division with National Collection of Industrial Microorganisms Center, NCL, Pune. The process performs the bio-catalytic production of biodiesel to make an example of green biotechnology. The process aims at downstream glycerol processing and making the industrial BD synthesis cost-effective by cutting down the cost of disposal of crude glycerol which is very cost intensive.

1.4.3.2. Pure alkali and alkaline earth oxides

The basic nature of alkali and alkaline earth oxides is supposed to crop up due to incidence of M^{2+} and O^{2-} ion in pairs in dissimilar coordinateon environments. The strongest base sites of highest strength arise at the sites at corner and edges and with low coordination defect or on surfaces with high Miller indices (Hattori, 1995). The following Fig.1.3 depicts the adsorption of methoxide ion over the basic sites of metal oxides.

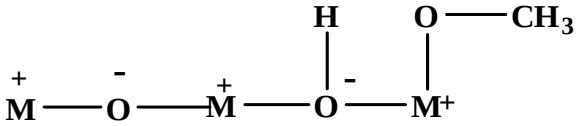

Fig. 1.3. Interaction of methanol to generate methoxide ion over pure metal-oxide, (M= metal atom). (Serio et al., 2008)

During methanolysis of triglycerides, it provides ample of sites for adsorption of methanol, where, O-H bonds quickly breakdown to give CH_3O^- anions and protons. Consequently, methoxide anions react with the substrate (oil or fat) to give away (FAMEs), fatty acid methyl esters. While oxides of Ca and Mg metals are more extensively employed from alkaline earth metal oxides for solid base catalysed transesterification, oxides of strontium have also been studied and applied in BD production (Su et al., 2013). The basic power of Group II metals oxides improves in the sequence of MgO < CaO < SrO < BaO. This is because of the decline of ionization enthalpy while on moving down the group, consequently weakens the M–O bond, hence, mounting the basic power of the oxides. A recurrent concern encountered for employing the bare metal oxides is their fairly high solubility in alcohol that leads to oozing out of metal into the BD and glycerol layers. Moreover, bare oxides also insist stiff reaction conditions like fairly high temperatures for biodiesel production (De lima et al., 2016)

CaO is one of the largely studied catalyst in the field of BD production owing to its high activity, accessibility and low cost. CaO derived from calcined snail shell has been used to produce BD. 92.5 % FAMEs yield was achieved after 1 h at 65 °C utilising 9:1 MeOH/oil molar ratio plus 3 wt% amount of catalyst (Kaewdaeng et al., 2017). A huge number of reports associated to use of CaO catalyst have been reported in last decade. All those reports on the transesterification using CaO disclosed the following issues.

a) Poisoning and deactivation of surface CaO basic sites by moisture and CO_2 adsorption after exposure to air to form calcium hydroxide and calcium carbonate.

b) Difficulties to accomplish CaO severance due to its dissolution in methanol.

c) Low action of used CaO after recycling compared to fresh CaO.

d) Possibility of side reactions together such as saponification and neutralization of FFA (Kesic et al., 2016).

1.4.3.3. Mixed- metal oxides

With an aim to perk up the activity of the catalyst, diverse mixed metal oxides have exclusively been studied for BD synthesis. The bare metal oxides pose a serious problem of leaching or oozing out into the reacting system of the active reacting species. Due, to leaching in bare metal oxides as catalysts, the speed of reaction reduces, demand of energy increases and hence the effective cost of the process. To perk up the overall performance and basicity of the catalyst, mixed metal oxides or alkali doped metal oxides have been well investigated for transesterification. The improved basicity of mixed oxide catalysts can be owed to the origin of O^- sites following the substitution of M^+ for M^{2+} and related charge inequity and associated defect generation (Montero et al., 2010). Perhaps, the activity and chemical behaviour of mixed- metal oxides is dissimilar from that of single oxide as the cations present in mixed-metal oxide can act in a supportive way and catalyze the various steps in methanolysis (Lee et al., 2014). The metal oxide present in larger amount acts as matrix or support while the metal present in comparatively lower amount is the doped metal. A variety of oxides of transition metals differing in Lewis base nature have also been studied and explored for BD production. In case of transition metal oxides as catalysts, lesser soap formation *via* saponification in the presence of high FFAs content was observed as compared to conventional homogeneous basic catalysts. Moreover, these offer less cost of production due to their inexpensive nature, easy availability and discerning nature of action. Their activity can be relayed on the existence of partially filled d-orbitals and their splitting with the approach of oxide ligand field (Gawande and Pandey, 2012). For biodiesel production, Zr metal has also been revealed to trigger and further stabilise the heterogeneous base catalysts (Torres et al., 2014). Earlier, bare zirconia alone has been employed as a catalyst owing to its both acidic as well as basic properties for catalysing one-pot esterification transesterification of low-quality vegetable oils (VOs) (Li et al., 2002). Mixed oxide of calcium oxide and zirconia $CaO\text{-}ZrO_2$ has been reported for methanolysis of rapeseed oil. The reaction employed 8 wt% of catalyst dose, 72:1 MeOH/oil molar ratio and could yield ~92% of

FAMEs at 120 °C within 6 h (Liu et al., 2015). Various other recently reported catalysts have been compared in Table 1.2.

Table 1.2. Basic mixed metal oxide catalysts reported in literature for transesterification of triglycerides.

		Reaction conditions							
Catalyst	**Triglyceride source**	**Temp (°C)**	**Pressure (MPa)**	**Time (h)**	**MeOH/oil molar ratio**	**Cat. amount (wt%)**	**Reusability**	**Yield (%)**	**Ref.**
C. brunneus-derived CaO	Rice bran	NR	NR	NR	35:1	0.5	7	93	Mazaheri et al., 2018
CaO-MgO	Soyabean	70	NR	2	12:1	1	5	98	Fan et al., 2016
CaO-LaO	Jatropha oil	240	8.2	0.17	21:1	1	NR	93	Hwa Teo et al., 2015
CaMgZn	Palm	60	NR	3	20:1	6	NR	97.5	Limmanee et al., 2013
Ca-O-Mg	E.Guineensis derived TGs	60	NR	6	15:1	4	5	99	Teo et al., 2017.
$MnCO_3$-ZnO	Soyabean	175	NR	1	18:1	4	17	94	Wana et al., 2014
CaO-CeO_2	Palm	65	NR	6	12:1	5	6	95	Wong et al., 2015
Na_2ZrO_3	Soyabean	65	NR	3	NR	3	4	98	Torres et al., 2014
Sr/MgO	Soyabean	65	NR	0.5	12:1	5	1	93	Tantirungrotechai et al., 2013
CaO-La_2O_3	Jatropha	160	NR	3	25:1	3	NR	98	Lee et al., 2015
CaO-cow bone	soyabean	60	NR	3	10:1	18	NR	92	Ayodeji et al., 2018
Sr/Ca	Palm	65	NR	0.5	9:1	5	NR	98	Li et al., 2016
CaO/MgO/ Fe_2O_3	Soyabean	70	NR	5	12:1	1	NR	93	Zhang et al., 2014
Cs/Na_2ZrO_3	Soyabean	65	NR	0.25	30:1	1	NR	99	Rodriguez et al., 2016
K/animal bones	Jatropha	70	NR	3	9:1	6	4	96	Nisar et al., 2017
CaO-NiO	Jatropha	65	NR	6	15:1	5	NR	85	Teo et al., 2014
Na-pumice	Soyabean	60	NR	2.7	24:1	12.86	3	99	De Luna et al., 2017
Ni/ZnO	Castor	55	NR	1	8:1	11	3	95	Baskar et al., 2018
Li_2ZrO_3	Waste oil	65	NR	1.25	12:1	5	9	99	Kaur and Ali, 2015

It can be observed from above table that most of the solid catalysts developed so far either don't give complete conversion of feedstock to BD or necessitate high temperature and pressures. Since, an industrial process has to be economically sound, very few catalysts bridge the gap between the industrial status demand and the overall performance of the literature reported catalysts.

1.4.4. Solid acid catalysts

It is supposed that heterogeneous acid catalysts possess brawny capability to reinstate uniphasic acid catalyst (Jacobson et al., 2008). The major rewards of utilising solid acid catalyst include (a) insensitivity to FFA, (b) simultaneous esterification as well as transesterification, (c) eradicate the tedious washing process of biodiesel, (d) trouble-free parting of the catalyst from reaction medium, ensuing the lesser level of product contamination, (e) simpler renewal of catalyst and (f) diminished corrosion crisis (Sharma et al., 2018). Solid acid catalysts can sustain their activity even in presence of 15% FFA contents. For transesterification, the idyllic and ultimate solid acid catalyst should encompass properties like consistent pore arrangement, a fair to elevated amount of strong acidic sites, plus a hydrophobic (water repelling) surface. Representative structure of sulphated metal oxide which is a very frequently employed solid acid catalyst has been depicted in Fig.1.4.

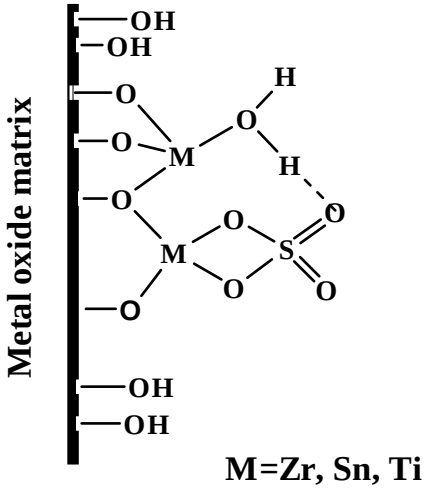

Fig. 1.4. Structure of sulphated metal oxides used for BD synthesis.

Mechanism of solid-acid catalysed transesterification is revealed in Fig. 1.5. Firstly, triglycerides form a Lewis complex (I) with the metal ion that activates the carbonyl group for nucleophilic attack by alcohol. Then, nucleophilic hit of alcohol on carbocation yields a tetrahedral intermediate (II) which is a hemiacetal species. Wobbly tetrahedral intermediate breaksdown with the support of solvent. After recurring twice, 3 new FAMEs are produced and the catalyst gets regenerated. During this process, formation of Lewis complex and activation of carbonyl (-C=O) group empowers the catalytic action by improving the electrophilicity of adjoining carbonyl C- atom (Lv et al., 2017).

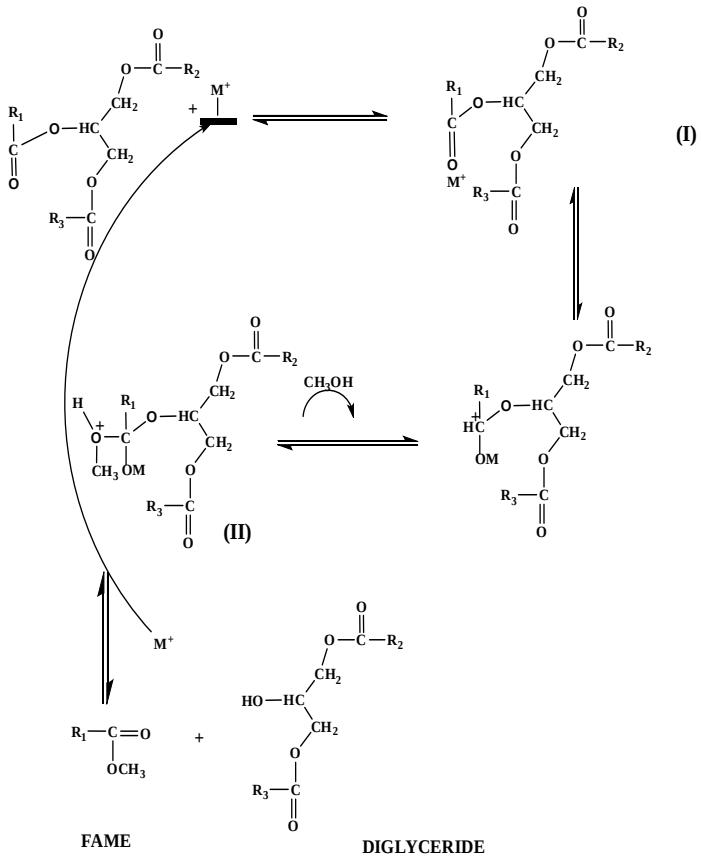

Fig. 1.5. Mechanism of solid-acid catalysed transesterification. (M= active site/metal ion, R_1, R_2, R_3 = carbon chains of fatty acid of triglyceride) (Lv et al., 2017).

To synthesise heterogeneous acid catalysts, different metal oxides have been utilised for immobilisation of sulphate group to prepare suphated metal oxides, potentially strong catalysts for BD production. These catalysts possess the knack of catalysing concurrent esterification and transesterification of the VOs having high content of FFAs. The transition metal oxides such as TiO_2, ZrO_2, SnO_2 etc. possess amphoteric character and can be modified with impregnation of suitable metals to prepare solid acidic or basic catalysts. In addition, Heteropolyacids are a class of acid catalysts, able to exhibit superacidity and possess lithe structures. Because of lofty solubility in the polar medium, HPAs are not suitable as solid catalysts in BD production (Kozhevnikov, 1998). Various reports are present in literature on the utility of solid acid catalysts for transesterification and esterification of diverse feedstocks. A comparison different literature reported solid acid catalysts used for BD synthesis has been sketched Table 1.3.

Table 1.3. Assessment of solid acid catalysts reported in literature for transesterification of triglycerides.

Catalyst	Triglyceride source	Reaction conditions				Remarks	Yield (%)	Ref.
		Temp (°C)	Time (h)	MeOH /oil molar ratio	Cat. amount (wt%)			
Bare ZrO_2	Palm	200	1	16:1	3	Can be used after modification or as support	65	Jitputti et al., 2006
Li_2ZrO_3	Waste oils	65	1.25	12:1	5	highly active, stable	99	Kaur and Ali, 2015
Tungstated ZrO_2	Soyabean	200	10	6:1	3	Highly stable	67	Jacobson et al., 2008
Tetragonal SO_4^{2-}/ZrO_2	Soyabean	150	6	20:1	3	Significant decativation	100	Shi et al., 2016
SO_4^{2-}/ZnO	Soyabean	65	4	6:1	4	Low yield	81.1	Istadi et al., 2015
Li/TiO_2	Canola	65	3	24:1	5	stable	98	Alsharifi et al., 2017
Sr/MgO	Soyabean	65	0.5	12:1	5	Not reusable	93	Tantirungrotechai et al., 2013
$W/Ti/SiO_2$	Waste cottonseed	65	4	30:1	5	Reusable for 4 cycles	98	Kaur et al., 2018
Zr/CaO	Jatropha	65	1.75	15:1	5	Effective for high FFA containing feedstock		Kaur and Ali, 2014
Ca/Sn	Soyabean	60	6	12:1	8	Incomplete conversion	89.3	Xie and Zhao, 2013
Mn/ZnO	Mahua	50	0.83	7:1	8	Reusable for 5 cycles	97	Baskar et al., 2017
Phosphotungstate/MCM-41	Oleic acid	60	14	40:1	4.4	Incomplete conversion, more reaction time	89	Singh and Patel, 2015
Cs-$H_3PW_{12}O_{40}$	Used VO	260	0.66	40:1	3	Harsh reaction conditions NR	92	Shin et al., 2012

Alike most of the solid base catalysts, even acidic counterparts that yielded complete conversion levels needed high reaction temperature. The reaction conditions employed or the overall performance of the catalyst from the commercial perspective are not found upto the mark for being accepted to catalyse the transesterification industrially.

1.5. Mesoporous silica

In year 1992, a new folks of well-ordered mesoporous materials came into light which paved the way to a new field of research for researchers. Mesoporous materials are known as mesoporous molecular filters or sieves, constitute a category of 3D-nanostructures having distinct mesoscale pores (2–50 nm diameter) and surface area ranging up to 1000 m^2/g. They occupy an exclusive and distinctive place between crystalline zeolites and various types of 3D ordered materials. These materials are formed by a process of self-assembly from combined solutions of metal alkoxides which are sol-gel precursors and structure-directing amphiphiles, frequently block-copolymers or surfactants. According to the classification by IUPAC, *micropores* possess a diameter < 2 nm, while, diameter of *mesopores* stays within 2-50 nm and diameter of *macropores* is > 50 nm. The pores can comprise unlike shapes *viz.* spherical or cylindrical (Sing et al., 1985).

Initially, mesoporous materials were designated as MCM-X (MCM stands for Mobil Crystalline of Materials), first synthesized in Mobile Corporation laboratories. In 1998, mesoporous silica was first prepared using non-ionic triblock polymers (Zhao et al., 1998) and designated as SBA-X (Santa Barbara Amorphous), X corresponds to a specific and particular surfactant and pore structure. This kind of surfactant fetches lot of interest, as it can be easily removed, is nontoxic in nature, easily biodegradable, and inexpensive (Munoz and Acuna, 2010). The synthesis carried out using non-ionic surfactants typically occurs in solutions with low-pHs. To cite an example, in SBA-15, there are cylindrical pores arranged in hexagonal fashion and synthesized using P123 surfactant whilst, in SBA-16, the pores are spherical in a bcc arrangement and synthesized using surfactant F127. It has been reported that relative to MCM-41 material, SBA-15 possesses more steady matrix to slot in the nanoparticles due to its thicker walls and relatively larger pore size. Moreover, SBA-15 has uniform pores with larger size to allow easy diffusion of larger molecules. (Bore et al., 2005).

Today, the SBA-15 mesoporous silica is most expansively and widely studied and is the subject of interest and attention for researches and its application for commercial purposes as well. SBA-15 silica displays very fascinating textural properties, *viz.* large surface areas, consistent-sized pores, solid scaffold and skeleton walls, plus corresponding textural porosity. The main benefit of SBA-15 material as matrix also includes greater surface-to-volume ratio, changeable scaffold compositions plus lofty thermal solidity (Rahmat et al., 2010). Bigger pore size to allow diffusion of bulkier molecules, inert nature of Si-O bond and tuneable surface make the mesoporous materials a versatile support material for the purpose of

synthesis and preparation of wide array and variety of catalysts (Kazemian et al., 2013). Since a long time after their first report of synthesis, mesoporous silicas have been applied in various fields of great utility. Mesoporous materials have been reported to act as a prospective supports for Pt particles (Joo et al., 2001), or as storeroom units for hydrogen or methane gases (Zhou et al., 2004). In a recent report, Iron oxide-supported SBA-15 acted as a great magnetic mesoporous adsorbent for Ni^{2+} for its removal from wastewater. The catalyst showed lofty adsorption potential of 352.9 mg/g within 240 min (Ulfa and Jannah, 2018). It has posed as a promising matrix for the restricted release of efavirenz drug in 120 min. time without any disruption in its order (Jesus et al., 2016). It has been also explored as a potential adsorbent for CO_2 with quite high adsorption capacity when compared to zeolites and activated charcoal (Do Nascimento et al., 2017). SBA-15 has also acted as support material for metal oxides such as CeO_2, MoO_3, WO_3 (Tiemann, 2008; Xie and Zhao, 2014 Kaur et al., 2018).

1.5.1. Synthesis of mesoporous silica

The method of sol gel synthesis is employed in synthesising mesoporous silica. A colloidal system constitutes the sol in which micelles are formed by surfactants. As the precursor of silica is added, its hydrolysis occurs and it forms a framework which encloses the liquid. The sol gel transition is slow and ultimately, sol gets converted to gel. As the calcination step of the gel is done, the surfactant evaporates and gets removed thereby leaving the network of porous silica. However, it is to be rememebered that there is firstly the silanol group formation with hydrolysis of alkoxide precursors as depicted in scheme 1.3.

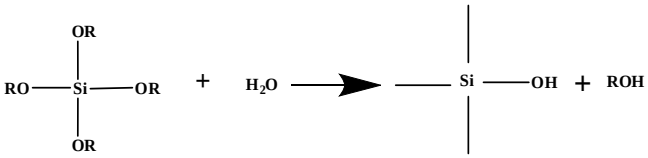

Scheme 1.3. Hydrolysis of silica precursor to form silanol groups (R= $-CH_2CH_3$, $-CH_3$, $-CH_2CH_2CH_3$, $-CH_2CH_2CH_2CH_3$).

After this, the polymerisation occurs and formation of Si-O-Si linkages takes place that forms the silica framework.

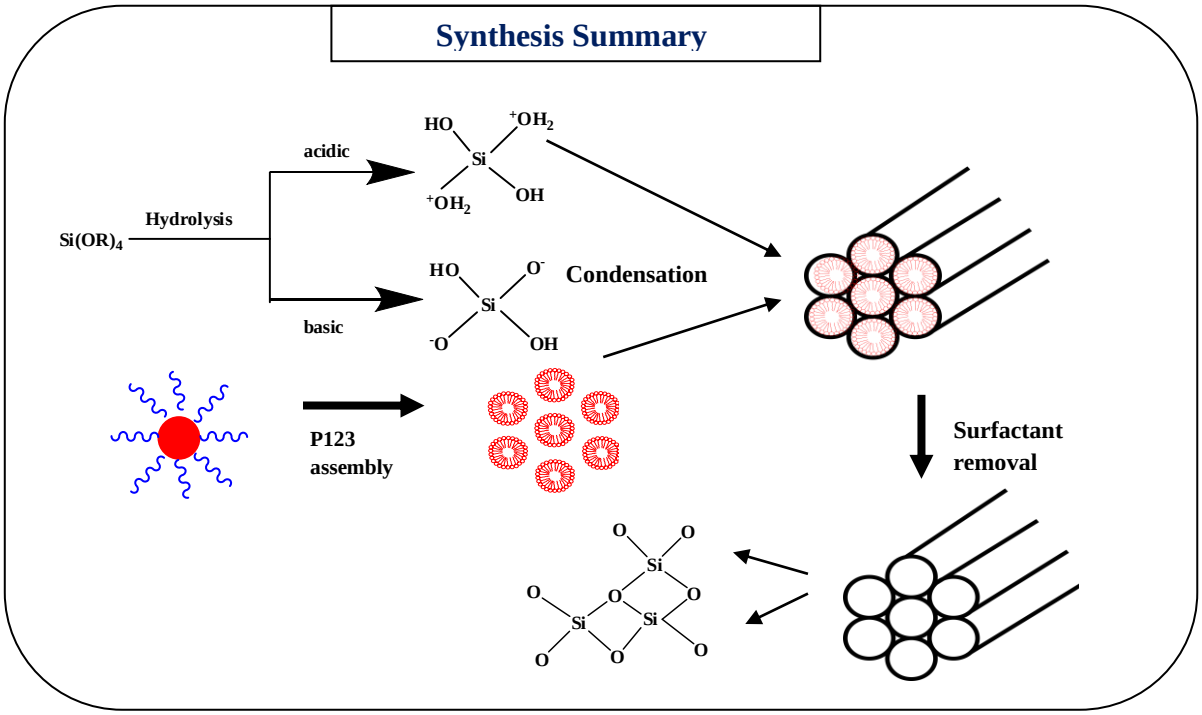

Fig. 1.6. Stepwise synthesis of mesoporous silica

For SBA-15 synthesis, pluronic 123 is utilised as surfactant. Under the trademark "pluronics", there are different non ionic polymers, triblock in nature, all consisting of polyethylene oxide (PEO), hydrophilic portion and polypropylene oxide chain (PPO), hydrophobic in nature (Jorgensen and Hvidt, 1997). Structures of various different types of surfactants (pluronics, cationic and anionic) have been in Fig. 1.7.

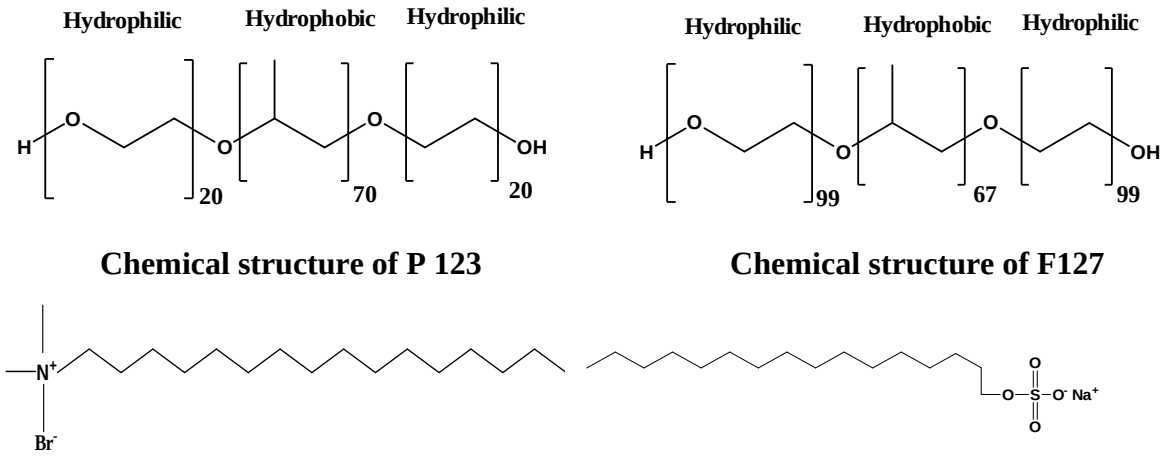

Fig. 1.7. Structures of different surfactants (non-ionic, cationic, anionic)

1.5.2. Micelle formation with pluronics

Initially, the surfactants are present at air/water interface, when their concentration in the medium is low. As the surfactant concentration increases, the surface energy reduces further till it reaches a crucial level. At this phase, the CMC (Critical Micelle Concentration) is attained where surfactant molecules begin to aggregate to form micelles. The CMC as well as micellar shape is decided by the nature of surfactant. The summative arrangement of amphiphilic molecules is decided by the factor known as critical packing parameter or CPP, {CPP=V/l.a}, {V = volume of hydrophobic non-polar chain [nm^3], a = area of the hydrophilic polar part [nm^2] and l [nm] is length of water loving/hydrophobic component of chain}. In case of pluronics, micelles comprise of hydrophobic/water repelling PPO core bounded by hydrophilic/water loving PEO chains (Wanka et al., 1994). If V~ A. l and CPP~ 1, then surfactant has small head groups and rigid chains and form bilayer micelle which is planar. For SBA-15 synthesis, cylindrical micelles have range of CPP $1/3<CPP<1/2$ and only in this case, hexagonal packing becomes feasible. If CPP>1, then reverse micelle is formed and packing of surfactant becomes quite tough. Vesicles are formed when CPP = 0.5-1 and spherical micelle is formed when CPP<0.33 (Israelachvili, 1997). The various packing arrangements of surfactants have been depicted in Fig.1.8.

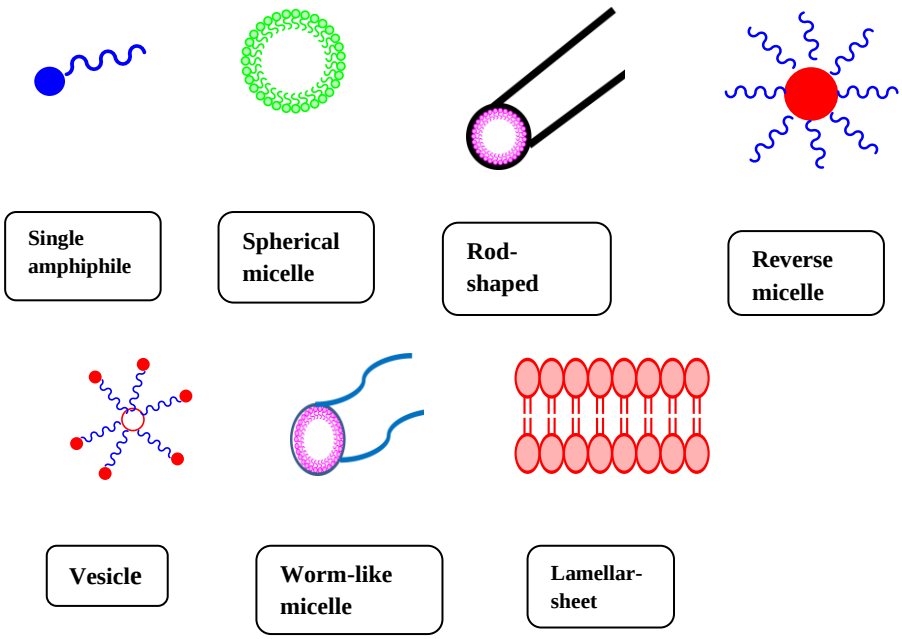

Fig. 1.8. Different packing arrangements of surfactants and micelle structures.

1.5.3. SBA-15 supported catalysts for BD production

When it comes to biodiesel production which is a burning area of interest for researchers, SBA-15 mesoporous silica has engrossed much interest and attention as a solid support. The SBA-15 silica can act as great support for acidic and basic catalysts without any disruption in its structure (Melero et al., 2012). These supported catalysts are likely to possess fairly good catalytic activities for transesterification. According to a report, 2 wt% of WO_3 was imbued over silica mesoporous particles (SMP). Under optimised reaction conditions, with 2 wt% of WO_3 loading, 4.5 wt% of catalyst amount, 9:1 MeOH/oil molar ratio, at 343 K, 96% of FAMEs yield was obtained within a duration of 45 min (Aziz et al., 2017). The lofty catalytic action of $2WO_3$/SMP can be ascribed to the elevated content of Lewis acid sites plus the existence of together inter and intrarparticle pores system of the catalyst which efficiently facilitated and increased reactants and products transport throughout the reaction course. The chemical structure of WO_3/SMP is depicted in Fig. 1.9.

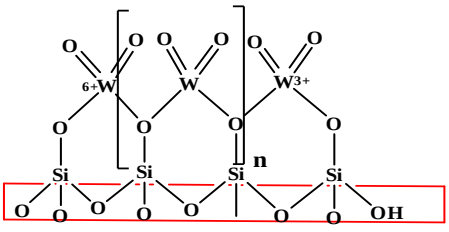

Fig. 1.9. Structure of Tungsten oxide impregnated mesoporous silica particles.

Ti-SBA-15 has been explored for concurrent esterification and transesterification. The basic mechanism of BD synthesis by this catalyst has been elaborated in Fig. 1.10.

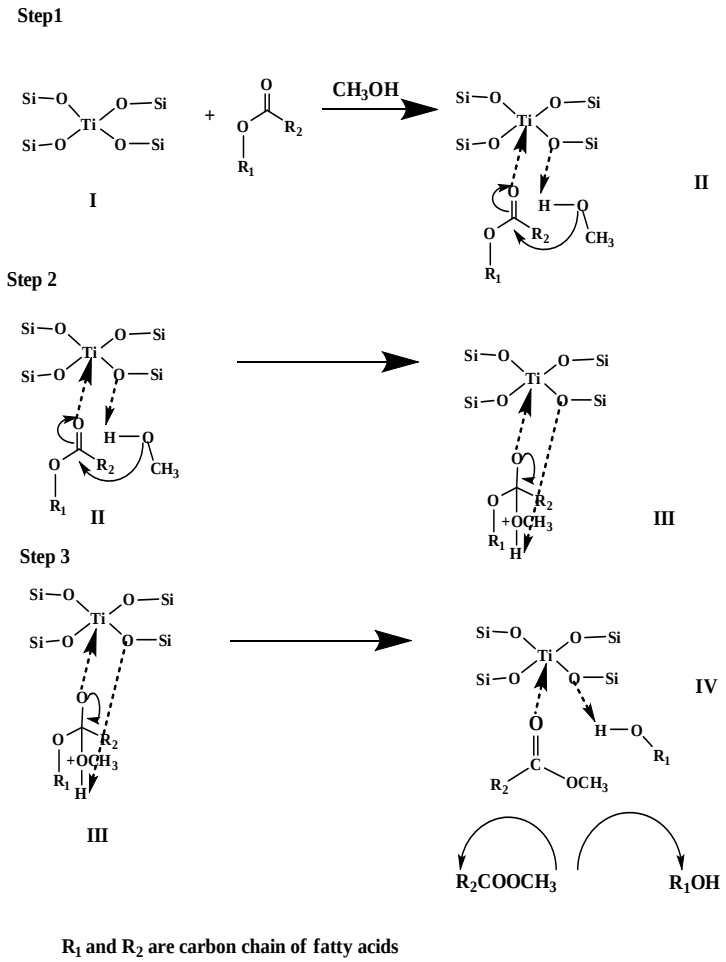

Fig. 1.10. Mechanism of transesterification by Ti-SBA-15 heterogeneous catalyst

Over the facade of Ti/SBA-15 catalyst, -C=O group of triglyceride gets coordinated to the tetrahedral Ti^{4+} species through O atom to form an intermediate (II). In the interim, CH_3OH gets triggered by stabilizing down the H atom *via* H-bonding with lattice oxygens in the adjacent tetrahedral Ti^{4+} moieties. The electrophilic C of Lewis complex experiences nucleophilic hit by stimulated CH_3OH to yield a tetrahedral intermediate (III). Then, electron on C-O gives reverse to C atom and O-R_1 moeity hits the H atom appended on vicinal -OH group, to produce the new intermediate (IV) yielding new fatty acid methyl ester and ROH molecule. To prepare an acidic SBA-15 supported catalysts, matrix of mesoporous silica is modified by impregnation with acidic character/ Lewis acids, *viz.* sulphonic acid, tungstate, zirconia etc.

A comparison of various mesoporous based acidic catalysts employed for BD synthesis along with their reaction conditions has been drawn in Table 1.4.

Table 1.4. Assessment of activity of acidic mesoporous heterogeneous catalysts for BD production.

Catalyst	TG source	Reaction conditions				Reusability (cycles)	Yield (%)	Ref.
		Temp (ºC)	Time (h)	MeOH/ oil molar ratio	Catalyst amount (wt%)			
M-SBA-15-SO_3H (M=Al,Ti)	Oleic acid	140	0.5	15:1	5	Non reusable	97	Munguia et al., 2017
Mesoporous polymer solid acid	Jatropha	160	8	50:1	6	4	94	Pan et al., 2016
SO_3H functionalised Mesoporous catalyst	Oleic acid	100	4	30:1	4	4	96	Pan et al., 2017.
Mesoporous SO_3H–$ZnAl_2O_4$ (microwave conditions)	Palm fatty acid distillate	60	0.3	9:1	1.5	7	95	Soltani et al., 2017
Mesoporous W/Ti/SiO_2	Waste cottonseed	65	4	30:1	5	4	98	Kaur et al., 2018
WO_3/mesoporous silica	Croton megalocarpus	70	0.75	9:1	4.5	Non reusable	96	Aziz et al., 2017
Mesoporous WO_3/SiO_2 spheres	Oleic acid	NR	6	40:1	3	5	97	Guochang et al., 2016
Al-SBA-15	Jatropha	180	24	12:1	NR	NR	99	Meloni et al., 2016
Ti/SBA-15	Jatropha	200	3	27:1	15	3	90	Chen et al., 2014
([Ps-im]HSO_4)/ SO_4^{2-}/ZrO_2-SiO_2	Ricebran oil	150	3	18:1	5	5	99	Fan et al., 2018
Mesoporous sulphated zirconia	Soyabean oil	120	4	12:1	4	NR	94.9	Luo et al., 2017
Mesoporous sulphonated carbon	Acidic oils (21-41 wt% FFA)	120	16.6	20:1 MeOH/ FFA	NR	Non reusable	91	Konwar et al., 2016

To prepare a basic mesoporous catalyst, matrix of mesoporous silica is modified by drenching with basic character carrying groups, Lewis bases, *viz.* MgO, CaO, modified alkali and alkaline earth metals etc. A comparison of various mesoporous based basic catalysts explored for BD synthesis along with their reaction conditions and overall performance has been drawn in Table 1.5.

Table 1.5. Assessment of activity of basic mesoporous heterogeneous catalysts for BD production.

Catalyst	TG source	Reaction conditions				Reusability (cycles)	Yield (%)	Ref.
		Temp (ºC)	Time (h)	MeOH/oil molar ratio	Catalyst amount (wt%)			
B.Cepacia/ Fe_3O_4/lipase on mesoporous silica	Waste cooking	35	35	6:1	25	5	91	Karimi, 2016
Na_2SiO_3	NR	28	12	12:1	5	NR	96	Yang et al., 2018
$CaSiO_3$	NR	28	24	27:1	23	NR	96	Yang et al., 2018
Mesoporous calcium titanate	Waste cottonseed	65	1	3:1	0.2	5	80	Yahya et al., 2016.
20-CeO_2/Li/SBA-15	Waste cottonseed	65	4	40:1	10	5	98	Malhotra and Ali, 2018
MgO-mesoporous silica	Jatropha	200	4	36:1	6	2	81.4	Andrew et al., 2015
Ca-Ce/SBA-15	Palm	85	6	20:1	5	15	96	Kawi et al., 2015
CaO-MoO_3/SBa-15	Soyabean	65	50	50:1	6	NR	83.2	Xie and Zhao, 2014
SBA-15-pr-NR_3OH	Soyabean	65	0.5	12:1	2.5	5	99	Xie and Fan, 2014
K_2SiO_3/AlSBA-15	Jatropha	60	3	9:1	3	4	95	Wu et al., 2014.
Mesoporous KOH/Fe_3O_4	Canola	65	3.26	12.3:1	9	3	93.5	Rezayan and Taghizadeh, 2018
Lipase/ mesoporous silica	Hevea Brasiliensis	35	NR	8:1	NR	10	93	Arumugam et al., 2018
1,3-dicyclohexyl-2-octylguanidine/ SBA-15	Soyabean	65	15	15:1	8	5	92.6	Xie et al., 2015
Mesoporous Magnetic sodium silicate	Soyabean	65	8	25:1	3	5	99.2	Xie et al., 2018
Mesoporous Ca/Al	Sunflower oil	70	NR	12:1	10	NR	84.2	Vardast et al., 2018

Largely, the above studied catalysts either produced < 96.5% FAMEs or insisted harsh conditions to carry out the reaction. For taking up of BD for using at commercial level, the FAME yield should be at least 96.5 %. The product with FAMEs yield lesser than 96.5% can't be addressed as BD at commercial level.

1.6. Conclusions

1) Biodiesel (BD) is a renewable, sulphur less, non toxic replacement and alternative for conformist and traditional diesel. Chemically, it is a mixture of fatty acid methyl esters produced *via* transesterification of triglycerides.

2) The application of heterogeneous catalysts would lead to trouble-free and effortless, inexpensive separation processes, lesser effluent generation as well as capitol and energy costs. Reusability of the catalyst is a chief advantage which may further make the process more cost-effective.

3) Mesoporous silica has gripped much interest as a solid support due to its exceptional properties like superior thermal stability, elevated surface area and downsizes mass transfer limitations and permits soaring concentration of active sites per unit weight of material.

4) The SBA-15 being thermally very stable can act as great support for both acidic as well as basic catalysts without any breakdown in its construction.

5) Most of the mesoporous based catalysts reported in literature were either able to yield < 96.5 % FAMEs or demanded heavy methanol to oil molar ratios and reaction temperatures.

1.7. Lacunae in literature

The high production cost limits the utility of BD at commercial scale. Here are listed the gaps that have been identified on the basis of literature for the catalysts used in BD production.

1) Major problem faced with utility of homogenous catalysts is their tricky and knotty separation from the reaction mixture. The BD produced in homogeneous catalysed process must be washed to get rid of the catalyst impurities. Moreover, such catalysts necessitate high quality feedstock which is almost free of moisture and FFA.
2) Most of the literature accounted heterogeneous catalysts demonstrate better activity under unkind reaction conditions. Major hitches associated with such catalysts are: (i) partial solubility of the catalysts in reaction mixture, (ii) extermination of the catalysts due to the atmospheric gases or moisture or reaction mixture (iii) non reusability or less reusability and (iv) Harsh reaction conditions
3) Most of the literature based mesoporous based catalysts demonstrate poor reusability as well as stability.
4) Many catalysts reported in literature were able to yield < 96.5 % FAMEs yield. Attempts need to be made to accomplish higher yields at reasonable or easy experimental conditions.

1.8. Objectives

1) Preparation of silica based mesoporous materials of appropriate pore size as a support material for the catalyst preparation.
2) Impregnation of active metals (e.g., Zr, K, Na, Ce, etc.) over prepared support to prepare the catalyst for transesterification reaction.
3) Evaluation of transesterification activity of the prepared catalysts and study the kinetics of the reaction.

The present work will focus on improvement in terms of activity and recyclability of prepared silica based mesoporous metal impregnated catalysts and employing a procedure of synthesis which is friendly for environment and cost-effective. Moreover, the work also centres to calculate the thermodynamic parameters which are a significant for transesterification.

References

Allen, C.A.W., Watts, K.C., Ackman, R. G., Pegg, M.J., 1999. Predicting the viscosity of biodiesel fuels from their fatty acid ester composition. Fuel 78, 1319-1326.

Alsharifi, M., Znad, H., Ang, M., 2017. Biodiesel production from canola oil using novel Li/TiO_2 as a heterogeneous catalyst prepared by wet impregnation method. Renewable Energy 114, 1077-1089.

Andrew, A., Katima, J., Lee, K.T., Mdoe, J.E.G., 2015. Solvent-free-MgO-functionalised mesoporous catalyst for jatropha oil transesterification. J. Nanotechnol. 2015, 1-7.

Arumugam, A., Thulasidharan, D., Jegadeesan, G.B., 2018. Process optimisation of biodiesel production from Hevea Brasiliensis oil using lipase immobilised on spherical silica aerogel. Renewable Energy 116, 755-761.

Asri, N.P., Machmudah, S., Wahyudiono., Budikarjono, S.K., Roesyadi, A., Goto, M., 2013. Palm oil transesterification in sub-and supercritical methanol with heterogeneous base catalyst. Chem. Eng. Processing. 72, 63–67.

Atadashi, I.M., Aroua, M.K., Aziz, A.A., 2010. High quality biodiesel and its diesel engine application.: a review. Renew. Sustain. Energ. Rev. 14, 1999-2008.

Ayodeji, A.A., Blessing, I.E., Sunday, F.O., 2018. Data on calcium oxide and cow bone catalysts used for biodiesel production. Data in brief 18, 512-517.

Aziz, M.A.A., Triwahyono, S., Jalil, A.A., Atabani, A.E., Ramli, Z., Majid, Z.A., Prasetyoko, D., 2017. Transesterification of croton megalocarpus oil to biodiesel over WO_3 supported on silica mesoporous- macroporous catalyst. Chem. Eng. J. 316, 882-892.

Babu, N.S., Sree, R., Prasad, P.S.S., Lingaiah, N., 2008. Room-temperature transesterification of edible and non edible oils using a heterogeneous strong basic Mg/La catalyst. Energy Fuels 22, 1965-1971.

Balat, M., Balat, H., Öz, C., 2008. Progress in bioethanol processing. Progr. Energy Combust. Sci. 34, 551-573.

Baskar, G., Selvakumari, I.A.E., Aiswarya, R., 2018. Biodiesel production from castor oil using heterogeneous Ni doped ZnO nanocatalyst. Bioresour. Technol. 250, 793-798.

Baskar, G., Gurugulladevi, A., Nishanthini, T., Aiswarya, R., Tamilarasan, K., 2017. Optimisation and kinetics of biodiesel production from mahua oil using managanese doped zinc oxide nanocatalyst. Renew. Energy 103, 641-646.

Bore, M.T., Pham, H.N., Switzer, E.E., Ward, T.L., Fukuoka, A., Datye A.K., 2005.The role of pore size and structure on the thermal stability of gold nanoparticles within mesoporous silica. J. Phys. Chem. B. 109, 2873-2880.

Bournay, L., Casanave, D., Delfort, B., Hillion, G., Chodorge, J. A., 2005. New heterogeneous process for biodiesel production:A way to improve the quality and value of crude glycerine produced by biodiesel plants. Catal. Today 106, 190-192.

Brunschwig, C., Moussavou, W., Blin, J., 2012. Use of bioethanol for biodiesel production. Prog. Energy Combust. Sci. 38, 283-301.

Calero, J., Luna, D., Sancho, E.D., Luna, C., Bautista, F.M., Romero, A.A., Posadillo, A., Verdugo, C., 2014. Development of a new biodiesel that integrates glycerol, by using CaO as heterogeneous catalyst, in the partial methanolysis of sunflower oil. Fuel 122, 94-102.

Chen, S.Y., Mochizuki, T., Abe, Y., Toba, M., Yoshimura, Y., 2014. Ti-incorporated SBA-15 mesoporous silica as an efficient and robust Lewis solid acid catalyst for production of high quality diesel fuels. Appl. Catal. B: Environ. 148-149, 345-346.

Cozzolino, M., Di Serio , M., Tesser, R., Santacesaria, E., 2007. Grafting of titanium alkoxides on high surface SiO_2 support: An advanced technique for preparation of nanostructured of TiO_2/SiO_2 catalysts. Appl. Catal. A: Gen. 325, 256-262.

Daud, N.M., Abdullah, S.R.S., Hasan, H.A., Yaakob, Z., 2015. Production of biodiesel and its wastewater treatment technologies: a review. Process Safe. Environ. 94, 487–508.

De Lima, A., Ronconi Machado, C., Mota, C., 2016. Heterogeneous basic catalysts for biodiesel production. Catal. Sci. Technol. 6, 2877-2891.

De Luna., M.D.G., Cuasay, J.L., Tolosa, N.C., Chung, T.W., 2017. Transesterification of soyabean oil using a novel heterogeneous base catalyst: synthesis and characterisation of Na-pumice catalyst, optimisation of transesterification conditions, studies on reaction kinetics and catalyst reusability. Fuel 209, 246-253.

Do Nascimento, A.R., De Figueredo, G.P., Da Costa, T.R., De F Melo, M.A., De A Melo, D.M., De Souza, M.J.B., 2017. Thermodynamics of CO_2 adsorption on mesoporous materials impregnated with nickel. Ceramica, 63, 524-529.

Eckey, E.W., 1956. Esterification and interesterification. J. Am. Chem. Soc. 33, 575-579.

Escobar, J.C., Lora, E.D., Venturini, O.J., Edgar E. Yanez, E.E., Castillo, E.F., 2009. Biofuels: Environment, technology and food security. Renew. Sustain. Energ. Rev. 13, 1275-1287.

Fan, M., Liu, Y., Zhang, P., Jiang, P., 2016. Blocky shapes Ca-Mg mixed oxides as water resistant catalyst for effective synthesis of biodiesel by transesterification. Fuel Process. Technol. 149, 163-168.

Fan, M., Liu, H., Zhang, P., 2018. Ionic liquid on acidic organic-inorganic hybrid mesoporous material with good acid-water resistance for biodiesel production. Fuel 215, 541-550.

Gawande, M.B., Pandey, R.K., 2012. Role of mixed metal oxides in catalysis science-versatile applications in organic synthesis. Catal. Sci. Technol. 2, 1113-1125.

Goering, C. E., Schwab, A. W., Daugherty, M. J., Pryde, E. H., Heakin, A. J., 1982. Fuel properties of Eleven vegetable oils. Trans ASAE. 85, 1472-1483.

Gorji, A., Ghanei, R., 2014. A review on catalytic biodiesel production. J.Bio & Env. Sci. 5, 48-59.

Guochang, C., Hongbin, Q., Jikang, C., Zhicai, W., Mingfu, Y., Cun-Yue, G., Xiaoming, W., 2016. Well-dispersed sulphated mesoporous WO_3/SiO_2 hybrid colloidal spheres: high-efficiency catalysts for synthesis of fatty acid alkyl esters. Fuel 163, 41-47.

Hattori., 1995. Heterogeneous basic catalysts. Chemical reviews. Chem. Rev. 95, 537-558.

Hawa Teo, S., Goto, M., Taufiq-Yap, Y.H., 2015. Biodiesel production from Jatropha curcas oil with Ca and La mixed oxide. J. Supercrit. Fluids 104, 243-250.

Helwani, Z., Othman.M.R., Aziz.N., Fernando, W.J.N., Kim. J., 2009. Technologies for production of biodiesel on green catalytic techniques. Fuel Process. Technol. 90, 1502-1514.

Islam, M.S., Ahmed, A.S., Islam, A., Aziz, S.A., Xian, L.C., Mridha, M., 2014. Study on emission and performance of diesel engine using castor biodiesel. J. Chem. 2014, 1-8.

Islam, A., Taufiq-Yap, Y.H., Chu, C.M., Chan, E.S., Ravindra, P., 2013. Study on design of heterogeneous catalysts for biodiesel production. Process Safe. Environ. 91, 131-144.

Israelachvili, J.N, 1997. Intermolecular and Surface Forces, Academic Press, London. Chapters 16-17.

Istadi, I., Buchori, L., Rahmawati, D.A., Intaningrum, D., 2015. Active acid catalyst of sulphated ZnO for transesterification of soyabean oil with methanol to biodiesel. Procedia Environ. Sci. 23, 385-393.

Jacobson, K., Gopinath, R., Meher, L.C., Dalai, A.K., 2008. Solid caid catalysed biodiesel production from waste cooking oil. Appl. Catal. B: 85, 86-91.

Jesus, R.A., Rabelo, A.S., Figueiredo, R.T., Da Silva, L.C.C., Codentino, I.C., Araujo, G.LB., Araujo, A.A.S., Mesquita, M.E., 2016. Synthesis and application of MCM-41 and SBA-15 as matrices for in-vitro efavirenz release study. J. Drug Deliv. Sci. Technol. 31, 153-159.

Jitputti, J., Kitiyanan, B., Rangsunvigit, P., Bunyakiat, K., Attanatho, L., Jenvanitpanjakul, P., 2006. Transesterification of crude palm oil and crude coconut oil by different solid catalysts. Chem. Eng. J. 116, 61-66.

Joo, S.H., Choi, S.J., Kwak, O.J., Liu, Z., 2001. Ordered nanoporous arrays of carbon supporting high dispersions of platinum nanoparticles. Nature 412, 169-172.

Jorgensen, E.B., Hvidt, S., 1997. Effect of salt on micellisation and gelation of a triblock copolymer studied by rheology and light scattering. Macromolecules 30, 2355-2364.

Jothiramalingam, R., Wang, M.K., 2009. Review of recent developments in solid acid, base and enzyme catalysts for biodiesel production via transesterification. Ind. Eng. Chem. Res. 48, 6162–6172.

Kaewdaeng, S., Sintuya, P., Nirunsin, R., 2017. Biodiesel production suing calcium oxide from river snail shell ash as catalyst. Energy Procedia 138, 937-942.

Karimi, M., 2016. Immobilisation of lipase onto mesoporous magnetic nanoparticles for enzymatic synthesis of biodiesel. Biocatal Agric. Biotechnol. 8, 182-188.

Kaur, M., Malhotra, R., Ali, A., 2018. Tungsten supported Ti/SiO_2 nanoflowers as reusable heterogeneous catalyst for biodiesel production. Renewable Energy 116, 109-119.

Kaur, N., Ali, A., 2014. Kinetics and reusability of Zr/CaO as heterogeneous catalyst for methanolysis and ethanolysis of jatropha curcas oil. Fuel Process. Technol. 119, 173-184.

Kaur, N., Ali, A., 2015. Lithium zirconate as solid catalyst for simultaneous esterification and transesterification of low quality triglycerides. Appl. Catal. A: Gen. 489, 193-202.

Kawi, S., Maneerung, T., Thitsartarn, W., 2015. highly active and durable Ca- doped Ce-SBA-15 catalyst for biodiesel production. Energy 89, 946-956.

Kazemian, H., Turowec, B., Siddiquee, M.N., Rohani, S., 2013. Biodiesel production using cesium modified mesoporous ordered silica as heterogeneous base catalyst. Fuel 103, 719–724.

Kesic, Z., Lukic, I., Zdujic, M., Mojovic, L., Skala, D., 2016. Calcium oxide based catalysts for biodiesel production: a review. Chem. Ind. Chem. Eng. Q. 22, 391−408.

Knothe, G., Steidley, K.R., 2005. Lubricity of Components of Biodiesel and Petrodiesel. The Origin of Biodiesel Lubricity. Energy Fuels 19, 1192-1200.

Konwar, L.J., Warna, J., Arvela, P.M., Mikkola, J.P., 2016. Reaction kinetics with catalyst deactivation in simultaneous esterification and transesterification of acidic oils to biodiesel over mesoporous sulphonated carbon catalyst. Fuel 166, 1-11.

Kozhevnikov, I. V., 1998. Catalysis by heteropolyacids and multicomponent polyoxometalates in liquid-phase-reactions. Chem. Rev. 98, 171-198.

Kresge, C.T., Leonowicz, M.E., Roth, W.J., Vartuli, J.C., Beck, J.S., 1992. Ordered mesoporous molecular sieves synthesized by a liquid-crystal template mechanism. Nature 359, 710-712.

Kulkarni, M. G., Dalai, A. K., Bakshi, N.N., 2006. Waste cooking oil- an economical source for biodiesel: a review. Ind. Eng. Chem. Res. 45, 2901-2913.

Larson, E.D., 2006. A review of life-cycle analysis studies on liquid biofuel systems for the transport sector. Energy Sustain. Dev. 2, 109–126.

Lee, A.F., Bennett, J.A., Manayil, J.C., Wilson, K., 2014. Heterogeneous catalysis for sustainable biodiesel production via esterification and transesterification. Chem. Soc. Rev. 43, 7887-7916.

Lee, J., Cho, W., Shim, W., 2004. Application of MCM-48 and SBA-15 materials for the separation of biochemicals dissolved in aqueous solution. Korean J. Chem. Eng. 21, 246-251.

Lee, H.V., Juan, J.C., Taufiq-Yap, Y.H., 2015. Preparation and application of binary CaO-La_2O_3 catalyst for biodiesel production. Renew. Energy 74, 124-132.

Li, H., Niu, S., Lu, C., Li, J., 2016. Calcium oxide functionalized with strontium as heterogeneous transesterification catalyst for biodiesel production. Fuel 176, 63-71.

Li, Y., He, D., Yuan, Y., Cheng, Z., Zhu, Q., 2002. Influence of acidic and basic properties of ZrO_2 based catalysts on isosynthesis. Fuel 81, 1611-1617.

Limmanee, S., Naree, T., Bunyakiat, K., Ngamcharussrivichai, C., 2013. Mixed oxides of Ca, Mg and Zn as heterogeneous base catalysts for synthesis of palm kernel oil methyl esters. Chem. Eng. J. 225, 616-624.

Liu, X., He, H., Wang, Y., Zhu, S., Piao, X., 2008. Transesterification of soyabean oil to biodiesel using CaO as solid base catalyst. Fuel 87, 216-221.

Liu, L., Wen, Z., Cui, G., 2015. Preparation of Ca-Zr mixed oxide catalysts through a birch-templating route for synthesis of biodiesel *via* transesterification. Fuel 158, 176-182.

Luo, Y., Liu, N., Mei, Z., Wang, H., Han, C., He, S., 2017. Synthesis of mesoporous sulphated zirconia nanoparticles with high surface area and their applies for biodiesel production as effective catalysts. Catal. Today 298, 99, 108

Lv, Pengmei., Wang, J., Xing, S., Li, Z., Fan, P., Wang, Z., 2017. Comparison between heterogeneous acid and base catalysed biodiesel production: catalytic mechanism and performance. 8th International symposium on acid base catalysis. Brazil

Malhotra, R., Ali, A., 2018. Lithium-doped ceria supported SBA-15 as mesoporous solid reusable and heterogeneous catalyst for biodiesel production *via* simultaneous esterification and transesterification of waste cottonseed oil. Renewable Energy 119, 32-44

Mazaheri, H., Masjuki, H.H., Amini, Z., Harrison, M.D., Kusomo, F., Alwi, A., 2018. Rice bran oil based biodiesel production using calcium oxide catalyst derived from C. Brunneus shell. Energy 144, 10-19.

Meloni, D., Perra, D., Monaci, R., Cutrufello, M.G., Rombi, E., Ferino, I., 2016. Transesterification of Jatropha curcas oil and soyabean oil over Al-SBA-15 catalysts. Appl. Catal. B: Environ. 184, 163-173.

Montero, J., Wilson, K., Lee, A., 2010. Cs promoted triglyceride transesterification over MgO nanocatalysts. Top. Catal. 53, 737-745.

Melero, J.A., Bautista, L.F., Iglesias, J., Morales, G., Sánchez-Vázquez, R., 2012. Zr-SBA-15 acid catalyst: optimisation of synthesis and reaction conditions for biodiesel production from low grade oils and fats. Catal. Today 195, 44-53.

Munguia, D.A.C., Rios, E.T., Alejandre, A.G., Rico, J.L., Gonzalez, H., 2017. Reaction study for esterification for oleic acid over M-SBA-15-SO_3H (M=Al, Ti) catalysts. Energy Procedia 142, 590-596.

Munoz, E.M.R., Acuna, R.H., 2010. Sol-gel derived SBA-16 mesoporous material. Int. J. Mol. Sci. 9, 3069-3086.

Nisar, J., Razaq, R., Farooq, M., Iqbal, M., Khan, R.A., Sayed, M., Shah, A., Rahman, I., 2017. Enhanced biodiesel production from jatropha oil using clacined waste animal bones as catalyst. Renewable Energy 101, 111-119

Pan, H., Li, H., Liu, X.F., Zhang, H., Yang, K.L., Huang, S., Yang, S., 2016. Mesoporous polymeric solid acid as efficient catalyst for transesterification of crude Jatropha curcas oil. Fuel Process. Technol. 150, 50-57.

Pan, H., Liu, X.F., Zhang, H., Yang, K.L., Huang, S., Yang, S., 2017. Multi SO_3H functionalised mesoporous polymeric acid catalyst for biodiesel production and fructose-to-biodiesel additive conversion. Renewable Energy 107, 245-252.

Pathak, S., 2015. Acid catalysed transesterification. J. Chem. Pharm. Res. 7, 1780-1786.

Rahmat, N., Zuhairi, A.A., Rahman Mohamed, A., 2010. A review: Mesoporous santa barbara amorphous-15, types, synthesis and its applications towards biorefinery production. Am. J. Appl. Sci. 7, 1579–1586.

Ramirez-Ortiz, J., Martinez, M., Flores, H., 2012. Metakaolinite as a catalyst for biodiesel production from waste cooking oil. Front. Chem. Sci. Eng. 6, 403-409.

Rezayan, A., Taghizadeh, M., 2018. Synthesis of magnetic mesoporous nanocrytalline KOH/ZSM-5-Fe_3O_4 for biodiesel production. Process optimization and kinetic study. Process Safe. Environ. 117, 711-721.

Rodriguez, D.A.T., Ibarra, I.C.R., Ibarra, I.A., Pfeiffer, H., 2016. Biodiesel production from soyabean and jatropha oils using cesium impregnated sodium zirconate as a heterogeneous base catalyst. Renew. Energy 93, 323-331.

Sharma, S., Saxena, V., Baranwal, A., Pandey, L.M., 2018. Engineered nanoporous materials mediated heterogeneous catalysts and yheir implications in biodiesel production. Materials Science for Energy Technologies 1, 11-21.

Shi, G., Yu, F., Wang, Y., Pan, D., Wang, H., Li, R., 2016. A novel one-pot synthesis of tetragonal sulphated zirconia with high activity for biodiesel production for the transesterification of soyabean oil. Renew. Energy 92, 22-29.

Shin, H.Y., An, S.H., Sheikh, R., Park, Y, H., Bae, S.Y., 2012. Transesterification of used vegetable oils with Cs-doped heteropolyacid in supercritical methanol. Fuel 96, 572-

Sing, K.S.W., Everett, D.H., Haul, R.A.W., Moscou, L., Pierotti, R.A., Rouquerol, J., Siemieniewska, T., 1985. Reporting physisorption data for gas solid systems with Special Reference to the Determination of Surface Area and Porosity. Pure & Appl. Chem. 57, 603-619.

Singh, S., Patel, A., 2015. Mono lacunary phosphotungstate anchored to MCM-41 as recyclable catalyst for biodiesel production via transesterification of waste cooking oil. Fuel 159, 720-727.

Soltani, S., Rashid, U., Nehdi, I.A., Muhtaseb, A.A., 2017. Sulfonated mesoporous zinc aluminate catalyst for biodiesel production from high free fatty acid feedstock using microwave heating system. J. Taiwan Inst. Chem. Eng. 70, 219-228.

Songstad, D.D., Lakshamanan, P., Chen, J., Gibbons, W., Hughes, S., Nelson, R., 2009. Historical perspective of biofuels: learning from the past to rediscover the future. In vitro Cell. Div. Biol. 45, 189-192.

Sreeprasanth, P.S., Srivastava, R., Srinivas, D., Ratnasamy, P., 2006. Hydrophobic, solid acid catalysts for production of biofuel and lubricants. Appl. Catal. A: Gen. 2, 148-159.

Su, M., Yang, R., Li, M., 2013. Biodiesel production from hempseed oil using alkaline earth metal oxides supporting copper oxide as bi-functional catalysts for transesterification and selective hydrogenation. Fuel 103, 398-407.

Tantirungrotechai, J., Thepwatee, S., Yoosuk, B., 2013. Biodiesel synthesis over Sr/MgO solid base catalyst. Fuel 106, 279-284.

Teo, S.H., Rashid, U., Yap, Y.H.T., 2014. Biodiesel production from crude Jatropha Curcas oil using calcium based mixed oxide catalysts. Fuel 136, 244-252.

Teo, S.H., Rashid, U., Yap, Y.H.T., 2017. Heterogeneous calcium-based bimetallic oxide catalysed transesterification of E. Guineensis derived triglyceride for biodiesel production. Energy Convers. Manage. 141, 20-27.

Tiemann, M., 2008. Repeated templating. Chem. Mater. 20, 961–971.

Torres, N.S., Ibarra, I.C.R., Pfeiffer, H., 2014. Sodium zirconate as a catalyst in soyabean oil transesterification reaction for biodiesel production. Fuel Process. Technol. 120, 34-39.

Ulfa, M., Jannah, A.M., 2018. Synthesis of mesoporous Fe_2O_3/SBA-15 and its application for Ni (II) ion adsorption. Orient. J. Chem. 1, 420-427.

Vardast, N., Haghighi, M., Dehghani, S., 2018. Sono-diespersion of calcium over Al-MCM-41 used as a nanocatalyst for biodiesel production from sunflower oil: Influence of ultrasonic irradiation, calcium content on catalytic properties and performance. Renew. Energy. 132, 979-988.

Wana, L., Liua, H., Skalab, D., 2014. Biodiesel production from soyabean oil in subcritical methanol using $MnCO_3$/ZnO as catalyst. Appl. Catal. B: Environ. 152-153, 352-359.

Wang, R., 1988. Development of biodiesel fuel. Taiyangneng Xuebao 9, 434-436.

Wang, Y., Wu, Z., 2005. In situ coating metal oxide on SBA-15 in one-pot synthesis. Microporous Mesoporous Mater. 123, 298-305. 84, 127-136.

Wanka, G., Hoffmann, H., Ulbricht, W., 1994. Phase diagrams and aggregation behaviour of poly(oxyethylene)-Poly(oxypropylene)-Poly(oxyethylene)triblock copolymers in aqueous solutions. Macromolecules 27, 4145-4159.

Wong, Y.C., Tan, Y.P., Taufiq-Yap, Y.H., Ramli, I., Tee, H.S., 2015. Biodiesel production *via* transesterification of palm oil by using CaO-CeO_2 mixed oxide catalysts. Fuel 162, 288-293.

Wu, H., Zhang, J., Liu, Y., Zheng, J., Wei,Q., 2014. Biodiesel production from Jatropha oil using mesoporous molecular sieves supporting K_2SiO_3 as catalysts for transesterification. Fuel Process. Technol.19, 114-120.

Xie, W., Fan, M., 2014. Biodiesel production by transesterification using tetraalkylammonium hydroxides immobilised onto SBA-15 as a solid catalyst. Chem. Eng. J. 239, 60-67

Xie, W., Han, Y., Wang, H., 2018. Magnetic Fe_3O_4/MCM-41 composite-supported sodium silicate as heterogeneous catalyst for biodiesel production. Renewable Energy 125, 675-681.

Xie, W., Zhao, L., 2013. Production of biodiesel by transesterification of soyabean oil using calcium supported tin oxide as heterogeneous catalyst. Energy Convers. Manage. 76, 55-62.
Xie, W., Zhao, L., 2014. Heterogeneous CaO-MoO_3-SBA-15 catalysts for biodiesel production from soyabean oil. Energy Convers. Manage. 79, 34-42.

Xie, W., Yang, X., Fan, M., 2015. 2015. Novel solid base catalyst for biodiesel production. Mesoporous SBA-15 immobilised with 1,3-dicyclohexyl-2-octylguanidine. Renewable Energy 80. 230-237.

Yahya, N.Y., Ngadi, N., Jusoh, M., Halim, N.A.A., 2016. Characterisation and parametric study of mesoporous calcium titanate catalyst for transesterification of waste cooking oil into biodiesel. Energy Convers. Manage. 129, 275-283.

Yang, X,X., Wang, Y.T., Yang, Y.T., Luo, J., Zhang, F., Yang, W.J., Bao, G.R., 2018. Catalytic transesterification to biodiesel at room temperature over several solid bases. Eenrgy Convers. Manage.164, 112-121.

Zabeti, M., Daud, W. M. A. W., Aroua, M. K., 2009. Activity of solid catalysts for biodiesel production: a review. Fuel Process. Technol. 90, 770-777.

Zhang, P., Han, Q., Fan, M., Fan, M., Jiang, P., 2014. A novel waste-water scale derived solid base catalyst for biodiesel production. Fuel 124, 66-72.

Zhao, D., Huo, Q., Feng, J., Chmelka, B.F., Stucky, G.D., 1998. Non ionic triblock and star diblock copolymer and oligomeric surfactant synthesis of highly ordered, hydrothermally stable mesoporous silica structures. J. Am. Chem. Soc. 120, 6024-6036.

Zhou, H., Zhu, S., Honma, I., Seki, K., 2004. Methane gas storage in self-ordered mesoporous carbon (CMK-3). Chem. Phys. Lett. 396, 252-255.

Materials and Methods

Abstract

This chapter throws light on chemicals and materials utilised as well as a facet of all the methods, characterisation and analysis techniques recurrently employed for the work in present thesis.

2.1. Chemicals

Waste cottonseed oil (WCO) and waste Soyabean oil (WSO) was obtained from local restaurants in Patiala. Prior to the reaction, WCO and WSO were filtered using ordinary filter paper to remove the suspended particulates from the oil. Virgin cottonseed oil (VCO) used for the transesterification reactions was procured from the local shops sited in Patiala. Jatropha oil (JO) was procured from Medors Biotech Pvt. Ltd. New Delhi (India). Methanol (99.8%) was purchased from Merck (India) Ltd. Tetraethyl orthosilicate (TEOS) and Pluronic 123 (EO_{20}-PO_{70}-EO_{20}), surfactant copolymer were obtained from Sigma–Aldrich (USA). Cerium (III) nitrate, Lithium carbonate (Li_2CO_3), Sodium carbonate (Na_2CO_3), Zinc oxide (ZnO), Potassium nitrate (KNO_3), Zirconium dioxide (ZrO_2) were purchased from Loba Chemie (India), were used without further purification. Oleic acid (99.9%) employed in esterification reaction, hexane, ethyl acetate, acetic acid (AR grade) and silica gel (TLC grade) used in the present study were purchased from Loba Chemie (India), were used without further purification. Trichloroacetic acid, *n*–butylamine and toluene (HPLC grade) employed for Hammett indicator study were purchased from Spectrochem Limited (India). The basic and acidic strengths of the catalysts were found out and estimated by the means of Hammett indicators study using following indicators: methyl orange ($H_0 \leq 3.1$), methyl red ($H_0 \leq 4.8$), neutral red ($H_0 \leq 6.8$), bromthymol blue ($H_0 \leq 7.2$), anthraquinone ($H_0 \leq 8.2$), phenolphthalein ($H_0 \leq 9.3$), Nile blue ($H_0 \leq 10.1$), tropaeolin ($H_0 \leq 11.1$), 2, 4-dinitroaniline ($H_0 \leq 15.0$), and 4- nitroaniline ($H_0 \leq 18.4$) purchased from Qualigens Fine Chemicals, India.

2.2. Thin layer chromatography (TLC)

The advancement of the transesterification reaction was observed by thin layer chromatography (TLC). The sample was withdrawn out of reaction mixture using a glass capillary after apposite intervals of time and mixture thus obtained was diluted in hexane, then subjected to TLC analysis, by employing silica gel over a glass plate as stationary and hexane/ethylacetate (95:5 v/v) as mobile phase. The development of TLC plate was carried out in iodine chamber. The BD spot was differentiated from the triglyceride spot on the basis of retention factor (R_f). Biodiesel shows superior mobility as compared to vegetable oil (VO) with the chosen solvent system.

2.3. Chemical analysis of vegetable oils

The free fatty acid content (FFA) and saponification values of waste cottonseed oil (WCO), virgin cottonseed oil (VCO), waste soyabean oil (WSO), jatropha oil (JO) were experimentally found out by following the method reported in literature (Aransiola et al., 2012) and obtained values have been given in Table 2.1.

Table 2.1. Chemical analysis of vegetable oils.

Feedstock	FFA content (wt%)	Saponification value (mg of KOH/g of sample
WCO	4.8	194.5
VCO	0.4	189.3
WSO	3.9	178
JO	9.7	188.5

2.4. Hammett indicator titration

The acidic strengths of catalysts were found out using the Hammett indicator- amine titration method (Xie et al., 2006). 0.05 g of catalyst was suspended in 5 mL of toluene. Next, 5 drops of methanolic solution of appropriate Hammett indicator (0.02M) were added. The resulting suspension was titrated against 0.01 M n-butyl amine till the observation of appropriate colour change. The amount of n-butyl amine consumed for titration was expressed as acidity of solid catalyst in terms of mmol/g of solid catalyst.

Further, the basic strength of catalyst was determined by using Hammett indicator-carboxylic acid titration method (Xie et al., 2006). 0.05 g of catalyst was suspended in 5 mL of toluene. Next, 5 drops of methanolic solution of appropriate Hammett indicator (0.02M) was added. The resulting suspension was titrated against 0.01 M trichloroacetic acid till the observation of appropriate colour change. The amount of trichloroacetic acid consumed for titration was expressed as basicity of solid catalyst in terms of mmol/g of solid catalyst.

2.5. Turnover frequency determination

The turnover frequency (TOF) was calculated from equation 2.1 using the literature reported method (Sani et al., 2014).

$$TOF = \{mol_{FAMEs}/f_m \times w_{cat} \times t\} \quad (2.1)$$

where mol_{FAMEs} is the number of moles of FAMEs ; w_{cat} is the amount of catalyst; t is the reaction time and f_m is active (acidic or basic) sites of catalyst (in mmol g^{-1}) calculated by Hammett indicator benzene carboxylic method of titration.

2.6. Reaction kinetics and determination of thermodynamic parameters

Theoretically, to accomplish entire transesterification, one mole of triglyceride needs 3 moles of alcohol. Hence, the overall order of transesterification reaction must be 4. However, with an aim to coerce the equilibrium towards the right side (product side), the reaction is executed in the company of superfluous amount of alcohol. Because, surfeit of alcohol is employed in the reaction, the transesterification reaction could be supposed to trail (pseudo) 1st order kinetic equation (Yacob et al., 2015).

$$-\ln (1-X_{me}) = kt \quad (2.2)$$

where, X_{me} is the FAMEs yield at time 't'.

The conversion values obtained at different time intervals at were put in the equation (2.2) to obtain the values of rate constants. To determine the energy of activation and (E_a), Arrhenius equation was employed which is given in equation 2.3.

$$\ln k = -Ea/RT + \ln A \quad (2.3)$$

where, R is the universal gas constant (8.3 J K^{-1} mol^{-1}), and T is the temperature of reaction in Kelvin, Ea is the activation energy (kJ mol^{-1}), A is pre–exponential factor (min^{-1}).

The activation energy of the reaction was computed from the slope of Arrhenius curve.

Eyring–Polanyi equation (2.4) was put in use to compute the enthalpy ($\Delta H^{\ddagger}$) and entropy of activation ($\Delta S^{\ddagger}$) for the reaction.

$$\ln(k/T) = -\Delta H^{\ddagger}/RT + \ln(k_B/h) + \Delta S^{\ddagger}/R \quad (2.4)$$

where k_B and h are the Boltzmann (1.38×10^{-23} J K^{-1}) and Planck (6.63×10^{-34} J s) constants, respectively. $\Delta H^{\ddagger}$ and $\Delta S^{\ddagger}$ were estimated from slope $\{-\Delta H^{\ddagger}/R\}$ and intercept $\{\ln (k_B/h) + \Delta S^{\ddagger}/R\}$ of this plot, respectively.

$\Delta H^{\ddagger}$ and $\Delta S^{\ddagger}$ were calculated from the slope $\{-\Delta H^{\ddagger}/R\}$ and intercept $\{\ln(k_B/h)+\Delta S^{\ddagger}/R\}$ of Eyring-Polanyi plot, respectively.

Further, the calculations were extended to calculate free energy of reaction. The Gibb's free energy ($\Delta G^{\ddagger}$) was determined by substituting the values of $\Delta H^{\ddagger}$ and $\Delta S^{\ddagger}$ in equation (2.5).

$$\Delta G^{\ddagger} = \Delta H^{\ddagger} - T\Delta S^{\ddagger} \quad (2.5)$$

2.7. Instruments

2.7.1. Powder X-Ray Diffraction (XRD)

Powder X-Ray diffraction (XRD) analysis was carried for structural analysis and phase identification of prepared catalysts on Panalytical X'pert Pro diffractometer, (Netherlands), operating at a voltage of 40 kV using monochromatic Cu Kα radiation (0.154 nm) in 2θ range of 0.5-5^{o} and 5–60°. The samples were scanned at scanning speed of 2°/minute.

2.7.2. Scanning-Electron Microscopy-Energy Dispersive X-Ray Analysis (SEM-EDS)

SEM-EDS analysis was executed to carry out the morphological study of the prepared catalysts on JEOL JSM 6510 LV equipment, (Japan). To perform the analysis, the sample was first ultrasonicated in ethanol for 2h. Next, over a sample holder, a drop of suspension was mounted using a carbon tape. The test sample was then encrusted with gold and visually analysed with the instrument to study the morphology of the particles. EDS was performed for qualitative estimation of elements in the samples and elemental mapping images were also recorded.

2.7.3. Field Emission Scanning Electron Microscopy (FE-SEM)

Detailed morphological attributes of prepared catalysts were examined by Field Emission Scanning Electron Microscopy on Jeol JSM 6100 equipment, (Japan), with image analyser. To prepare the sample, miniature quantity of powdered sample was ultrasonicated in ethanol and little amount of sample was then mounted over sample holder with the aid of carbon tape.

2.7.4. High Resolution Transmission Electron Microscopy (HR-TEM)

The High Resolution Transmission Electron Microscopy (HR-TEM) was carried out on FEI Tecnai G2 F-20 equipment, (U.S.A.). Before analysis, the test sample was dispersed in solvent ethanol and ultrasonicated for 30 min. The suspension was placed onto a porous carbon film on the copper grid. The samples were air dried before analysis and images were recorded with instrument.

2.7.5. X-ray Photoelectron Spectroscopy (XPS)

In order to determine the oxidation state and binding energy of the elements present in the prepared catalyst, X-ray photoelectron spectroscopy (XPS) study was performed on KRATOS-AXIS DLD equipment, (U.K.) spectrometer with monochromatic Al Kα radiation at 1486.60 eV operating at 10 kV. The samples were initially degassed for 4 h duration inside XPS chamber for curtailing air contamination over the surface of sample. To trounce the charging crisis, charge neutralizer of 2 eV was applied and binding energies of all the elements were calibrated using C 1s binding energy (284.6 eV) of standard hydrocarbons.

2.7.6. Brunauer–Emmett–Teller Surface Area Analysis

Surface area of samples was determined by using BET (Brunauer–Emmett–Teller) Surface Area Analyser using Microtec Belsorp Miniell equipment (Japan) with multipoint technique. Before the analysis, 0.1 g of sample was pre- treated at 150 °C under nitrogen atmosphere for 3 h in order to confiscate all the physisorbed moisture from the catalyst surface. The surface area of the samples was calculated using BET (Brunauer–Emmett–Teller) method from adsorption–desorption isotherms.

2.7.7. Fourier Transform- Infra Red Spectroscopy

Fourier Transform Infra- Red (FT-IR) spectrum of the samples was analysed on Agilent Cary-660, (U.S.A.) spectrophotometer in the range 400-4000 cm^{-1}. KBr pellet was employed to obtain the spectra of prepared samples at room temperature. Lewis acidity characteristics of the prepared catalyst were studied by pyridine adsorption method. To carry out the study, pyridine was adsorbed on the surface of the catalyst at room temperature. The sample was dried for 2 h at 50 °C and subsequently heated at 300 °C for 10 min for the desorption of pyridine. Then, FTIR diffuse reflectance spectra of the catalyst was recorded.

2.7.8. Fourier Transform- Nuclear Magnetic Resonance (FT-NMR)

In order to characterise the fatty acid methyl esters (FAMEs) produced during transesterification reactions, H^1 NMR spectra was recorded on Bruker Avance–II (400 MHz), (U.S.A.) spectrophotometer using $CDCl_3$ as solvent.

Chemical shifts were expressed as parts per million (ppm) employing tetramethylsilane (TMS) as an internal standard. The FAMEs yield was quantified by putting the appropriate values in equation as reported in literature (Knothe, 2000).

$$\text{FAMEs yield (\%)} = \{2I_{(methoxy)}/3I_{(methylene)}\} \times 100 \quad (2.6)$$

where, $I_{(methoxy)}$ and $I_{(methylene)}$ are the integration values of methoxy (3.6 ppm) and methylene (2.3 ppm) protons, respectively in proton NMR spectrum of fatty acid methyl ester

2.7.9. Microwave Plasma-Atomic Emission Spectroscopy Technique (MP-AES)

The metal ion concentration of Si, Ce, Li, Zn, Na metals in FAMEs and glycerol layers to test the oozing out of metal ions was estimated using microwave plasma-atomic emission spectroscopy technique (MP-AES) on Model 4100, Agilent Technologies, U.S.A. equipment and ESICO microprocessor model 1382 E Flame Photometer. For the analysis, 0.5 g of sample was digested in 5 mL of HNO_3 (16 M) in order to remove all the organic matter. The solution was then filtered and the volume was made upto 50 mL in a volumetric flask with deionised water.

2.7.10. Flame Photometer

The metal ion concentration of Na and K metals in FAMEs and glycerol layers in chapters 5 and 6 was determined using ESICO microprocessor model 1382 E Flame Photometer, India. For the analysis, 0.5 g of recovered reaction sample was digested in 5 mL of HNO_3 (16 M) in order to remove all the organic matter. The solution was then filtered and the volume was made upto 50 mL in a volumetric flask with water.

2.7.11. Experimental set up for transesterification

All transesterification reactions were carried out in a 100 mL, two-necked round bottom flask which was equipped with oil bath, water-cooled reflux condenser and a magnetic agitator and a thermometer. In a typical reaction of transesterification, the flask was charged with 10 g of vegetable oil and assorted with desired molar concentration of methanol as well as catalyst and stirred at a specific temperature for fixed reaction duration. The reaction mixture so obtained was left in separatory funnel for 10 h to part the two layers, upper biodiesel layer and the lower glycerol layer. The FAMEs thus produced were quantified using ^{1}H-NMR analysis.

Water cooled condenser

Clamp stand for holding

Round bottom flask with reaction mixture

Hot plate and magnetic stirrer for heating

(a)

(b)

Fig. 2.1 (a) Experimental set up for transesterification and (b) Picture of final product

References

Aransiola, E.F., Daramola, M.O., Ojumu, T.V., Aresmu, M.O., Solomon, B.O., 2012. Nigerian Jatropha curcas oil seeds : Prospects for biodiesel production in Nigeria. Int. J. Renewable Energy Res. 2,317-325.

Knothe, G., 2000. Monitoring a progressing transesterification reaction by fiber- optic near infrared spectroscopy with correlation to ^{1H} nuclear magnetic resonance spectroscopy. J. Am. Oil Chem. Soc. 7, 489-493.

Sani, Y.M., Daud, W.M.A.W., Aziz, A.R.A., 2014. Activity of solid acid catalysts for biodiesel production. Appl. Catal. A: Gen. 470, 140-161.

Xie, W., Peng, H., Chen, L., 2006. Calcined Mg-Al hydrotalcites as solid base catalysts for methanolysis of soyabean oil. J. Mol. Catal. A: Chem. 246, 24-32.

Yacob, A.R., Bello, A.M., Ruskam, A., Kabo, K.S., 2015. Catalytic performance by kinetics evaluation of novel KOH-modified ZnO in heterogeneous transesterification of rice bran oil to biodiesel. 6th International Conference on Environmental Science and Technology 84, 101-107

Lithium - Ceria Supported SBA-15 as Mesoporous Reusable and Heterogeneous Catalyst for Biodiesel Production *via* Concurrent Esterification and Transesterification of Waste Cottonseed Oil

Abstract

Li^{+} and Ce^{4+} loaded SBA-15 has been synthesized under normal atmospheric condition (without using hydrothermal treatment) and following wet impregnation route. The catalyst has been characterised by using different techniques viz., BET method for surface area measurements, FE-SEM for surface morphology study, XPS for the determination of catalyst composition and element oxidation state. The catalyst was found to possess both acidic and basic sites and hence, successfully employed for the simultaneous esterification and transesterification of waste cottonseed oil. Under optimized reaction conditions of catalyst concentration of 10 wt%, methanol to oil molar ratio of 40:1 at 65 °C, the catalyst was able to give > 98 % fatty acid methyl ester yield within 4 h of reaction time. The catalyst was recovered and reused during 5 successive runs without any significant loss of activity. The activation energy (E_a) for the reaction was found to be 57.7 kJ mol^{-1}, while $\Delta H^{\ddagger}$, $\Delta G^{\ddagger}$ and $\Delta S^{\ddagger}$ were found to be 59.4 kJ mol^{-1}, + 95.9 kJ $mol^{-1}$and - 0.108 kJ mol^{-1}, respectively. On the basis of thermodynamic parameters, the reaction is expected to be endothermic, non spontaneous and following an associative pathway.

Keywords: Heterogeneous catalysts, mesoporous, basicity, transesterification, reusability.

3.1. Introduction

Homogeneous alkali catalysts are more effective in comparison to the acid catalysts for vegetable oil transesterification reaction, however require high quality feedstock which does not contain free fatty acids (FFA) and any moisture content. A major disadvantage of homogeneous catalysts is the formation of single phase of catalyst and final product, thus making the product purification step more cumbersome. Moreover, due to the formation of solitary phase of product and catalyst, the product purification stage to separate out the catalyst becomes even more burdensome. Another limitation of homogeneous alkali catalysts is their deactivation by FFA (> 0.5 wt%), and/or moisture (> 0.3 wt%) contents *via* saponification (Sharma et al., 2018).

In order to employ the high FFA holding feedstock for BD production using basic catalysts, FFA is esterified in a beginning step by using acid catalyst pursued by the transesterification. However, if preliminary step is missed, this reaction gives undesirable products owing to formation and the catalyst gets deactivated from hastening the transesterification further. This also hampers the purification process of BD, together with glycerol separation and water washing. The key limitations of the 2-step process involve the application of acerbic acids which demand (i) acid resistance and intricately devised reactors, (ii) obligatory acid neutralization trailed by product washing (iii) discarding of effluents, generated during the washing step (Gorgi and Ghanei, 2014).

A solid catalyst developed in this context which can concurrently carry out esterification and transesterification can be very advantageous and beneficial from both environmental and industrial perspective. Solid catalysts are easily separated from the reaction mixture by simple physical processes with no need of neutralisation, thereby, providing a process which is more benign environmentally (Endalew et al., 2011). Heterogeneous catalysts reduce the production cost and harmful effluent generation thus making the BD production more eco-friendly. Reusability is also one of the major advantages of solid catalyst hence, making the BD production a cost effective process at industrial level.

A variety of mesoporous based solid catalysts have been reported in literature for biodiesel production. Transesterification using CaO- MoO_3 based on mesoporous silica has been reported to yield 83.2% FAMEs yield from methanolysis of soybean oil at 65 °C, employing 6 wt% of catalyst amount, 50:1 MeOH/oil molar ratio and 40 wt% loading of CaO- MoO_3, in the reaction time of 50 h (Xie and Zhao, 2014). In another reaction, jatropha oil was converted into its corresponding FAMEs by employing acidic heterogeneous catalyst Mica-

Ph-SO_3H catalyst which was prepared by modifying the silane mica clay. Under the optimized reaction conditions, the catalyst was found to yield the complete conversion of feedstock into FAMEs within 150 min of reaction time at a stirring speed of 800 rpm (Negm et al., 2017).

In literature, lithium/CaO and ceria/silica based catalysts, individually, have been employed for the preparation of biodiesel (Kaur and Ali, 2014a; Bhagiyalakshmi et al., 2013). Latest studies on solid catalysts have shown that the performance of bimetallic catalysts is more than that of uni-metal catalysts due to greater thermal stability and activity of the former (Park et al., 2007). In order to explore the combined effect of Li^{+1} and Ce^{+4} in a single catalyst, in present chapter, both the metal ions were immobilized over mesoporous silica surface. In the present catalyst, owing to the presence of acidic as well as basic sites, it has been successfully employed as reusable heterogeneous catalyst for the simultaneous transesterification and esterification of high free fatty acid (FFA) containing waste cotton seed oil (WCO) with FFA and moisture content of 4.8 wt% and 0.27% wt% respectively. Cottonseed oil is inexpensive and widely available in India as well as less fit for edible purposes and hence was selected as feedstock.

3.2. Experimental section

3.2.1 Synthesis of SBA-15 support

SBA-15 support was synthesised by employing Pluronic 123 as the structure directing agent and tetraethyl orthosilicate (TEOS) as the source of silica. In a typical synthesis, 8 g of Pluronic 123 was stirred with 80 ml of distilled water for 1h. To this, 360 ml of 2 M hydrochloric acid (HCl) was added, stirred for another 2 h followed by the addition of 18 ml of TEOS at room temperature (40 ºC). Resulting mixture was stirred for another 24 h, and aged at 80 ºC for 48 h under static condition. The solid thus formed was recovered through filtration, washed with ethanol, dried and finally calcined at 600 ºC for 5 h.

3.2.2 Catalyst Preparation

In synthesis of Li^+ and Ce^{+4} impregnated SBA-15, wet impregnation method was employed. In a typical procedure, 5 g of SBA-15 was suspended in 40 ml of distilled water and to this 10 ml solution of cerium (III) nitrate of desired concentration was added to obtain 5-25 wt% of Ce loaded SBA-15. In the next step, 10 mL Li_2CO_3 solution containing 0.80 g of Lithium carbonate was added to achieve 3 wt% of Li with respect to SBA-15. The resulted slurry was

stirred for 6 h at room temperature (35-38 ºC), then dried at 110 ºC for 24 h and calcined in muffle furnace at 550 ºC for 5 h. The catalysts so prepared were designated as *x*-CeO_2/Li_2O/SBA-15, where *x* is the wt% of Ce on SBA-15.

3.2.3 Transesterification and esterification of triglycerides

All the transesterification reactions were carried out in a 100 ml two necked round bottom flask equipped with a water cooled condenser, oil bath, magnetic stirrer and a thermometer. In a usual reaction, reaction flask was charged with 10 g of waste cottonseed oil (WCO), desired amounts of methanol and catalyst, and resulted mixture was agitated at desired temperature.

Esterification reaction was also carried out in the similar reaction set up but employing oleic acid (OA) as a substrate in place of WCO. In order to monitor the progress of reaction, the samples were withdrawn from reaction mixture after fixed time intervals, centrifuged to remove the solid catalyst and liquid phase was subjected to proton NMR analysis to quantify the products formed.

Methyl esters of WCO: **^{1}H–NMR** ($CDCl_3$, 400 MHz, δ ppm): 5.34 (m, −CH=CH−), 3.6 (s, $-OCH_3$), 2.77 (m, $-CH=CH-CH_2-CH=CH-$), 2.3 (m, $-CH_2-CO-$), 2.03 [m, $-CH_2-(CH_2)n-$], 1.6−1.25 [m, $-(CH_2)n-$], 0.88 (m, $-CH_2-CH_3$).

3.3. Results and discussion

3.3.1. Catalyst characterisation

3.1.1.1. Powder XRD study

Small angle powder XRD patterns (Fig. 3.1a) of SBA-15, shows the characteristic peak at 2θ ~ 0.80°, which could be indexed to (100) plane, characteristic of *p*6*mm* hexagonal symmetry and 2D hexagonal structure of SBA-15. Small angle XRD patterns of CeO_2/Li_2O/SBA-15 show the similar type of diffraction patterns. This shows the retention of long range mesoscopic order of SBA-15 even after impregnation of ceria and lithium. However, upon lithium and ceria loading, reflection corresponding to (100) plane showed a tendency to shift to slightly higher angle from 0.80° to 0.82°. Moreover, there is also a slight shift in angle corresponding to (110) reflection as a shift in the peak can be observed with the increase in loading of ceria. This may be attributed to slight change in the wall properties of mesoporous silica due to partial blocking or filling of mesopores by ceria particles (Li and Rudolph, 2008).

The wide angle powder XRD patterns of CeO_2/Li_2O/SBA-15 are shown in the Fig. 3.1b. The pattern shows the characteristic peaks of CeO_2 at 2θ values of 28.6° (111) , 33.2° (200), 47.6° (220) and 56.6° (311), which indicates the formation of fluorite-type cubic structure of ceria (space group: *Fm3m*) (JCPDS file no. 34-0394). No peak corresponding to oxide of Li was observed in the spectra indicating the homogeneous distribution of Li into the lattice of CeO_2/SBA-15 material.

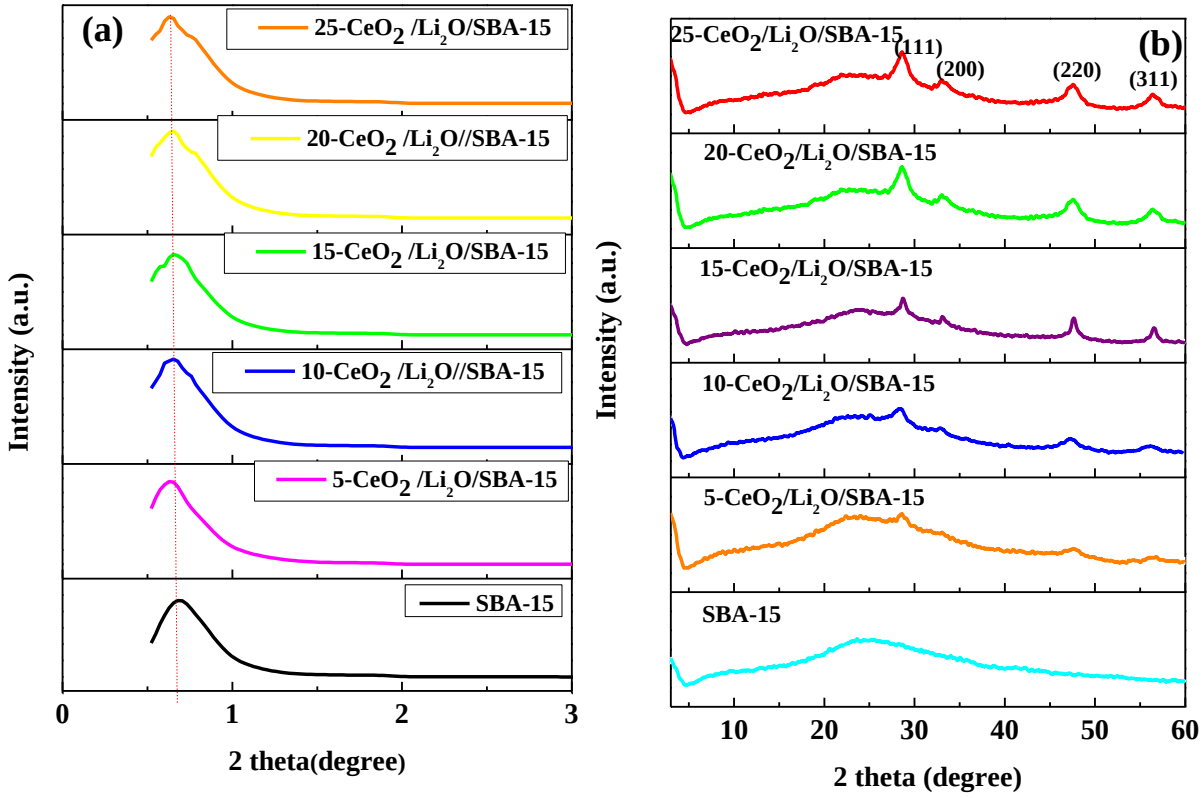

Fig. 3.1. a) Low angle and b) wide angle XRD patterns of SBA-15, CeO_2/Li_2O/SBA-15 catalysts.

3.3.1.2. Porosity and Surface area Study

In order to study the BET surface area of the prepared materials, N_2-adsorption/desorption isotherms of CeO_2/Li_2O/SBA-15 were measured. Table 3.1 shows the textural properties of prepared catalysts. All the isotherms are type IV with H_1 hysteresis loops, (Fig. 3.2a) which are characteristics of the mesoporous materials (Luo et al., 2008). A sharp nature of adsorption as well as desorption branches (at a relative pressure of 0.4- 0.6) is due to a narrow pore size distribution in bare SBA as well as CeO_2 and Li_2O impregnated SBA-15

(Vunain et al., 2013). The sharpness of the inflection curve is indicative of uniform pore size distribution.

Table 3.1. Surface area, average pore size and average pore volume of prepared samples.

Sample name	Surface area ($m^2 g^{-1}$)	Average pore volume ($cm^3 g^{-1}$)	Average pore diameter (nm)
SBA-15	148	0.67	6.66
5-CeO_2/Li_2O/SBA-15	121.65	0.62	5.24
20-CeO_2/Li_2O/SBA-15	112.46	0.60	5.12
25-CeO_2/Li_2O/SBA-15	103.65	0.59	4.58

As shown in Fig. 3.2b, Barrett-Joyner-Halenda (BJH) method was employed to calculate the pore size from Nitrogen-sorption isotherms, which indicates the gradual decrease in average pore size with the increase in ceria concentration in SBA material. Table 1 clearly depicts the decline in surface area, average pore size and average pore volume with the increase in ceria contents in SBA. The decrease in the average pore size and average pore volume of the prepared samples can be attributed to the dispersion of ceria into the pores of SBA-15 (Sareen et al., 2015).

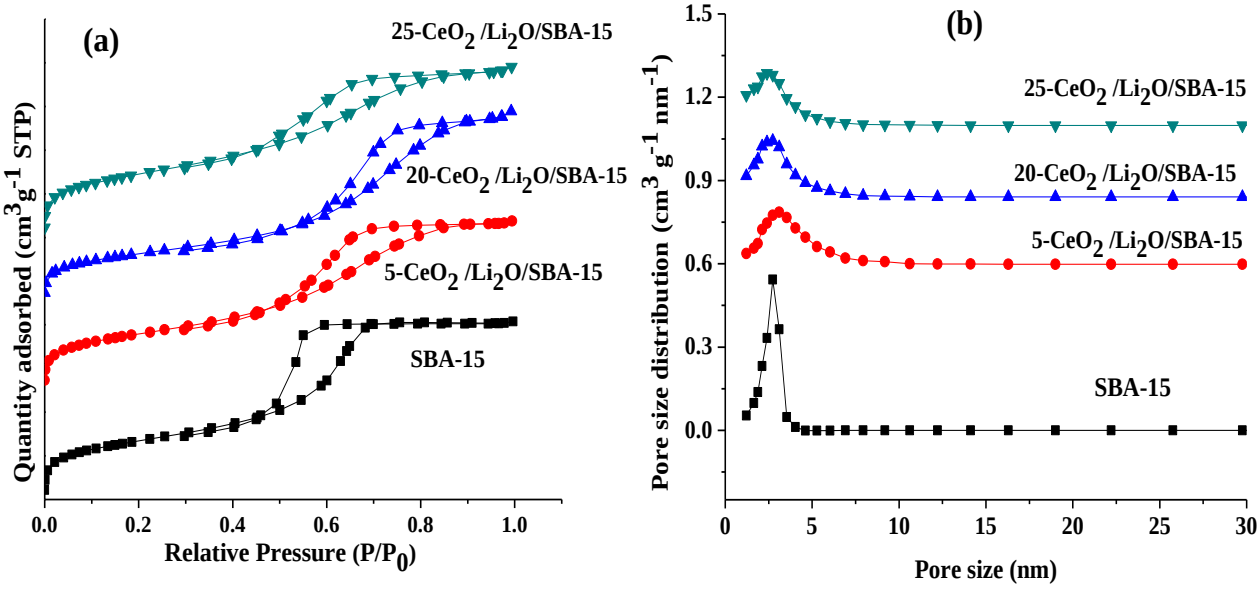

Fig. 3.2. a) N_2 adsorption–desorption isotherms and b) pore size distribution of SBA-15 and CeO_2/Li_2O /SBA-15 catalysts.

3.3.1.3. Pyridine adsorption DRIFT spectra

In order to show the presence and type of acidic site over the catalyst surface, FTIR spectra of pyridine, adsorbed on SBA-15 and CeO_2/Li_2O/SBA-15 have been compared in Fig 3.3. The absence of any pyridine band in the FTIR spectra of SBA-15, supported the lack of acidic sites over bare mesoporous silica. However, in the FTIR spectra of ceria supported SBA-15, a band at 1440 cm^{-1} was observed to support the presence of Lewis acidic sites in the prepared catalyst (Rajagopal et al., 1995). This band could be ascribed to the co-ordinately bonded pyridine with the Lewis acid sites of the catalyst (Parry, 1963). Absence of any band at 1540 cm^{-1}, ruled out the presence of any Bronsted acid site in the prepared catalyst.

Lewis acid sites have been reported to catalyze the esterification of fatty acids (Park et al., 2010) and hence, the catalyst could catalyze the esterification as well as transesterification activity owing to the presence of Lewis acidic as well basic sites.

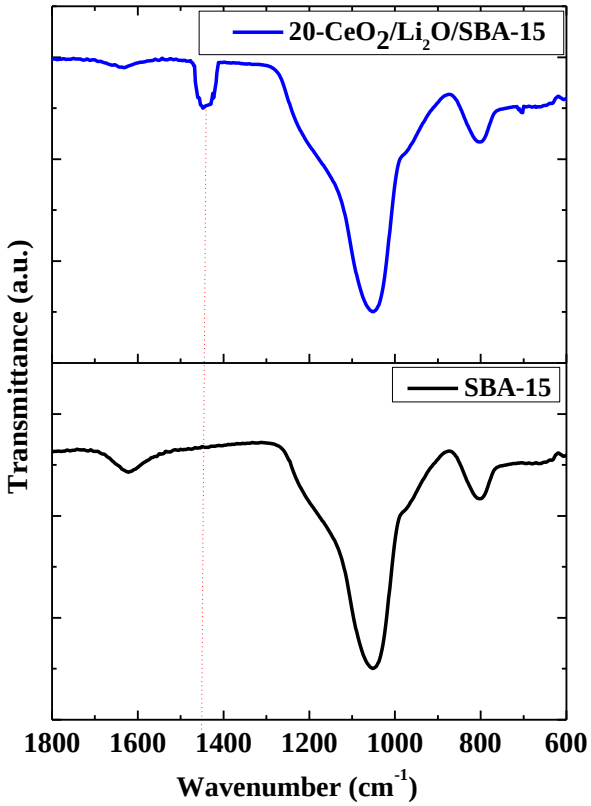

Fig. 3.3. Pyridine adsorbed FTIR spectra of bare SBA-15 and 20- CeO_2/Li_2O/SBA-15 catalyst.

3.3.1.4. FE-SEM Analysis

The samples of SBA-15 and 20-CeO_2/Li_2O/SBA-15 were characterised by FE-SEM to study the surface morphology of the catalyst. As could be seen from the FE-SEM images of SBA-15 and 20- CeO_2/Li_2O/SBA-15 (Fig. 3.4a), smooth and spherical nature of synthesised SBA-15 particles in agglomerated form was observed. A clear change in particle shape and morphology was observed upon lithium and ceria loading over SBA-15 material (Fig. 3.4b) and agglomerates of 20- CeO_2/Li_2O/SBA-15 in asymmetrical shape were observed.

The EDS spectra of SBA-15 and 20- CeO_2/Li_2O/SBA-15 are depicted in Fig. 3.4c and 3.4d respectively. It is clear from the results that only Si and O are present in SBA-15 support and no other impurity or elements were detected which confirmed that SBA-15 support was composed of pure silica. The EDS spectra of the active catalyst shows the presence of ~ 22 wt% Ce which is close to the theoretical ceria loading of 20 wt%. Lithium could not be detected by EDS analysis due to atomic mass detection limit of EDS instrument. The corresponding elemental mapping of the 20- CeO_2/Li_2O/SBA-15 catalyst is shown in Fig. 3.5. The mapping also confirms the loading of Ce in the siliceous matrix of SBA-15.

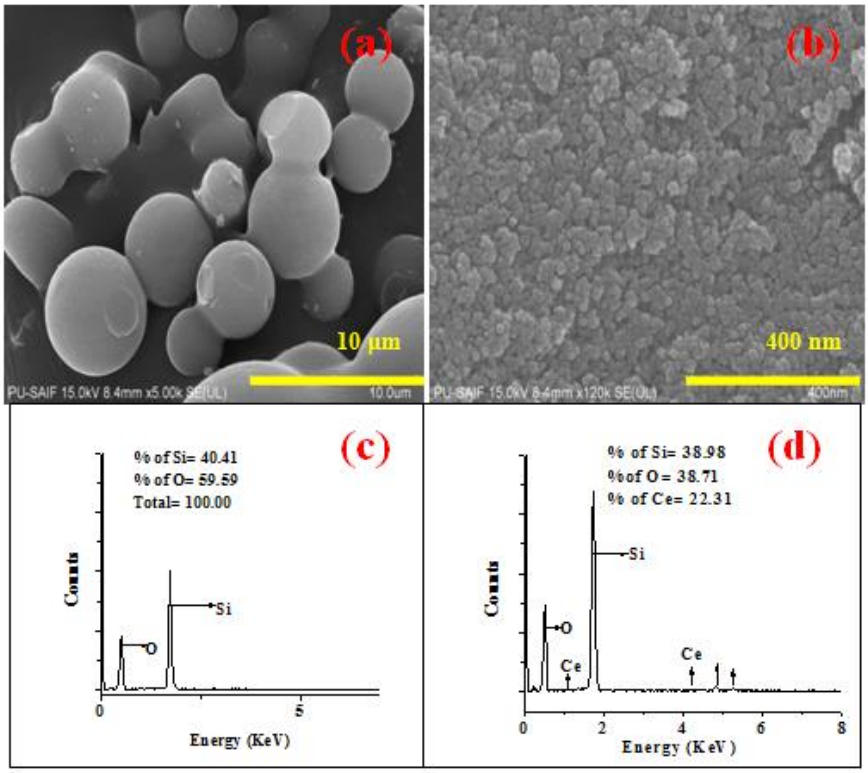

Fig. 3.4. FE-SEM images of (a) bare SBA-15 support (b) 20-CeO_2/Li_2O/SBA-15 (c) EDS spectra of SBA-15 (d) EDS spectra of 20-CeO_2/Li_2O/SBA-15.

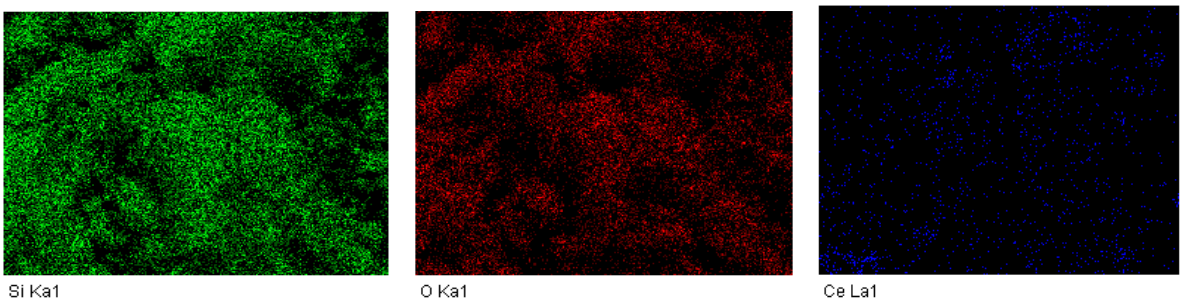

Fig. 3.5. Elemental mapping of 20-CeO_2/Li_2O/SBA-15 catalyst.

3.3.1.5. HRTEM analysis

HRTEM image of SBA-15 (Fig. 3.6a) showed the well defined nano-channels arranged in highly ordered fashion. The observed structure was found similar to that of typical mesoporous SBA-15 as reported in literature (Wu et al., 2014) which further confirmed the formation of mesoporous SBA material. The lattice fringes arranged in the parallel fashion could be seen to support the presence of monoloayers in a well packed arrangement.

The mesoporous structure maintained even after the lithium and ceria impregnation and particles showed crystalline structures with a interplanar spacing of 0.32 nm (Fig. 3.6b), which was close to the reported value of 0.31 nm (Hailstone et al., 2009) corresponding to (111) plane of ceria in fluorite structure. The dark spots against the lighter background in the HRTEM images clearly show the impregnation and presence of ceria crystallites on the mesoporous matrix (Fig. 3.6c). The selected area electron diffraction (SAED) pattern (Fig. 3.6d), revealed polycrystalline nature of catalyst owing to the presence of multiple rings made up of small bright spots. The fluorite structure of ceria is also supported by aforementioned and XRD studies.

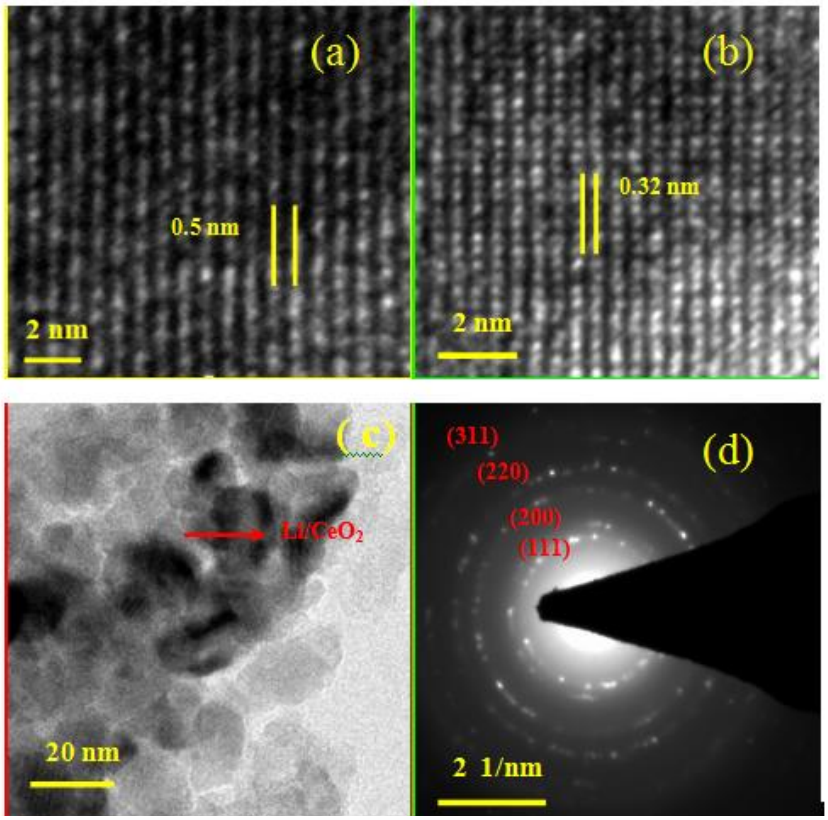

Fig. 3.6. HR-TEM images of (a) hexagonal arrays of SBA-15, (b) lattice fringes corresponding to (111) plane and fluorite structure of ceria, (c) 20- CeO_2/Li_2O/SBA-15 dark spots signify the loading of Li and CeO_2 on SBA-15, and (d) SAED pattern of 20-CeO_2/Li_2O/SBA-15

3.3.1.6. XPS Study

In order to determine the electronic state of the elements present in 20-CeO_2/Li_2O/SBA-15, XPS study was employed. As shown in Fig. 3.7, the peak observed at 103.1 eV supports the presence of silicon corresponding to Si 2p state (Pal et al., 2014). The peak observed at 103.6 eV is due to Si-O bond at the surface, whereas the peak observed at be 104.4 eV due to the $SiOH_2^+$ species over the catalysts (Wagner et al., 1982; Negrila et al., 2008). The peak at 917.2 eV refers to Ce $3d_{3/2}$ state which is the characteristic for Ce in +4 oxidation state present in CeO_2 (Cho et al., 2013). The peak corresponding to the O 1s, could be deconvoluted into three peaks and out of these, the strong peak at 532.8 can be assigned to the oxygen of non-crystalline of SBA-15. The two weaker peaks at 529.5 eV and 531 eV can be attributed to the lattice oxygen of CeO_2 and weakly bonded oxygen of water molecule,

respectively (Reddy et al., 2008). Since, the presence of lithium could not be detected in EDS analysis, the prepared catalyst was analyzed by XPS study to confirm presence of Li in the catalyst. The peak observed at 56.4 eV can be attributed to Li^{1+} 1s state to support the presence of Li in the prepared catalyst (Aurbach et al., 1996).

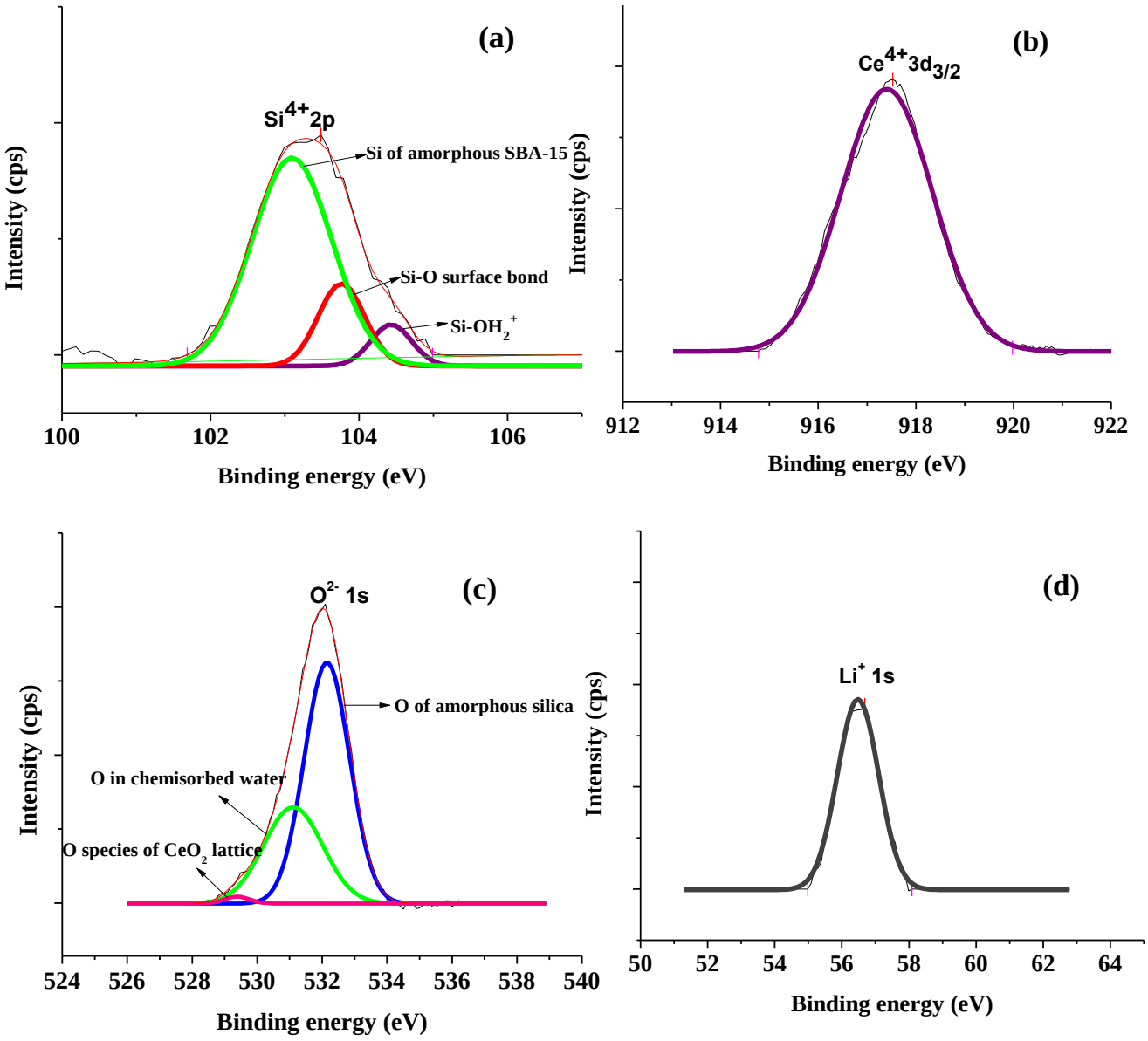

Fig. 3.7. XPS spectra of (a) Si (b) Ce (c) O and (d) Li present in 20-CeO_2/Li_2O/SBA-15 catalyst.

3.3.1.7. Hammett indicator study

The Hammett indicator test was employed to quantify the acidic and basic sites present over the catalyst surface. In order to quantify the acidic and basic sites, the catalyst was titrated

with *n*-butylamine and trichloroacetic acid, respectively. It can be clearly seen from Table 3.2, bare SBA-15 was found to show weak acidic as well as basic sites which were not able to catalyze the transesterification of WCO. On increasing the CeO_2 loading over SBA support, the acidic as well as basic sites were found to increase which resulted in the higher catalytic efficiency (TOF).

Table 3.2. Comparison of acidic and basic strengths, and TOFs for the CeO_2/Li_2O/SBA-15 catalyzed transesterification.

Catalyst	Acidity				Basicity				Total acidity (mmol g^{-1})	Total basicity (mmol g^{-1})	TOF ($\times 10^{-3}$ h^{-1})
	($H_0 \leq +3.1$)	($H_0 \leq +4.8$)	($H_0 \leq +6.8$)	($H_0 \leq +7.2$)	($H_0 \leq +4.8$)	($H_0 \leq +6.8$)	($H_0 \leq +7.2$)	($H_0 \leq +8.2$)			
SBA-15	NCC	NCC	0.15	NCC	0.25	0.24	NCC	NCC	0.15	0.49	-
5-CeO_2/Li_2O/SBA-15	NCC	0.08	0.20	0.30	0.52	0.13	0.13	NCC	0.58	0.78	1.2
10-CeO_2/Li_2O/SBA-15	0.07	0.16	0.24	0.51	0.69	0.31	0.12	NCC	0.98	1.12	1.3
15-CeO_2/Li_2O/SBA-15	0.10	0.15	0.26	0.65	1.10	0.31	0.21	NCC	1.16	1.62	1.4
20-CeO_2/Li_2O/SBA-15	0.14	0.38	0.40	0.52	2.73	0.73	0.40	0.36	1.44	4.22	1.7
25-CeO_2/Li_2O/SBA-15	0.15	0.39	0.41	0.55	2.03	1.19	0.40	0.62	1.50	4.24	1.7

**NCC stands for No colour change.*

**TOF is calculated at 50% conversion level on the basis of basic sites; Reaction conditions = MeOH to oil molar ratio of 40 : 1 at 65 °C reaction temperature, in the presence of 10 wt% of catalyst with respect to oil at 600 rpm stirring speed.*

**Indicators used:* methyl orange ($H_0 \leq 3.1$), methyl red ($H_0 \leq 4.8$), neutral red ($H_0 \leq 6.8$), bromthymol blue ($H_0 \leq 7.2$), anthraquinone ($H_0 \leq 8.2$)

3.3.2. FAMEs characterization by ^{1}H NMR

The competence of prepared catalyst has been evaluated for the transesterification of a variety of WCO. The FAMEs produced were characterized and quantified with proton NMR technique. The technique is not merely rapid, easy, and non destructive but also did not require any derivatisation of the products. The ^{1}H NMR spectrum of WCO shows a multiplet at 4.15-4.34 ppm owing to the existence of glyceridic protons. The peaks present at 0.8-2.8 ppm in the NMR spectrum of FAMEs as well as WCO (Fig. 3.8) are due to the presence of saturated hydrocarbon (HC) protons of fatty acids. The unsaturated ^{1}H of fatty acid carbon chain in WCO and FAMEs appear at 5.25 ppm. However, in ^{1}H NMR spectrum of FAMEs, a new peak emerges at 3.6 ppm due to -OCH_3 protons, whereas peaks corresponding to the glyceridic protons were no longer seen, thus, supporting the formation of fatty acid methyl

ester on methanolysis of WCO. FAMEs produced during the transesterification of WCO were quantified by following equation (2.6) as discussed in chapter 2.

$$\text{FAMEs yield (\%)} = \{2I_{(\text{methoxy})}/3I_{(\text{methylene})}\} \times 100 \quad (2.6)$$

where, $I_{(\text{methoxy})}$ and $I_{(\text{methylene})}$ are the integration values of methoxy (3.6 ppm) and methylene (2.3 ppm) protons, respectively in proton NMR spectrum of fatty acid methyl ester.

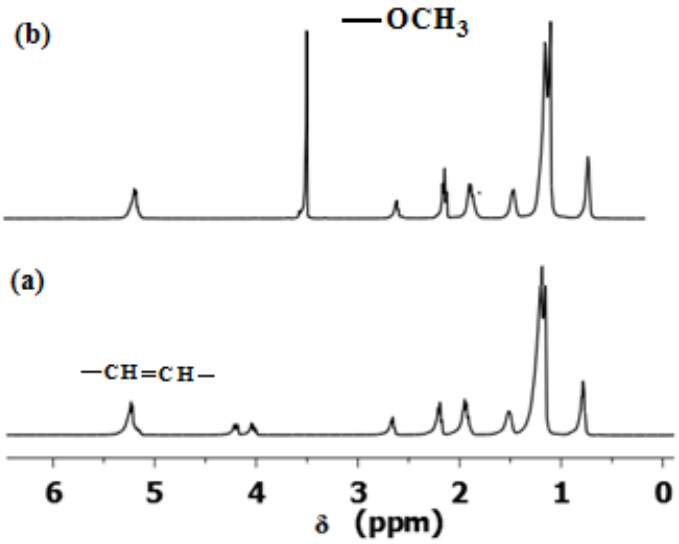

Fig. 3.8. Comparison of the ^{1}H NMR spectra of (a) waste cottonseed oil and (b) FAMEs.

3.3.3. Catalytic activity of CeO_2/Li_2O/SBA-15

Owing to the presence of acidic as well as basic sites, the esterification as well as transesterification activity of the prepared catalyst has been evaluated. To demonstrate the transesterification activity, WCO and methanol were employed as substrate. To achieve the maximum FAMEs yield in the least possible time the reaction parameters were investigated by varying one parameter at a time from the followings: (i) impregnated CeO_2 concentration, (ii) catalyst concentration, (iii) reaction temperature, and (iv) methanol to oil molar ratio. In addition, esterification reaction was also carried out by employing oleic acid as reactant to test the activity of catalyst towards esterification.

3.3.3.1. Effect of CeO_2 concentration on FAMEs yield

CeO_2 consists of both Lewis acid and basic sites and these sites are responsible for the catalytic activity. To determine the optimum amount of ceria concentration for the best

catalytic activity, a series of catalysts were prepared by loading of fixed weight percentage of lithium and impregnating 5-25 wt % of CeO_2 on SBA-15. All reactions were performed at 65°C employing the 40:1 methanol to oil molar ratio in the presence of 10 wt % of catalyst.
As the concentration of certain catalyst was increased from 5 to 20 wt %, the rate of reaction increased and complete conversion of WCO into FAMEs was achieved in 4 h (Fig. 3.9a). Similar trends were reflected by the TOF of the catalyst, which were found to increase from 1.2×10^{-3} to 1.7×10^{-3} h^{-1} on increasing the ceria loading (Table 3.2). A further increase in ceria concentration (from 20-25 wt %) was not found to affect the TOF to the significant extent and hence, 20-CeO_2/Li_2O/SBA-15 was selected to optimise the other reaction parameters. The maximum number of active sites was observed with 25 wt% CeO_2 loading. However, both the catalysts (with 20 wt% and 25 wt % CeO_2 loading) exhibited similar TOFs. Hence, 20 wt% of CeO_2 loading was chosen as most favourable CeO_2 concentration. The results are in line with the similar findings been reported in literature, where optimum activity was observed at 20 wt% loading of active species and increasing the loading amount further was not able to affect the reaction rate significantly (Brahmkhatri and Patel, 2011).

3.3.3.2. Effect of concentration of catalyst

In order to investigate the catalyst concentration, transesterification reactions were carried out at 65 °C, using a 40:1 methanol to oil molar ratio and varying the 20-CeO_2/Li_2O/SBA-15 amount from 6 to 11 wt% (catalyst/oil). The results have been summarized in Fig. 3.9 b, which shows that an increase in catalyst concentration up to 10 wt% was found to boost the rate of reaction. This could be attributed to the increase in the number of catalytic sites on increasing the catalyst concentration. However, a further increase in catalyst concentration (11 wt%) was not found to reduce the reaction duration and hence, transesterification study was performed in the presence of 10 wt% catalyst. This could be attributed to the high viscosity of the reaction mixture due to excess catalyst amount that leads to inefficient mixing of the reactants. The excess amount of catalyst, also leads to the formation of emulsion, that leads to the gel formation. This hinders the glycerol separation and, hence, declines the apparent FAMEs yield (Kim et al., 2004; Encinar et al., 2005).

3.3.3.3. Effect of reaction Temperature

To find the optimum reaction temperature, transesterification reactions were carried out in presence of 10 wt % of 20-CeO_2/Li_2O/SBA-15 employing 40:1 methanol to oil molar ratio

and varying the temperatures in the range of 35-65 °C (Fig. 3.9c). As the temperature was increased from 35°C to 65 °C, the rate of reaction was found to increase significantly. The reaction could not be completed at 35°C, even after quite longer durations of 50 h. However, the reaction time was reduced to 4 h as the temperature was increased to 65°C. Any further increase in the reaction temperature was not found to increase the efficiency of catalyst to any significant extent (Fig. 3.9c). Hence, 65 °C was selected as the optimum temperature to achieve the complete transesterification in minimum possible time. Higher temperature will lead to an increase the methanol evaporation from the reaction mixture. The methanol so vaporized will no longer be in contact with the catalyst or oil, and hence, the catalyst activity will not increase when reaction temperature is raised beyond 65 °C (Bo et al., 2007).

3.3.3.4. Effect of methanol/oil molar ratio on FAMEs yield

Methanol to oil molar ratio is one of the important parameters which has a considerable affect on the FAMEs yield as well as on production cost. The minimum methanol to oil molar ratio must be 3:1 for 100% conversion of vegetable oil to biodiesel. However, transesterification being a reversible process, is usually performed with an excess of methanol in order to shift the equilibrium in forward direction for achieving the maximum FAMEs yield. Heterogeneous catalysts, due to the phase difference, catalyze the reaction at relatively slower rate and hence, required more time for the completion of the reaction. In a view to achieve the higher FAMEs yield in lesser time during the reactions catalyzed by heterogeneous catalysts, higher alcohol to oil molar ratios (upto 275:1) have been reported in literature (Leclercq et al., 2001).

The transesterification reactions were carried out at 65 °C using 10 wt% of 20-CeO_2/Li_2O/SBA-15 and varying the alcohol to oil molar ratios from 12:1 to 50:1 (Fig. 3.9d). The reaction rate was found to increase with increase in methanol to oil molar ratio and the reaction time reduced significantly when 40:1 methanol to oil molar ratio was employed. Further increment in the methanol to oil molar ratio upto 50:1 was not found to reduce the duration of reaction to any considerable extent. Hence, 40:1 methanol to oil molar ratio was selected for the optimum activity of the present catalyst. A methanol to oil molar ratio greater than the 50:1 will interfere in the FAMEs and glycerol layers separation due to an increase in glycerol solubility. As a result, a fraction of the diluted glycerol will remain the BD phase and thus decline apparent BD yield because of foam formation. Moreover, when glycerol will

remain in solution, it will drive the reaction equilibrium towards the reactant side, thus, declining the BD yield (Barnwal and Sharma, 2004)

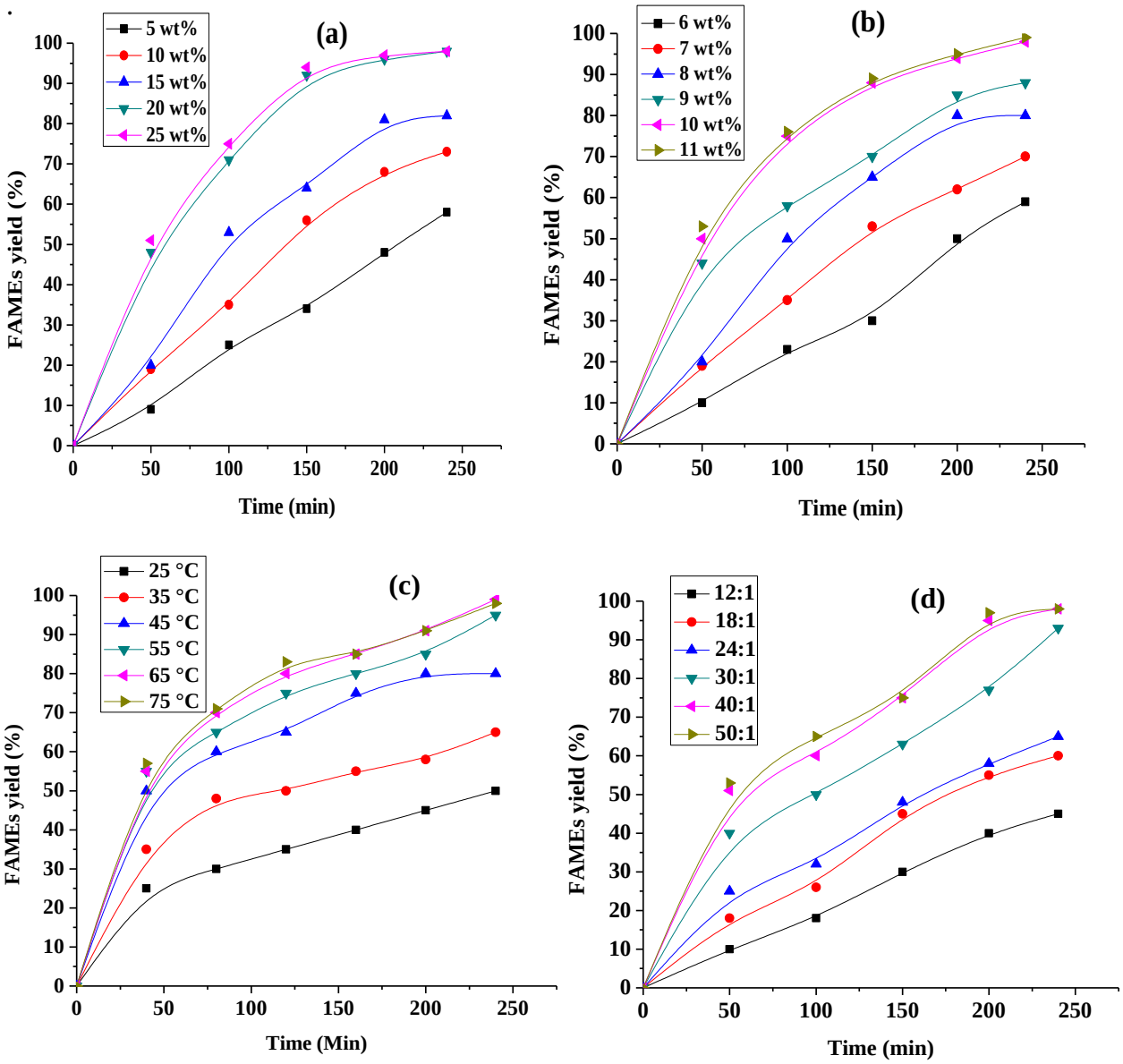

Fig. 3.9. Effect of (a) CeO_2 concentration on SBA-15, (b) catalyst concentration, (c) reaction temperature and (d) methanol/oil molar ratio on methanolysis of WCO.

3.3.4. Effect of FFA content on catalyst activity

In the presence of homogeneous catalyst, presence of > 0.5 wt% FFA contents in feedstock was found to deactivate the catalyst *via* saponification reaction. Conventionally, the

transesterification of high FFA-containing oils is carried out in a two-step process, viz., (i) acid-catalyzed esterification of high FFA containing vegetable oil (VO) followed by (ii) base catalyzed transesterification of ester rich VO. Hence, to avoid such tedious two step process, it is desirable to prepare a catalyst which can esterify the FFA and transesterify the waste cooking oil simultaneously in one pot system.

Very few reports have been cited in literature where a single catalyst is able to catalyze the simultaneous esterification as well transesterification reactions (Kaur and Ali, 2014b).

Tungstophosphoric acid modified hydrous zirconia has been employed as heterogeneous catalyst for simultaneous esterification and transesterification of poor quality canola oil (with 20% FFA content). The reaction was carried out at very high temperature 200 °C and yielded 90% FAMEs (Kulkarni et al., 2006).

As supported by the Hammett indicator test, 20-CeO_2/Li_2O/SBA-15 was found to possess both acidic as well basic sites. Out of these, former is expected to catalyze the esterification and later the transesterification reaction. To demonstrate the esterification activity of 20-CeO_2/Li_2O/SBA-15, oleic acid and methanol (1: 40 molar ratio) were reacted in the presence of the prepared catalyst at 65 °C for 4 h. After the stipulated time, ^{1}H NMR analysis spectra was recorded and appearance of peak at 3.6 ppm supported the formation of methyl oleate and quantified as ~ 27% methyl oleate to support the esterification activity of the catalyst (Fig. 3.10)

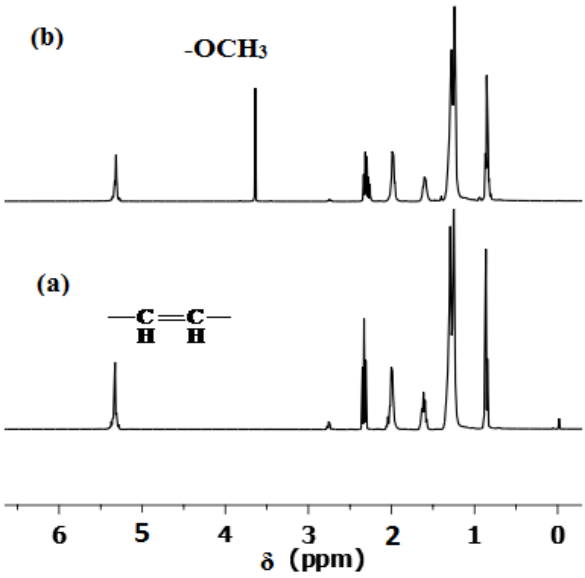

Fig. 3.10. Comparison of the ^{1}H NMR spectra of (a) oleic acid and (b) corresponding FAMEs.

^{13}C NMR spectra of oleic acid and corresponding methyl ester have also been compared in Fig. 3.11. The peak emerging at 13-35 ppm is due to terminal $–CH_3$ group and saturated carbons and the peaks appearing at 128-130 ppm is due to unsaturated carbons in both molecules. A new peak appeared at 51 ppm on esterification of oleic acid which supported the presence of $–OCH_3$ group.

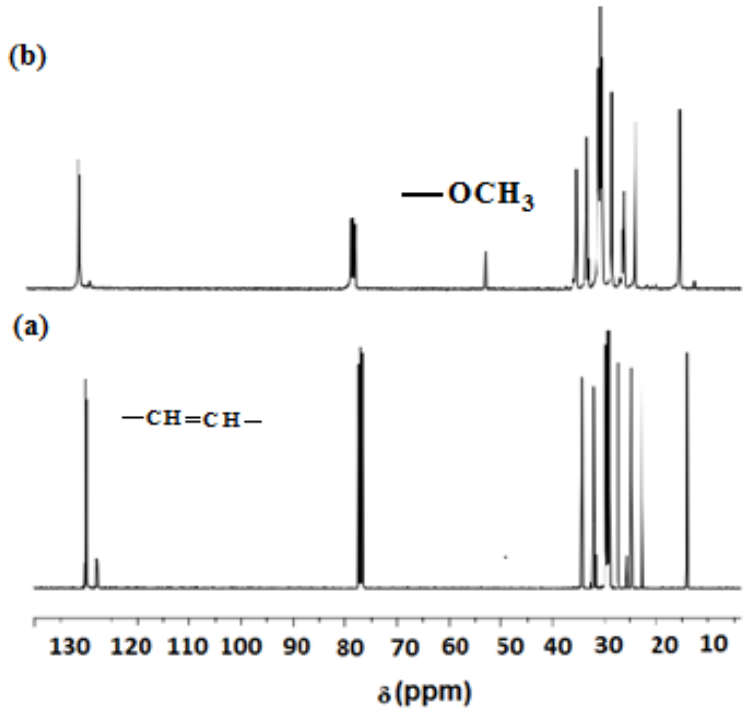

Fig. 3.11. Comparison of the ^{13}C NMR spectra of (a) oleic acid and (b) corresponding FAMEs.

In the present chapter, the prepared catalyst was found to catalyze the complete transesterification of WCO having FFA contents as high as 4.8 wt%. To find the maximum FFA tolerance of the catalyst, transesterification reactions of WCO were carried out under optimised conditions by adding 1-6 wt% of palmitic acid in the reaction mixture. Presence of up to 4 wt% of palmitic acid was not found to reduce the catalytic activity as shown in Fig. 3.12. However, a further increase in palmitic acid concentration, 5 wt% and above, was found to reduce the catalyst activity as the FAMEs yield was found to decline to 91%. Thus, 20-CeO_2/Li_2O/SBA-15 was found to be effective and yielding complete conversion of WCO even in the presence of 8.8 wt % FFA contents (4.8 FFA of WCO + 4 wt% added palmitic acid). When FFA contents in feedstock were increased beyond 9.8 wt% (5 wt% of added FFA + 4.8 wt% FFA already present) FAMEs yield was found to decrease. This can be

attributed to the strong interactions of polar carboxylic acid group (-COO^-) of FFA with the active sites present in catalyst which resulted in the partial blockage of active sites of catalyst (Kaur and Ali, 2014b).

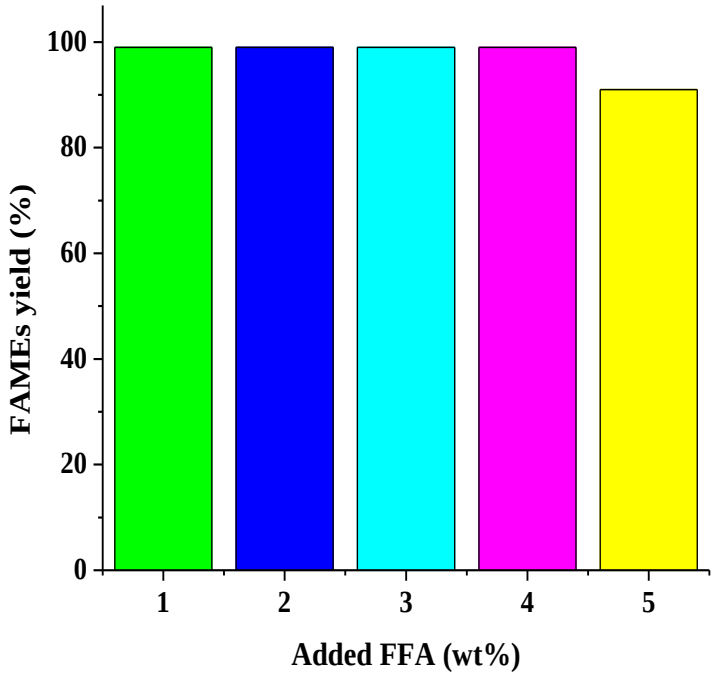

Fig. 3.12. Effect of added FFA content on the FAMEs on 20-CeO_2/Li_2O/SBA-15 catalyzed methanolysis of WCO (Reaction conditions: MeOH/oil molar ratio = 40:1; Catalyst amount = 10 wt% of oil; Temperature = 65 °C).

3.3.5. Reusability of catalyst and homogeneous contribution

Reusability is a very important and advantageous feature in case of heterogeneous catalysts as it makes the separation of catalysts easier and the post production process much less expensive and tedious. To evaluate the catalyst reusability and decay in its activity, transesterification with 20-CeO_2/Li_2O/SBA-15 was carried out under the optimised conditions. The used catalyst was recovered through filtration, then washed with hexane and dried at 120 °C and then calcined at 550 °C. The catalyst so regenerated was employed for transesterification for 6 successive runs under the similar experimental conditions and method of regeneration. It was observed that the reused catalyst gave complete conversion of triglyceride to FAMEs for 5 consecutive runs and the activity of the catalyst declined in the

6th run yielding 60% biodiesel yield. The TOF the catalyst declined significantly after 5th cycle itself as shown in Fig. 3.13.

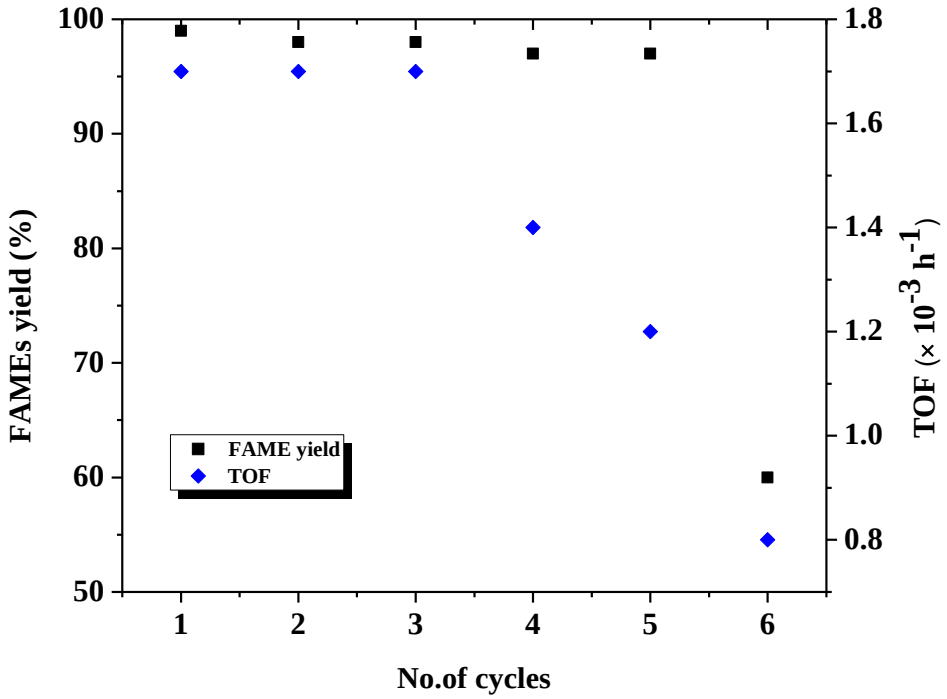

Fig. 3.13. Reusability of 20-CeO_2/Li_2O/SBA-15 catalyst (Reaction conditions: MeOH/oil molar ratio = 40:1; Catalyst amount = 10 wt% of oil; Temperature = 65 °C).

Leaching of the active species is a frequently encountered problem in the heterogeneous catalysts. The concentration of Ce and Li metal was quantified in FAMEs by using MP-AES technique. During initial runs, Ce metal was not detected in the reaction mixture, however, after the fifth run, 146 and 71 ppm of Ce was observed in BD and glycerol layer, respectively (Table 3.3). Small quantity of Li was also detected in last 2 runs as demonstrated in Table 3.3. Thus, during the initial four catalytic cycles no active metal was found in the reaction mixture to maintain that the catalyst is reasonably stable. In a blank experiment bare CeO_2 was employed as a catalyst to carry out the transesterification reaction of WCO. Analysis of cerium metal in BD layer show the presence of 144 ppm of Ce and no cerium was detected in glycerol layer. Thus, the active catalytic species immobilised on mesoporous silica is clearly an advantageous option over unsupported catalyst, since it significantly reduces the leaching of active metal into the reaction mixture making it a better counterpart.

Table 3.3. Dissolved metal ion concentration (ppm) in reaction mixture after every catalytic cycle.

Catalytic run	Metal concentration (ppm)					
	Biodiesel layer			Glycerol layer		
	Si	**Li**	**Ce**	**Si**	**Li**	**Ce**
I	19.0	*ND*	*NF*	9.0	*ND*	*NF*
II	10.*0*	*ND*	*NF*	6.5	*ND*	*NF*
III	7.0	*ND*	*NF*	11.0	*ND*	*NF*
IV	75.8	*ND*	*NF*	60.8	*ND*	*NF*
V	37.3	14.6	*NF*	47.3	8.2	*NF*
VI	153	24.8	146	94.3	13.6	71

**NF= not found., *ND= not determined*

Dissolution of the ceria, an active ingredient of the catalyst, from the matrix resulted in the decline of catalyst activity. The loss of cerium from the catalyst was further supported by comparing the powder XRD patterns of the fresh and reused catalyst as shown in Fig 3.14. The diffraction peaks corresponding to the CeO_2 phase were observed in the form of weak XRD patterns in reused catalyst to support the major loss of ceria from the matrix after fifth run.

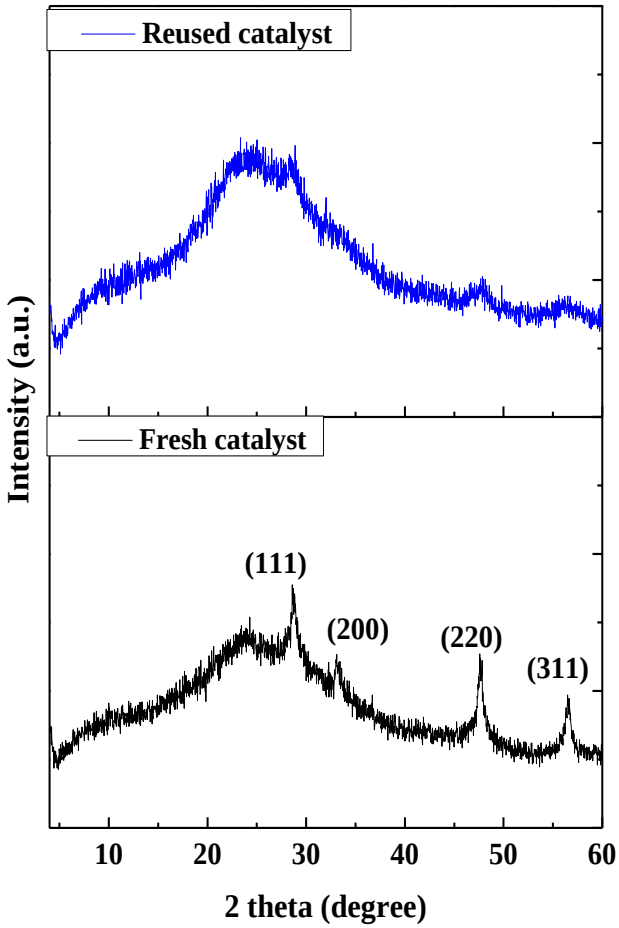

Fig. 3.14. Comparison of the powder XRD patterns of fresh and reused 20-CeO_2/Li_2O/SBA-15.

To further support the decline in the cerium content of the catalyst, EDS analysis of reused catalyst was performed. The spectra depicted 13.6% content of Ce in reused catalyst as compared to 22% Ce in case of fresh catalyst. Decline in the activity of catalyst upon repeated use can be attributed to the partial loss of cerium metal from the catalyst.

Leaching leads to decline in the activity of catalyst and the leached species can catalyse the reaction similar to homogeneous catalysts. Hence, it becomes important to find the homogeneous contribution of the catalyst while studying its reusability.

As discussed in reusability study, during first five catalytic runs Si was found to leach out in the reaction mixture whereas active metals Ce was not detected and Li was found in minor quantities. To further ensure the heterogeneous mode of activity of the prepared catalyst, hot filtration test was performed under optimized conditions. The catalyst was recovered by filtration after 1 h of reaction and reactants (without catalyst) were again heated for 3 h. It can

be seen from the Fig. 3.15, that there was no rise in FAMEs yield when the reaction was performed in absence of catalyst. This observation clearly proves (i) the heterogeneous mode of catalyst activity and (ii) the leached metal ions have no contribution in catalytic activity.

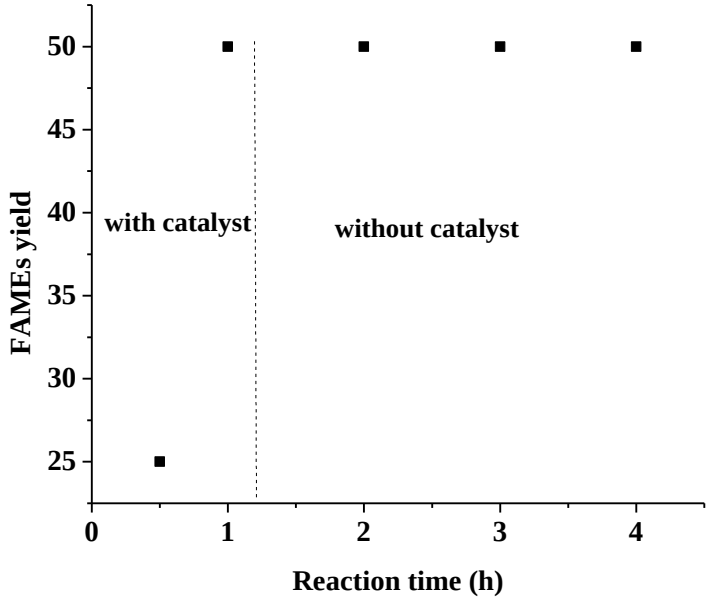

Fig. 3.15. Hot filtration test for 20-CeO_2/Li_2O/SBA-15 catalyzed transesterification.

Thus, from the above observation, it can be inferred that there is no significant homogeneous contribution in 20-CeO_2/Li_2O/SBA-15 activity because of leached species.

3.3.6. Kinetic study

For the completion of triglyceride transesterification, theoretically, each triglyceride molecule required 3 molecule of alcohol and overall order of the reaction must be 4. However, in most of the experimental work to push the equilibrium towards the forward direction and to increase the FAMEs yield in lesser reaction duration, such reaction is usually performed in the presence of excess alcohol (Wang et al., 2011). Hence, the transesterification of triglycerides, in presence of excess methanol, has been reported to follow the pseudo first order kinetics equation (2.2).

$$-\ln (1-X_{me}) = kt \qquad (2.2)$$

where, X_{me} is the FAMEs yield at time 't'.

The tranesterification reactions were carried out at different 35 to 65 °C under optimized conditions to determine the rate constants at these temperatures. The conversion values at

different temperatures were put in the equation (2.2) to obtain the values of respective rate constants. The plot of $-\ln(1-X_{me})$ *versus* '*t*' has been shown in Fig.3.16a.

The plot is linear in nature that proves that reaction has followed kinetics of first order (Zhang et al., 2010). The rate constant value at 65 °C from the plot has been found to be 0.017 min^{-1}.

With an aim to calculate energy of activation and (E_a), Arrhenius equation was employed which is given in equation (2.3).

$$\ln k = -Ea/RT + \ln A \qquad (2.3)$$

where, R is the universal gas constant (8.3 J $K^{-1}mol^{-1}$, and T is the temperature of reaction in Kelvin, Ea is the activation energy (kJ mol^{-1}), A is pre–exponential factor (min^{-1}).

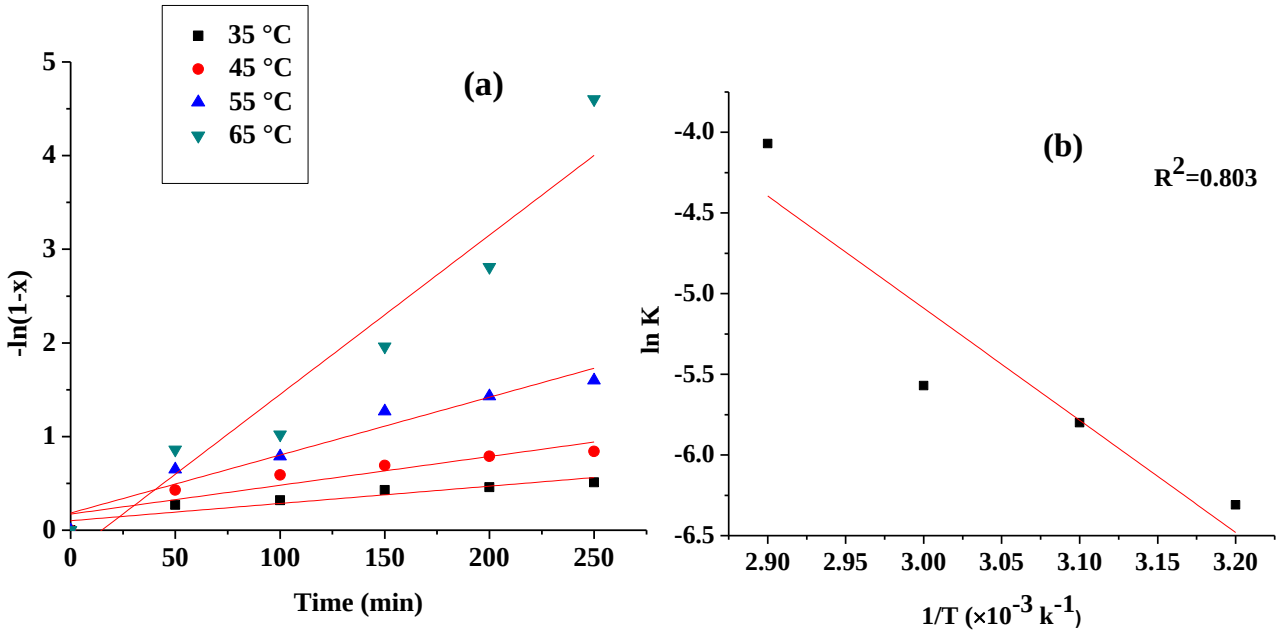

Fig. 3.16. (a) A plot of –ln(1–Xme) *versus* reaction time (t) at different temperatures (Reaction conditions: MeOH/oil molar ratio = 40:1; catalyst amount = 10 wt% of oil) and (b) Arrhenius plot for methanolysis of WCO in presence of 20-CeO_2/Li_2O/SBA-15.

From the Arrhenius plot (Fig. 3.16b), the activation energy was found to be 57.7 kJ mol^{-1} which is within the reported range (33-84 kJ mol^{-1}) for the methanolysis of vegetable oils (Sun et al., 2008). A value of Ea > 25 kJ mol^{-1}, further supports that reaction is controlled chemically and not by diffusion or mass transfer limitations (Patel and Brahmkhatri, 2013).

The activation energy for the transesterification reactions are frequently reported in literature, *e.g.*, 12-tungstophosphoric acid supported on SBA-15 has been employed for biodiesel

synthesis and E_a value of 44.6 kJ mol^{-1} was reported for the reaction (Brahmkhatri and Patel, 2011). Another study for mesoporous SnO_2/WO_3 (Sarkar et al., 2010) catalyzed reaction reported the activation energy value of 39.5 kJ mol^{-1}. However, very few reports have extended their work to calculate the thermodynamic parameters *viz.*, $\Delta H^{\ddagger}$ (enthalpy of reaction), $\Delta S^{\ddagger}$ (entropy of activation of reaction) and $\Delta G^{\ddagger}$ (free energy of reaction).

Eyring–Polanyi equation (2.4) was employed to calculate the enthalpy ($\Delta H^{\ddagger}$) and entropy of activation ($\Delta S^{\ddagger}$) for the reaction.

$$\ln(k/T) = -\Delta H^{\ddagger}/RT + \ln(k_B/h) + \Delta S^{\ddagger}/R \qquad (2.4)$$

where k_B and h are the Boltzmann (1.38×10^{-23} J K^{-1}) and Planck (6.63×10^{-34} J s) constants, respectively.

A linear plot was observed between ln(k/T) and 1/T as shown in Fig. 3.17, $\Delta H^{\ddagger}$ and $\Delta S^{\ddagger}$ were obtained from slope {$-\Delta H^{\ddagger}/R$} and intercept {ln (k_B/h)+$\Delta S^{\ddagger}/R$} of this plot, respectively.

From the curve, $\Delta H^{\ddagger}$ and $\Delta S^{\ddagger}$ were found to be 59.4 kJ mol^{-1} and - 0.108 kJ mol^{-1} respectively.

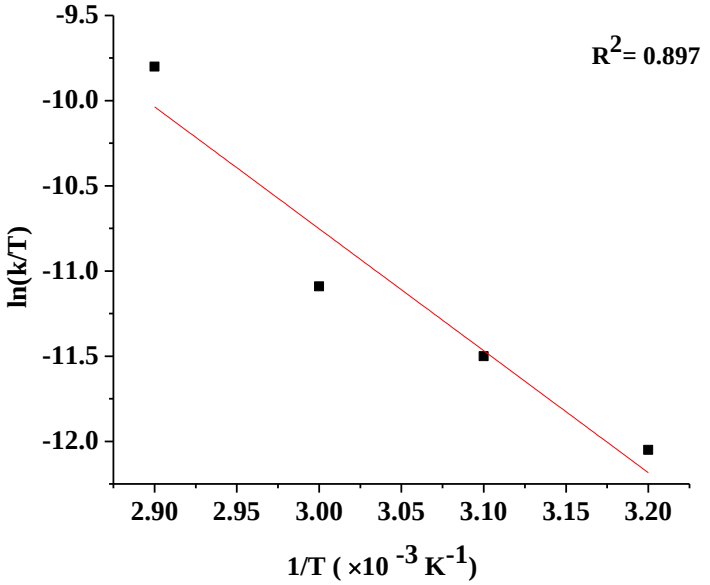

Fig. 3.17. A plot of ln(k/T) *versus* 1/T.

The Gibb's free energy ($\Delta G^{\ddagger}$) for the reaction was determined by substituting the values of $\Delta H^{\ddagger}$ and $\Delta S^{\ddagger}$ in equation (2.5)

$$\Delta G^{\ddagger} = \Delta H^{\ddagger} - T\Delta S^{\ddagger} \qquad (2.5)$$

The $\Delta G^{\ddagger}$ for the present transesterification reaction was found to be + 95.9 kJ mol^{-1}.

From the positive value of $\Delta G^{\ddagger}$, it can be inferred that 20-CeO_2/Li_2O/SBA-15 catalysed methanolysis of WCO is not a spontaneous reaction and the energy level of transition state is higher than that of reactants (Pogaku et al., 2012).

A negative value of $\Delta S^{\ddagger}$ shows that transition state possesses more order than that of reactants present in ground state. Thus, 20-CeO_2/Li_2O/SBA-15 catalysed transesterification has followed an associative pathway (Espenson, 2002). Positive value of $\Delta H^{\ddagger}$ shows that the reaction is endothermic in nature and requires external heating to form the transition state and go in forward direction (Beall, 1994).

In a report (Kaur and Ali, 2014b) during the 2Sr:Zr catalyzed transesterification of WCO, $\Delta H^{\ddagger}$, $\Delta S^{\ddagger}$ and $\Delta G^{\ddagger}$ values were found to be 45.9 kJ mol^{-1}, -0.121 kJ mol^{-1}, and 88.2 kJ mol^{-1} respectively which is comparable with the corresponding values reported in present chapter. Elsewhere, during the catalyst-free transesterification under supercritical conditions the $\Delta H^{\ddagger}$, $\Delta S^{\ddagger}$ and $\Delta G^{\ddagger}$ were found to be 31.3 kJ mol^{-1}, -0.023 kJ mol^{-1}, and 153.6 kJ mol^{-1}, respectively (Onga et al., 2013). Thus, the present thermodynamic study in presence of heterogeneous catalyst, as well as reported work indicates the endothermic nature of the reaction and formation of an ordered transition state during the reaction.

3.4. Conclusions

In the present study, 20-CeO_2/Li_2O/SBA-15 has been prepared by wet impregnation method and utilised as an effective heterogeneous catalyst for simultaneous esterification and transesterification of low quality cottonseed oil. Under most favourable reaction conditions (catalyst concentration 10 wt%, methanol to oil molar ratio of 40:1 at 65 °C), the transesterification of waste cottonseed oil was found to follow (pseudo) first order kinetics. The activation energy for the methanolysis of waste cottonseed oil was found to be 57.7 kJ mol^{-1}. A negative value of $\Delta S^{\ddagger}$ supported that 20-CeO_2/Li_2O/SBA-15 catalysed transesterification has followed an associative pathway, while positive value of $\Delta H^{\ddagger}$ shows that the reaction is endothermic in nature. The catalyst solubility study ruled out any homogeneous contribution in catalytic activity. The catalyst was recovered and recycled for 5 successive runs without any significant loss in activity.

References

Aurbach, D., Weissman, I., Schechter, A., 1996. X-Ray photoelectron spectroscopy studies of lithium surfaces prepared in several important electrolyte solutions. A comparison with previous studies by Fourier transform infrared spectroscopy. Langmuir 12, 3991-4007.

Barnwal, B.K., Sharma, M.P., 2004. Prospect of Biodiesel Production from vegetable oil in India. Renew. Sustain. Energy. Rev. 238-246.

Beall, H., 1994. Probing Student Misconceptions in Thermodynamics with In-Class Writing. J. Chem. Educ.71, 1056-1057.

Bhagiyalakshmi, M., Vinoba, M.,Grac, A.N., 2013. Transesterification of Jatropha oil over ceria-impregnated ZSM-5 for the production of biodiesel. Bull. Korean Chem. Soc. 34, 3059-3064.

Bo, X., Guomin, X., Lingfeng, X., Ruiping, W., Lijing, G., 2007. Transesterification of palm oil with methanol to biodiesel over a KF/Al_2O_3 heterogeneous base catalyst, Energy Fuels 21, 3109–3112.

Brahmkhatri, V., Patel, A., 2011. 12-Tungstophosphoric acid anchored to SBA-15: An efficient, environmentally benign reusable catalysts for biodiesel production by esterification of free fatty acids. Appl. Catal. A: Gen. 403, 161-172.

Cho, E.B., Yim, S., Kim, D., Jaroniec, M., 2013. Surfactant-Assisted synthesis of Mesoporous Silica/Ceria−Silica Composites with High Cerium Content under Basic Conditions. J. Mater. Chem. A. 1, 12595−12605.

Encinar, J.M., Gonzalez, J.F., Rodriguez, R. A., 2005. Biodiesel from used frying oil, variables affecting the yield and characteristics of biodiesel. Ind. Eng. Chem. Res. 44, 5491-5499.

Endalew, A. K., Kiros, Y., Zanzi, R., 2011. Inorganic heterogeneous catalysts for biodiesel production from vegetable oils. Biomass Bioenergy. 35, 3787-3809.

Espenson, J.H., 2002. Chemical Kinetics and Reaction Mechanisms, second ed. McGraw-Hill, India.

Gorji, A., Ghanei, R., 2014. A review on catalytic biodiesel production. J.Bio & Env. Sci. 5, 48-59.

Hailstone, R.K., DiFrancesco, A.G., Leong, J.G., Allston, T.D., Reed, K.J., 2009. A Study of Lattice Expansion in CeO_2 Nanoparticles by Transmission Electron Microscopy. J. Phys. Chem. C. 113, 15155–15159.

Kaur, M., Ali, A., 2014a. Ethanolysis of waste cottonseed oil over lithium impregnated calcium oxide: kinetics and reusability studies. Renew. Energy 63, 272-279.

Kaur, N., Ali, A., 2014b. One pot transesterification and esterification of waste cooking oil via ethanolysis using Sr:Zr mixed oxide as solid catalyst. RSC Adv. 4, 43671-81.

Kim, H. J., Kang, B. S., Kim, M. J., Park, Y. M., Kim, D. K., Lee, J. S., Lee, K. Y., 2004. Transesterification of vegetable oil to biodiesel using heterogeneous base catalyst. Catal. Today 93-95, 315-320.

Kulkarni, M.G., Gopinath, R., Meher, L.C., Dalai, A.K., 2006. Solid acid catalysed biodiesel production by by simultaneous esterification and transesterification. Green Chem. 8, 1056–1062.

Leclercq E., Finiels A., Moreau C., 2001. Transesterification of rapeseed oil in the presence of basic zeolites and related solid catalysts. J. Am. Oil Chem. Soc. 78, 1161-1165.

Li, E., Rudolph, V., 2008. Transesterification of Vegetable Oil to Biodiesel over MgO-Functionalized Mesoporous Catalysts. Energy Fuels 22, 145-149.

Luo, Y., Hou, Z., Li, R., Zheng, X., 2008. Rapid synthesis of ordered mesoporous silica with the aid of heteropolyacids. Microporous Mesoporous Mater. 109, 585-590.

Negm, N.A., Sayed, G.H., Habib, O.I., Yehia, F.Z., Mohamed, E.A., 2017. Heterogeneous catalytic transformation of vegetable oils into biodiesel in one-step reaction using super acidic sulfonated modified mica catalyst. J. Mol. Liq. 237, 38-45.

Negrila, C.C., Cotirlan, C., Ungureanu, F., Logofatu, C., Ghita, R.V., Lazarescu, M.F., 2008. ARXPS analysis of silicon oxide films. J. Optoelectron. Adv. Mater. 6, 1379-1383.

Onga, L.K., Kurniawana, A., Suwandi, A.C., Linb, C.X., Zhao, X.S., Ismadji, S., 2013. Transesterification of leather tanning waste to biodiesel at supercritical condition: Kinetics and thermodynamic studies. J. Supercrit. Fluids. 75, 11-20.

Pal, N., Cho, E.B., Kim, D., 2014. Synthesis of Ordered Mesoporous Silica/Ceria-Silica Composites and their High Catalytic Performance for Solvent-Free Oxidation of Benzyl Alcohol at Room Temperature. RSC Adv. 4, 9213−9222.

Park, S. H., Kim, B. H., Selvaraj, M., Lee, T. G., 2007. Synthesis and Characterization of Mesoporous Ce-Mn-MCM-41 Molecular Sieves. J. Ind. Eng. Chem. 13, 637−643.

Park, Y.M., Chung, S.H., Eom, H.J., Lee, J.S., Lee, K.Y., 2010. Tungsten oxide zirconia as solid superacid catalyst for esterification of waste oil (dark oil). Bioresour. Technol.101, 6589–6593.

Parry, E.P., 1963. An Infrared Study of Pyridine Adsorbed on Acidic Solids. Characterization of Surface Acidity. J. Catal. 2, 371-379.

Patel, A., Brahmkhatri, V., 2013. Kinetic study of oleic acid transesterification over 12-tungstophosphoric acid catalyst anchored to different mesoporous silica supports. Fuel Process. Technol. 113, 141-149.

Pogaku, R., Raman, J.K., Ravikumar, G., 2012. Evaluation of Activation Energy and Thermodynamic Properties of Enzyme-Catalysed Transesterification Reactions. Adv. Chem. Eng. Sci. 2, 150-154.

Rajagopal, S., Marzari, J.A., Miranda, R., 1995. Silica-Alumina-supported Mo Oxide catalysts: Genesis and Demise of Bronsted-Lewis Acidity. J. Catal. 151, 192–203.

Reddy, B.M., Bharali, P., Saikia, P., Park, S.E., Vanden Berg, M.W.E., Muhler, M., Gru¨nert, W., 2008. Structural Characterization and Catalytic Activity of Nanosized $Ce_xM_{1-x}O_2$ (M = Zr and Hf) Mixed Oxides. J. Phys. Chem. C. 112, 11729–11737.

Sareen, S., Mutreja, V., Singh, S., Pal, B., 2015. Highly dispersed Au, Ag and Cu nanoparticles in mesoporous SBA-15 for highly selective catalytic reduction of nitroaromatics. RSC Adv. 5, 184-190.

Sarkar, A., Ghosh, S. K., Pramanik, P., 2010. Investigation of the catalytic efficiency of a new mesoporous catalyst SnO_2/WO_3 towards oleic acid esterification. J. Mol. Catal. A: Chem. 327, 73-79.

Sharma, S., Saxena, V., Baranwal, A., Pandey, L.M., 2018. Engineered nanoporous materials mediated heterogeneous catalysts and yheir implications in biodiesel production. Materials Science for Energy Technologies 1, 11-21.

Sun, H., Hu, K., Lou, H., Zheng, X., 2008. Biodiesel production from transesterification of Rapeseed oil using KF/Eu2O3 as a Catalyst. Energy Fuels 22, 2756–2760.

Vunain, E., Jalama, K., Enus, R.M., Meijboom, R., 2013. The effect of recrystallization time on pore size and surface area of mesoporous SBA-15. J. Sol-Gel Sci. Technol. 68, 270–277.

Wagner, C.D., Passoja, D.E., Hillery, H.F., Kinsiky,T.G., Six, H.A., Jansen, W.T., 1982. Auger and photoelectron line energy relationships in aluminium-oxygen and silicon-oxygen compounds. J. Vac. Sci. Technol. 21, 933-944.

Wang, J.X., Chen, K.T., Huang, S.T., Chen, C.C., 2011. Application of Li_2SiO_3 as a heterogeneous catalyst in the production of biodiesel from soyabean oil. Chinese Chem. Lett. 22, 1363-1366.

Wu, H., Zhang, J., Liu, Y., Zheng, J., Wei,Q., 2014. Biodiesel production from Jatropha oil using mesoporous molecular sieves supporting K_2SiO_3 as catalysts for transesterification. Fuel Process. Technol.19, 114-120.

Xie, W., Zhao, L., 2014. Heterogeneous CaO-MoO_3-SBA-15 catalysts for biodiesel production from soyabean oil. Energy Convers. Manage. 79, 34-42.

Zhang, L., Sheng, B., Xin, Z., Liu, Q., Sun, S., 2010. Kinetics of transesterification of palm oil and dimethyl carbonate for biodiesel production at the catalysis of heterogeneous base catalyst. Bioresour. Technol.101, 8144-8150

5-Na/ZnO Based Mesoporous Silica as Reusable Solid Catalyst for Biodiesel Production *via* Transesterification of Virgin Cottonseed Oil

Abstract

5-Na/ZnO loaded SBA-15 has been prepared by one-pot method in atmospheric conditions (without employing hydrothermal treatment) and following wet impregnation method. The prepared catalyst was characterised by using several techniques viz., BET method for determination of surface area, FE-SEM for morphology of catalyst, XPS study to determine the oxidation state of constituent elements. The catalyst was utilised for transesterification from virgin cotton seed oil and the catalyst activity was found to be dependent on its basic strength. Under optimal reaction conditions of catalyst amount 12 wt%, methanol to oil molar ratio of 24:1 at reaction temperature of 65 °C, the prepared catalyst yielded > 98 % fatty acid methyl ester in 4 h of reaction duration. The catalyst was able to yield conversion level as good as ~ 74 % even in 5^{th} cycle after regeneration. Leaching of < 5ppm metal content was observed in 4^{th} and 5^{th} cycle which was within the ASTM specified limitations. The thermodynamic parameters for the reaction *viz.*, activation energy E_a, $\Delta H^{\ddagger}$, $\Delta S^{\ddagger}$, $\Delta G^{\ddagger}$ were calculated as 77.3 kJ mol^{-1}, 74.2 kJ mol^{-1}, -0.064 kJ $mol^{-1}$and, + 93.2 kJ mol^{-1}respectively.

Keywords: Transesterification, Basicity, Virgin Cotton seed oil, Reusability, Heterogeneous catalyst

4.1. Introduction

To triumph over the problems associated to homogeneous base catalysts, BD synthesis by using heterogeneous catalysts has gained significant attention over the past decade. In the past few years, ordered mesoporous materials have gained a lot of attention in catalysis field due to their tunable pore size, high thermal stability, inert nature, ease of surface modification and high surface area (Tu et al., 2006). Such properties can be effectively employed to confine particles of active metals within the nano-channels of ordered mesoporous materials. In comparison to the MCM-41, SBA-15 has much more stable matrix to incorporate the nanoparticles because of its thicker walls and relatively larger pore size (Bore et al., 2005). However, most of the reported mesoporous based catalysts either demand high reaction temperature, and/or demonstrate poor reusability. Further, in most of the cases the FAMEs yield is also below the acceptable value of 96.5 %. In this chapter, in-situ synthesis of SBA-15 was performed along with simultaneously happening impregnation of active catalytic species. From the commercial aspect, the in-situ synthesis of siliceous support along with drenching with active species could remarkably contribute in cutting down the synthesis time and input energy costs.

In the present chapter, 5-Na/ZnO catalyst has been supported over mesoporous silica to improve the catalyst stability as well reusability during the triglyceride transesterification. Unlike previous chapter, the catalytically active species (Na/ZnO) was impregnated over SBA-15 in one pot preparation process to bank the time and energy employed during the catalyst preparation. The prepared heterogeneous catalyst was utilised for the BD production via transesterification of virgin cotton seed oil (VCO) with methanol. The primary reason for the selection of the cotton seed oil is its low price in comparison to other edible oils in India, and less preference as edible oil (Jha et al., 2012).The catalyst reusability and its tolerance towards high free fatty acid (FFA) levels were also evaluated.

4.2. Experimental section

4.2.1 Synthesis of 5-Na/ZnO

Sodium loaded ZnO was primed by employing wet impregnation method. In the typical synthesis, 10 g of commercially available ZnO was suspended in 100 mL of distilled water and to this 20 mL Na_2CO_3 aqueous solution (0.6 M) was added. The resulting mixture was

kept for stirring for 4 h, dried at 100 °C for 20 h, finally calcined at 400 °C for 8 h and designated as 5-Na/ZnO-400.

4.2.2. Synthesis of 5-Na/ZnO/SBA-15 catalyst

Prepared 5-Na/ZnO was impregnated over silica during a single step. During the catalyst preparation, 2 g of Pluronic acid P123 was dissolved in 65 mL HCl (1.6 M) and to this appropriate amount of 5-Na/ZnO was added while stirring for 1 h. To the resulted mixture, TEOS (4.25 g) was added with continuous stirring at 50 °C. The resulting molar composition of the mixture obtained was 1TEOS:0.02P123:p(5-Na/ZnO):6HCl:192H_2O, where p varies with loading level of 5-Na/ZnO (6-12 wt%).The mixture thus obtained was stirred for another 24 h at 50 °C, dried at 100 °C under static conditions for 24 h and finally calcined at 600 °C for 6 h in order to remove the organic template. The samples so obtained were assigned as x-Na/ZnO/SBA-15, where x represents the mass percentage of 5-Na/ZnO.

In addition, pure SBA-15 was also synthesised in order to carry out a blank reaction and to compare its physical properties with x-Na/ZnO/SBA-15.

4.2.3. Transesterification of Triglycerides

All transesterification reactions were carried out in a 100 mL, two-necked round bottom flask which was equipped with oil bath, water-cooled reflux condenser, a magnetic agitator and a thermometer. In a typical reaction of transesterification, the flask was charged with 10 g of VCO and assorted with desired molar concentration of methanol as well as catalyst and stirred at a specific temperature for fixed reaction duration. The reaction mixture so obtained was kept in a separatory funnel for 10 h to separate the two layers, the upper biodiesel and the lower glycerol layer. The FAMEs thus produced were quantified using ^{1}H-NMR analysis by applying equation (2.6) as mentioned in chapter 2.

In ^{1}H NMR of FAMEs, a new peak emerged at 3.6 ppm due to -OCH_3 protons, while peaks consequent to glyceridic protons could no longer be detected hence, opinionating the formation of fatty acid methyl esters on transesterification of VCO.

4.3. Results and discussion

4.3.1 Catalyst characterisation

4.3.1.1. Powder XRD study

Fig. 4.1a illustrates the powder XRD patterns of SBA-15 and 5-Na/ZnO modified SBA-15 synthesised *via* one-pot method. Low angle XRD patterns of all the samples show diffraction peak of high intensity at 2θ ~ 1.1° which is characteristic of *p*6*mm* hexagonal symmetry of SBA-15 and can be indexed to (100) plane. This clearly indicates that modification of SBA-15 with 5-Na/ZnO does not disturb the hexagonal symmetrical features and mesoporous nature of SBA-15 host. This indicates no significant structural change in mesoporous silica structure has taken place upon 5-Na/ZnO impregnation. However, shifting of the reflection of (100) plane towards lower angles at 0.71° upon 5-Na/ZnO loading can be explained on the basis of slight changes in the unit cell parameters because of development of strain in SBA-15 on incorporation of large sized 5-Na/ZnO moiety (Charan and Rangarao, 2015).It is also clear from the XRD results that the support is thermally stable and treatment at high temperature of 600 °C does not obviously collapse the mesostructural silica.

Powder XRD patterns of x-Na/ZnO/SBA-15 are shown in Fig. 4.1b. The peaks appearing at 2θ = 22° and 25° are attributed to the presence of amorphous SBA-15 (JCPDS card number 01-075-1526). The diffraction peaks observed at 2θ = 31.7°, 34.1°, 36.1°, 47.05°, 56.4°, could be ascribed to the existence wurtzite hexagonal form of ZnO (JCPDS card number01-071-3830). The presence of sodium in ZnO was not found to affect the wurtzite structure of ZnO. Presence of diffraction peaks at 2θ = 38.8°, 43.7°, 45.4°, 49.01°, support the formation of $Na_2Si_2O_5$during the catalyst preparation (JCPDS card number 00-022-1396). The crystallite size of the 5-Na/ZnO/SBA-15 catalyst particle was determined using Debye–Scherer method (Qadri et al., 1999) and found to be ~ 16 nm.

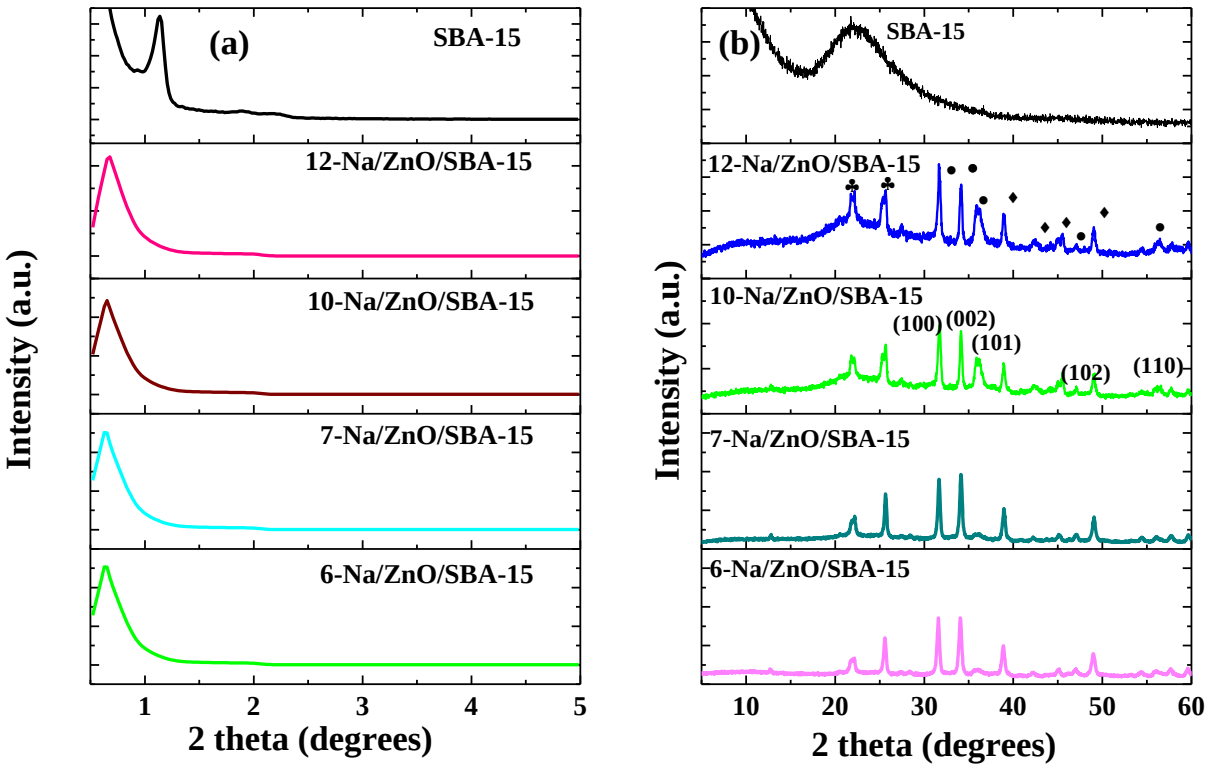

Fig. 4.1. (a) Low angle and (b) wide angle XRD patterns of x-Na/ZnO/SBA-15 catalysts. (• = wurtzite ZnO, ♦ = Sodium silicate, ♣ = amorphous silica).

4.3.1.2. Study of textural properties

With an aim to study the textural properties of the samples, nitrogen sorption isotherms were measured. Nitrogen adsorption-desorption isotherms for SBA-15 and 5-Na/ZnO loaded SBA-15 have been shown in Fig. 4.2a. It can be clearly seen that all the isotherms are type IV in nature according to the IUPAC classification. This indicates the mesoporous nature is maintained even when 5-Na/ZnO is loaded onto the SBA-15 matrix *via* one-pot method. The hysteresis loop observed for all isotherms is indicative of porosity and appears because of capillary condensation taking place in mesopores. However, on loading with 5-Na/ZnO, adsorption hysteresis, changed from H1 to H4. This change in the hysteresis loop could be ascribed to narrowing of pores of SBA-15 due to impregnation of 5-Na/ZnO (Sing et al., 1985).The textural properties of 5-Na/ZnO functionalised SBA-15 have been summarised in Table 4.1. It can be clearly observed that surface area and pore volume decreased strongly when SBA-15 was coated with 5-Na/ZnO with different loading levels. The decline in

surface area and pore volume is due to appearance of 5-Na/ZnO species in the mesopore channels and partial filling of the mesopores of SBA-15 (Sareen et al., 2015). However, it is clear from the Table 4.1, that the pore size of 5-Na/ZnO impregnated SBA-15 was greater than that of bare SBA-15 support. This observation is not unusual although. The increase in pore size can be attributed to the attachment of 5-Na/ZnO species to surface silanol groups outside the walls of pores. Therefore, pores of the SBA-15support may have expanded, because of entry of the active species (5-Na/ZnO in this study) into the pores or the attachment of 5-Na/ZnO outside the walls of pores (Berrichi et al., 2007).

Table 4.1. Textural properties, surface area, pore size and pore volume of the prepared samples.

Sample name	Surface area ($m^2 g^{-1}$)	Pore volume ($cm^3 g^{-1}$)	Pore diameter(nm)
SBA-15	442.1	0.64	4.31
6-Na/ZnO/SBA-15	115.7	0.61	32.4
10-Na/ZnO/SBA-15	17.8	0.027	29.7
12-Na/ZnO/SBA-15	13.2	0.024	29.2

Barrett-Joyner-Halenda (BJH) method was employed to compute the pore size distribution (PSD) from the adsorption branch of N_2- sorption isotherms which depicted the narrow and broad pore-size distribution of SBA-15 support material and 5-Na/ZnO impregnated SBA-15 respectively, (Fig. 4.2b). However, the decrease in the pore size can be attributed to the dispersion of 5-Na/ZnO particles on the surface of mesopores and their entry into the mesopores, hence occupancy of some pore space. The bare SBA-15 demonstrates higher surface area in comparison to the Na/ZnO impregnated SBA-15. Incorporation of the active sites over the mesoporous support, was found to reduce the surface area, however, basic sites over the resulted catalyst were found to increase which were primarily responsible for the transesterification activity. This is why the metal soaked catalyst exhibited high catalytic activity despite having the low surface area. Similar results have been reported in literature also where catalytic activity has been shown to rely more on its basic strength rather than the surface area (Sankaranarayanan et al., 2012; Patil and Deng, 2009).

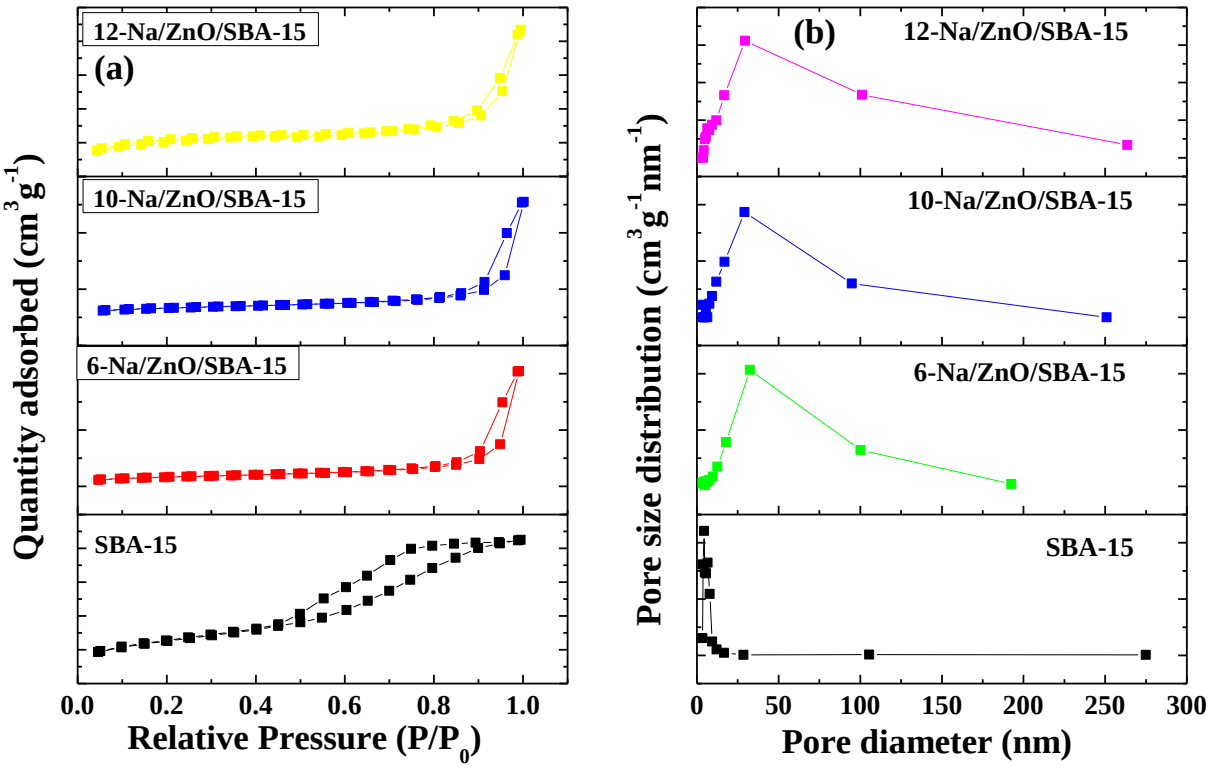

Fig. 4.2. (a) N_2 adsorption–desorption isotherms and (b) pore size distribution of x-Na/ZnO/SBA-15 catalysts.

4.3.1.3. FE-SEM study

10-Na/ZnO/SBA-15 catalyst was characterised by FE-SEM technique in order to study the morphology of the prepared catalyst. The FE-SEM analysis (Fig. 4.3a) show the aggregates of nearly oval or hexagonal particles and these aggregates consist of small sized primary particles. The particles tend to stay agglomerated and stacked over each other. The corresponding elemental mapping of the catalyst is demonstrated by coloured images (Fig.4.3b).The mapping of the catalyst depicted the homogeneous distribution of Na and Zn species in the siliceous framework.

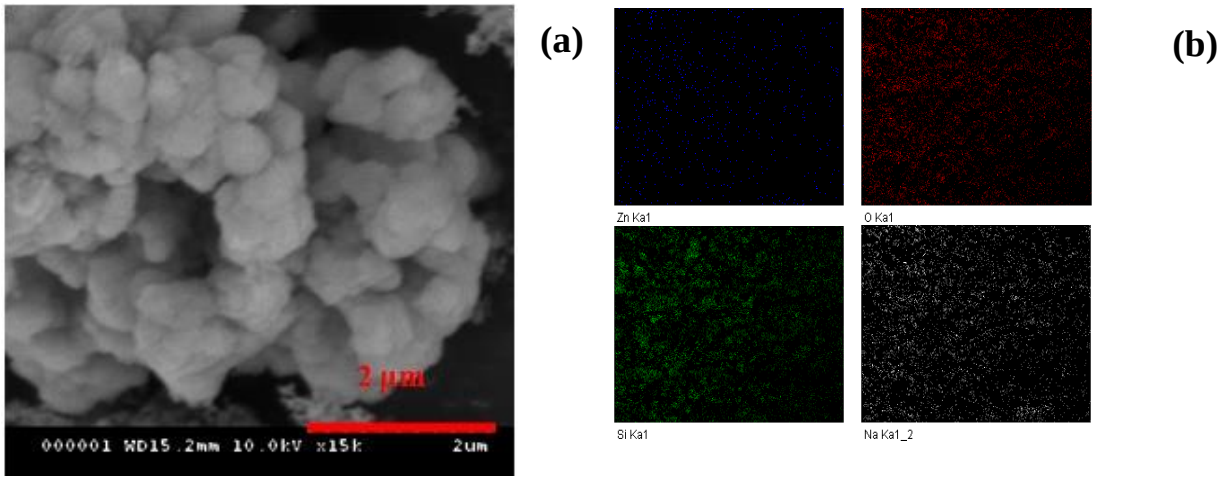

Fig. 4.3. (a) FE-SEM image of 10-Na/ZnO/SBA-15 (b) Elemental mapping of 10-Na/ZnO/SBA-15 catalyst.

4.3.1.4. HRTEM study

HRTEM analysis of 5-Na/ZnO functionalised SBA-15 is depicted in Fig 4.4.The micrographs revealed the well defined arrays of mesoporous channels arranged in 2D hexagonal *p*6*mm* structure which is characteristic of SBA-15 (Wu et al., 2014). Presence of cubic shaped 5-Na/ZnO particles over SBA-15 surface can be clearly seen against the lighter background of SBA-15 matrix (Fig.4.4a). It is clear from the HRTEM analysis that the functionalisation of SBA-15 with 5-Na/ZnO *via* one-pot method didn't disrupt its morphology and hexagonal structure, which is a characteristic of SBA-15.

At lower resolution (Fig 4.4b) HRTEM analysis of the catalyst confirms the homogeneous distribution of 5-Na/ZnO particles over the surface of SBA-15 matrix which is in agreement with the XRD study. Presence of Na and Zn in the EDS analysis of 10-Na/ZnO/SBA-15 further supports the Na/ZnO impregnation over the SBA-15 surface (Fig. 4.4c). The SAED pattern (Fig. 4.4d) of the catalyst depicts the crystalline character of catalyst due to the presenceof diffraction spots, corresponding to the (100), (002), (101), (102) planes of wurtzite crystal structure of ZnO which is also consistent with the aforementioned XRD analysis of the same catalyst. The presence of slightly diffused character in the rings is due to the amorphous nature of SBA-15 material present in the catalyst.

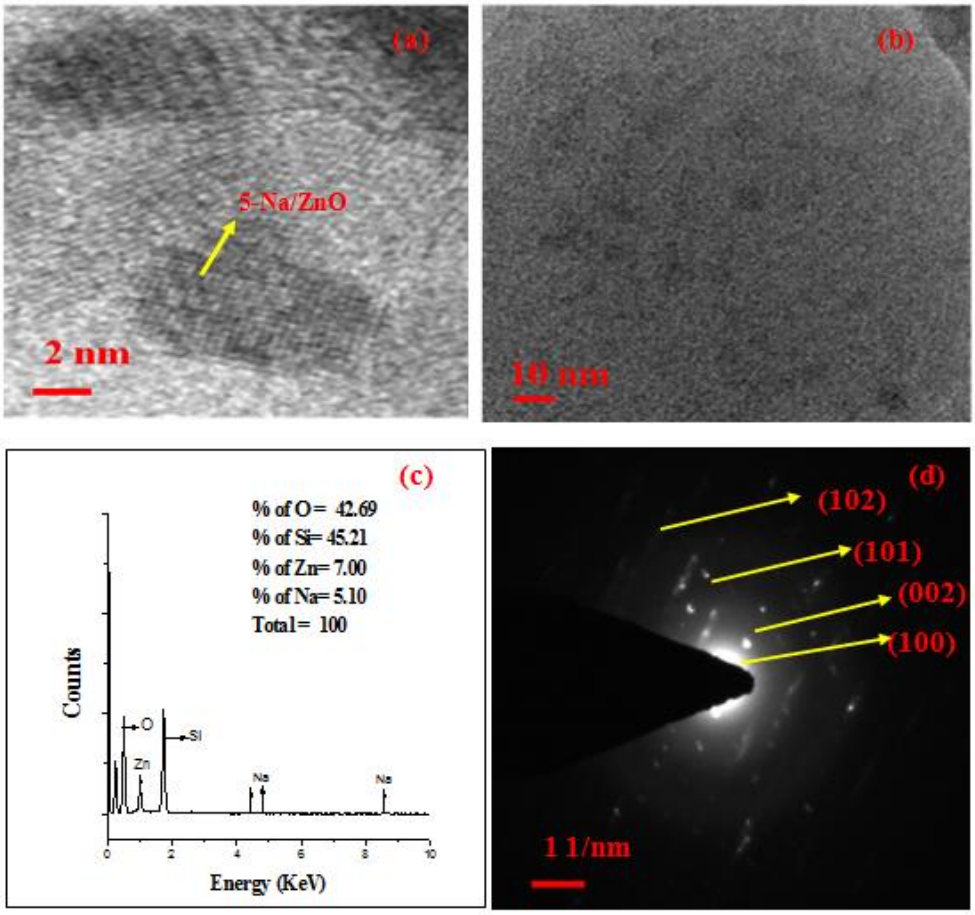

Fig. 4.4. HR-TEM images of (a) hexagonal arrays of SBA-15 and loading of 5-Na/ZnO species on SBA-15 and (b) dark spots signify the loading of 5-Na/ZnO on surface of silica, (c) EDS pattern of 10-Na/ZnO/SBA-15 and (d) SAED pattern of 10-Na/ZnO/SBA-15 catalyst.

4.3.1.5. Hammett indicator study

In order to quantify the strength and number of surface basic sites, Hammett indicator test was performed. The test was performed using trichloroacetic acid as titrant to quantify the basic sites of the prepared catalysts. As could be clearly seen from Table 4.2, the bare SBA-15 support material, although possesses some inherent basicity, but it was not found strong enough to initiate the catalytic activity for transesterification. 5-Na/ZnO impregnation increases the Lewis basic sites in the catalyst and these Lewis basic sites are responsible to initiate the transesterification reaction of the triglyceride molecules. As the 5-Na/ZnO concentration was increased, the basicity of the catalyst was found to increase. However, maximum activity of the catalyst was observed at 10 wt% loading of the active moiety,5-

Na/ZnO on SBA-15 and hence, it was selected as the optimum catalyst for carrying out the further studies.

Table 4.2. Comparison of basic strengths, and TOFs for the x-Na/ZnO/SBA-15 catalysts.

Catalyst	Indicators used				Total basicity (mmol g^{-1})	TOF ($\times 10^{-4}$ h^{-1})
	Bromothymol blue ($H_0 \leq +7.2$)	Phenolphthalein ($H_0 \leq +9.3$)	Nile blue ($H_0 \leq 10.1$)	Trapeolin ($H_0 \leq +11.1$)		
SBA-15	NCC	0.12	0.36	0.39	0.87	-
6-Na/ZnO/SBA-15	0.26	0.45	0.60	0.69	2.0	6.8
7-Na/ZnO/SBA-15	0.43	0.61	0.71	0.82	2.57	7.8
8-Na/ZnO/SBA-15	0.58	0.79	0.92	1.4	3.69	8.3
10-Na/ZnO/SBA-15	0.69	1.3	1.4	1.8	5.19	11
12-Na/ZnO/SBA-15	0.71	1.4	1.45	1.9	5.46	11

** NCC stands for no colour change*

**TOF is calculated at 50% level of conversion ; Reaction conditions = methanol to oil molar ratio of 24 : 1 at a Temperature of 65 °C, in the presence of 12 wt% of catalyst with respect to oil at 600 rpm stirring speed.*

4.3.1.6. XPS study

In order to further confirm the incorporation of active metallic species into SBA-15 and determine their elemental state, XPS analysis was carried out. As depicted in Fig. 4.5a, the peak present at 103.3 eV corresponds to Si 2p signal arising from silica of SBA-15 support (Pal et al., 2014). The peak observed at 102.8 eV is due to Si-O bond at the surface, whereas the peak observed at 104.1 eV due to the $SiOH_2^+$ species over the catalysts (Wagner et al., 1982; Negrila et al., 2008). The peak due to O 1s could be fitted into 3 gaussian peaks (Fig. 4.5b).The small peak at 530.6 corresponds to lattice oxygen present in ZnO. Another peak at 532 eV is due to chemisorbed oxygen or weakly bonded oxygen of absorbed water. The strong peak at 533 eV is due to oxygen present in amorphous SBA-15 support (Reddy et al., 2008). The peak appearing at 1070.6 corresponds to Na 1s signal (Precht et al., 2016) (Fig. 4.5c) whereas the peak present at 1021.8 eV is due to (Lu et al., 2009) the core level of Zn $2p_{3/2}$ signal in ZnO (Fig. 4.5d).

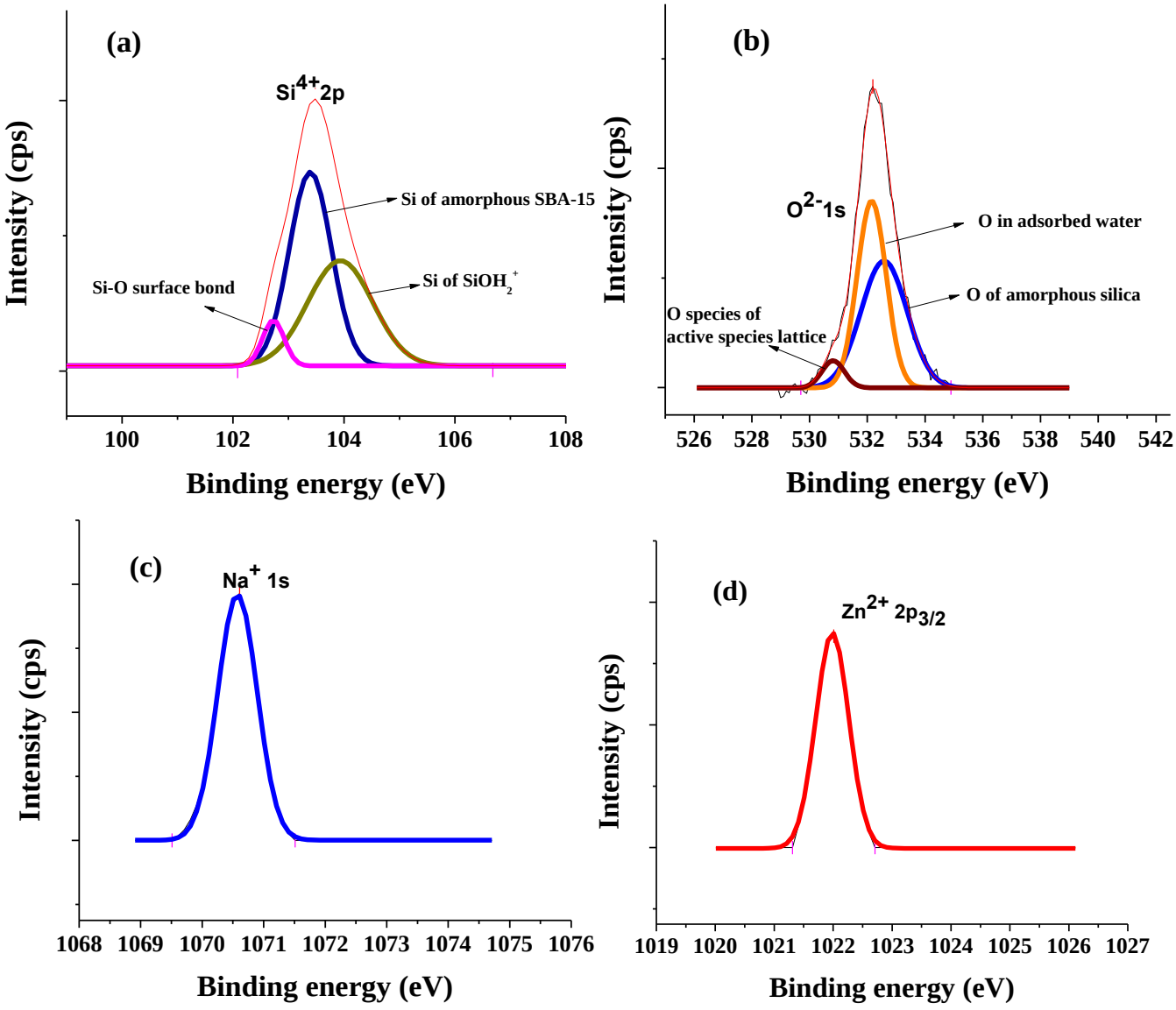

Fig. 4.5. XPS spectra of (a) Si (b) O (c) Na and (d) Zn present in 10-Na/ZnO/SBA-15 catalyst.

4.3.1.7. FT-IR spectroscopy

FT-IR spectra of bare SBA-15 and 10-Na/ZnO/SBA-15 have been compared in Fig. 4.6. In the FTIR spectra of untainted SBA-15, peaks observed at 1,050 and 800 cm^{-1} can be attributed to Si–O–Si asymmetric and symmetric stretching vibrations, respectively. The peak centred at 1630 cm^{-1} can be assigned to bending vibrations of the adsorbed water molecules (Vunain et al., 2013).Upon Na/ZnO impregnation over SBA material, few additional peaks were observed at 450, and 590-620 cm^{-1} due to Na-O bond, and Zn-O stretching modes,

respectively (Andrews, 1969; Babu et al., 2013). The peak observed at 970 cm^{-1} is due to the Si-O-Zn/Na to support the loading of 5-Na/ZnO over SBA-15.

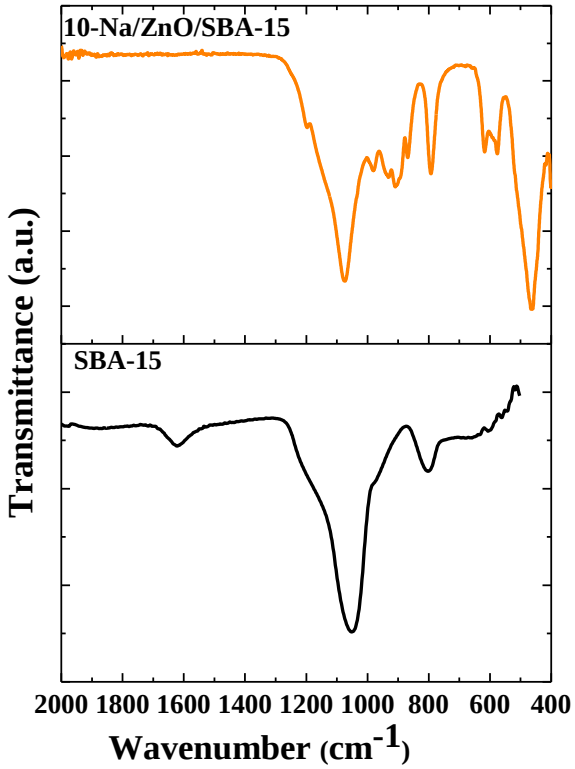

Fig. 4.6. FTIR spectra of bare SBA-15 and 10-Na/ZnO/SBA-15 catalyst.

4.3.2. Investigation of reaction parameters

The catalytic activity and efficiency of the prepared catalysts was tested for methanolysis of VCO. Keeping in mind the economic factors, it is imperative to determine the parameters which are finest to make BD production economically sound. The reaction parameters for transesterification were optimised with an objective to achieve the maximum yield of FAMEs in least possible time. The optimised reaction conditions were achieved by changing one parameter at one timeout of the following: (i) impregnated 5-Na/ZnO concentration, (ii) concentration of catalyst (iii) molar ratio of methanol to oil and (iv) reaction temperature

4.3.2.1. Effect of 5-Na/ZnO amount on BD production

SBA-15 is a thermally stable mesoporous material which acts as a great support material with high surface area to impregnate and confine the active metals into the nano-channels of mesoporous materials. Owing to the narrow pore size distribution (2-50 nm), SBA-15 has also been reported as an excellent molecular sieve for the small molecules as well as large biomolecules (Wu et al., 2014; Lee et al., 2004). It has been employed as an adsorbent for CO_2 with much more adsorption capacity than zeolites and even activated charcoal (Do Nascimento et al., 2017). The appropriate SBA-15 pore size has also been proven advantageous for the product selectivity, *e.g.*, during the core-shell composite molecular sieves catalyzed aromatisation reaction, improved selectivity for the xylene production was obtained (Shi et al., 2016). In another report, SBA-15 functionalized with amine group was tested for adsorptive exclusion of lead (II) out of aqueous solutions. The results revealed that adsorption as high as 93% was achieved in the range of pH 5-6 (Morales et al., 2012).

Nevertheless, SBA-15 alone has very less inherent basicity/acidity as also supported by the Hammett indicator study (Table 4.2) and hence, native SBA-15 required high temperature and pressure to catalyze the chemical reactions. In our study as well as in literature bare SBA-15, was found to show almost no activity when employed as a catalyst during the transesterification of triglycerides (Li and Rudolph, 2008). However, the activity of the SBA-15 could be improved by impregnating it with the appropriate active species (5-Na/ZnO in present chapter).

To determine the optimal amount of 5-Na/ZnO impregnation on SBA-15, a string of catalysts wereprepared by altering 5-Na/ZnO concentration from 6-12 wt%. Transesterification reactions were carried out at 65 °C, using a 24:1 MeOH/oil molar ratio and 12 wt% (with respect to oil) of catalyst amount. The complete transesterification of VCO was achieved in 4 h (Fig. 4.7a) when 5-Na/ZnO concentration was increased from 6 to 10 wt%. The rise in reaction rate with increasing the 5-Na/ZnO amount on SBA-15 is expected because there will be a consequent rise in amount of basic sites in the catalyst as given in Table 4.2. A further increase in 5-Na/ZnO concentration (from 10 to 12 wt %) was not found to significantly affect the FAMEs yield on transesterification of VCO. Hence, 10 wt% of 5-Na/ZnO on SBA-15 was chosen as the optimum concentration of active catalytic species. Any further increase in concentration of 5-Na/ZnO (from 10-12 wt %) was not found to significantly affect the FAMEs yield. In the present chapter, maximum content of active basic sites were observed

with 12 wt% loading of active moiety. But, both the catalysts (with 10 wt% and 12 wt% loading) depicted similar TOFs. Hence, 10 wt% of 5-Na/ZnO loading was selected as most favourable concentration for loading on mesoporous silica. The observations are in queue with the similar results reported in literature, where any further increase beyond a certain level in the loading of active species did not upshot the reaction rate (Brahmkhatri and Patel, 2011). High activity of the catalyst was obtained due to its robustly basic sites. As clearly mentioned in Hammett indicator study, the basicity of the catalyst increases as the amount of impregnated active species increases. Impregnation of active species (5-Na/ZnO) gives rise to the Lewis basic sites in catalyst which are accountable to commence the transesterification reaction.

4.3.2.2. Effect of amount of the catalyst

For any chemical process, the quantity of catalyst required has a very significant effect on the production cost. To evaluate the optimal catalyst amount, the methanolysis reactions were carried out at 65 °C, utilising a 24:1 MeOH/oil molar ratio in the presence of 10-Na/ZnO/SBA-15 catalyst and the concentration of catalyst was mottled from 6 to 14 wt% (catalyst/oil). The FAMEs yield was found to show an increment with the increase in catalyst concentration from 6 to 12 wt% as shown in Fig.4.7b.This is obvious because the increase in the catalyst concentration provides more amount of active catalytic sites. The rate of reaction increased proportionally with catalyst concentration from 6 to 12 wt%. Any further augment in catalyst amount (12 to 14 wt%) didn't affect the reaction rate and yield to any significant extent. Thus, all the reactions were carried out with 12 wt% catalyst at 65 °C temperature.

The reason for this observation could be that high amount of catalyst makes the reaction mixture thicker and raises its viscosity. This leads to ineffective mixing of the reactants, which in turn, leads to lesser contact between the triglyceride and methanol thus, making the biodiesel formation slow and decreases FAMEs yield. It is also important to mention that the addition of excessive amount of catalyst causes formation of an emulsion, which as a consequence, leads to the gel formation. This hinders separation of glycerol and, thus, declining the apparent FAMEs yield (Kim et al., 2004 ; Encinar et al., 2005).

4.3.2.3. Effect of methanol to oil molar ratio

One of the major parameters determining the rate of transesterification of triglyceride and FAMEs yield is the MeOH/oil molar ratio. Ideally, the stoichiometric molar ratio necessary, for transesterification reaction to go to completion is 3:1 (methanol/triglyceride). Since the transesterification reaction is reversible, it is frequently carried out by utilising surplus amount of alcohol to facilitate the forward reaction and prevent the back reaction (Kulkarni et al., 2006). The excess alcohol will improve the FAMEs yield by shifting equilibrium towards the forward direction.

In order to determine the optimal methanol/oil molar ratio, a string of methanolysis reactions were performed with 12 wt% of 10-Na/ZnO/SBA-15at 65 °C and varying MeOH/oil molar ratio from 10:1 to 30:1.It was found that reaction rate increased as the methanol/oil molar ratio was raised from 9:1 to 24:1. The reaction went to completion within 4 h when 24:1 methanol to oil ratio was taken. Any further increment in the methanol/oil molar ratio did not affect the rate of reaction to any significant extent and complete conversion was obtained within time not less than 4 h (Fig. 4.7c).

Therefore, 24:1 methanol to oil molar ratio was chosen to be optimum to achieve complete transesterification of VCO and all transesterification reactions were executed by employing the same MeOH/ oil molar ratio in the present chapter. If molar ratio of MeOH to oil greater than 24:1 is employed, it will cause the interference of excess methanol in the glycerol separation from the BD layer because of better glycerol solubility. Consequently, some amount of the diluted glycerol persists in the BD phase which causes decline in apparent BD yield due to foam formation. Moreover, if glycerol persists in solution, it causes the reaction equilibrium shift towards the backward direction, hence, decreasing the BD yield (Barnwal and Sharma, 2004).

4.3.2.4. Effect of reaction temperature

Temperature has a momentous role in transesterification reaction. As the reaction temperature is increased, the reaction rate and FAMEs yield also tends to increase. Nevertheless, literature reports that, if given sufficient time, transesterification can satisfactorily proceed at ambient temperatures when alkaline catalysts are used (Srivastava and Prasad, 2000).

In the present chapter, 10-Na/ZnO/SBA-15 catalyzed transesterification was carried out at different temperatures in order to evaluate the effect of reaction temperature on rate of reaction by employing 24:1 MeOH/oil molar ratio of oil to methanol and 12 wt% of catalyst.

It was observed that the rate of methanolyis augmented when reaction temperature was raised from 35 to 65 ºC as shown in Fig. 4.7d. Anymore increase in reaction temperature was not found to affect the FAMEs yield or reaction rate significantly. This observation can be attributed to the formation of vapours of methanol and its consequent loss from the reaction mixture. High temperature will lead to evaporation and subsequent loss of methanol from the reaction mixture. The vaporized methanol will no more remain in contact with the reactants for enough time and thus, the biodiesel yield will not improve (Bo et al., 2007) on increasing the reaction temperature beyond 65 °C. Thus, present chapter reports more than 98% FAMEs yield even at 65 °C and one atmosphere pressure to suggest the efficacy of the catalyst. Similar observation was also well documented in literature, *e.g.*, in a recent research mesoporous calcium titanate and W/Ti/SiO_2 has been utilised for BD production where the optimum reaction temperature observed was 65 °C and further increment could not help the reaction rate to improve any further (Yahya et al., 2016; Kaur et al., 2018). Literature also reports the transesterification at temperatures as high as 200 °C in closed reactor under high pressure condition. For an instance, Ti/SBA-15 has been reported for methanolysis of jatropha oil (Chen et al., 2014). The catalyst employed temperature of 200 °C and yielded 90% FAMEs yield within 3 h time. Similarly, MgO/SBA-15 was used for transesterification of jatropha oil employing 6 wt% of catalyst at 200 °C temperature and yielded 81.4% conversion levels (Li and Rudolph, 2008). Maintaining, such a high temperature during the reaction not only will demand the high energy but also requires the complicated reactor design to sustain the high pressure generated during the reaction.

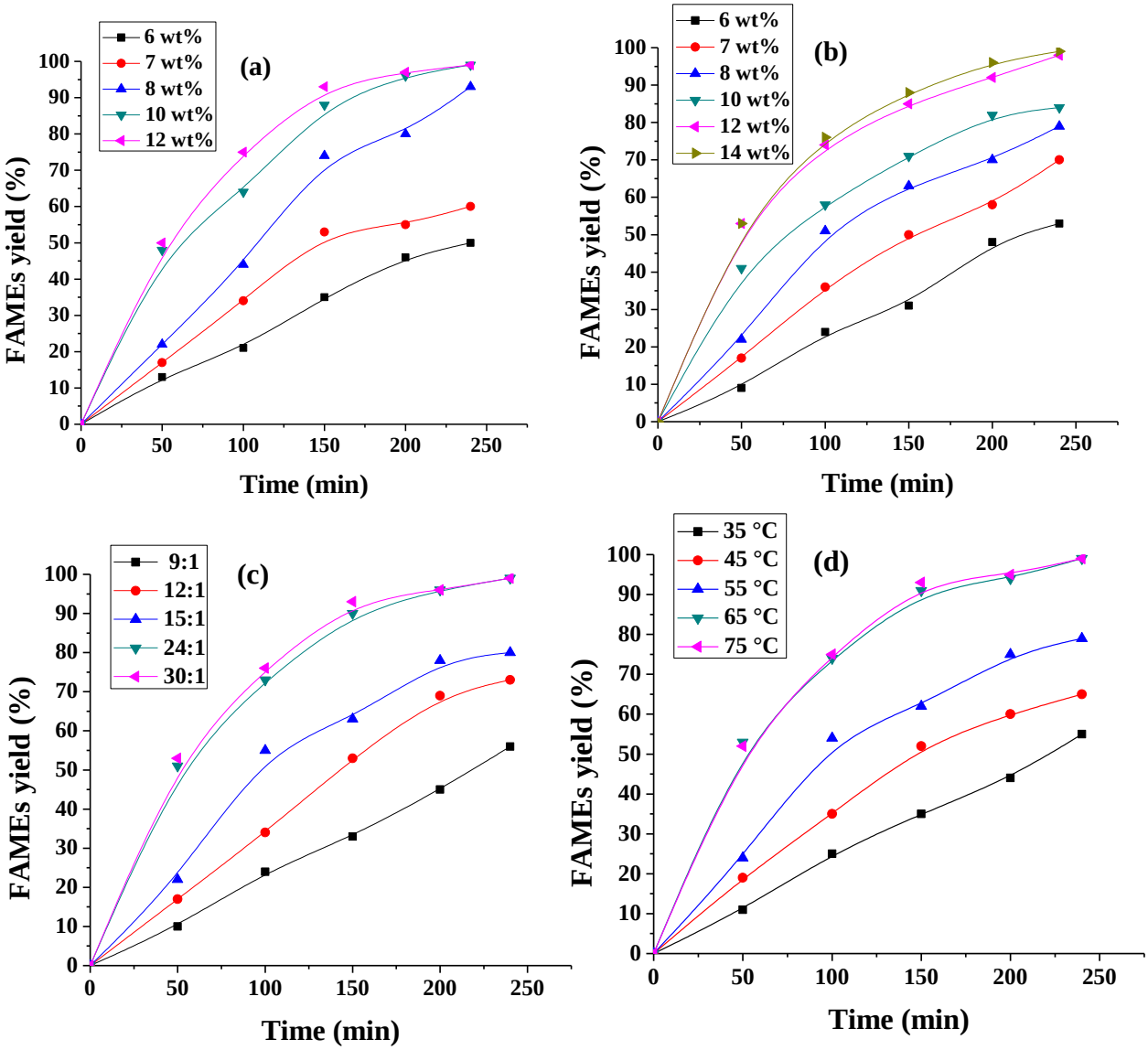

Fig. 4.7. Effect of (a) 5-Na/ZnO concentration on SBA-15, (b) catalyst concentration, (c) methanol/oil molar ratio and (d) reaction temperature on methanolysis of VCO.

4.3.3. Plausible Mechanism:

The plausible mechanism for the FAMEs formation during the transesterification reaction is demonstrated in Fig. 4.8. In the present study, the bare silica support was not found to demonstrate any catalytic activity and hence, transesterification activity of the catalyst could be attributed to the Lewis basic sites (O^{2-}) originating from the impregnated 5-Na/ZnO species. The literature reports (Eckey, 1956) the formation of strong nucleophile, methoxide anion (CH_3O^-), *via* proton abstraction by Lewis basic sites which is considered as reaction initiating step as shown in Fig. 4.8 as step-I. This anion is strongly basic in nature and in step-

II, attacks the carbonyl carbon of triglyceride molecule (1) which is electrophilic in nature. This paves the way to the intermediate formation of a tetrahedral alkoxycarbonyl (2) over the surface of catalyst (Ma and Hanna, 1999). Subsequently, in step-III, the intermediate (2) reacts with the H^+, formed during the methanol deprotonating in step-I, to form the intermediate (3).In the ultimate step-IV, intermediate (3) disintegrates to yield the FAME and diglyceride molecule (Faungnawakij et al., 2012). Diglyceride molecule further reacts with another methoxide ion to yield monoglyceride and another FAME molecule. The reaction repeats again with monoglyceride to finally yield glycerol and third FAME molecules.

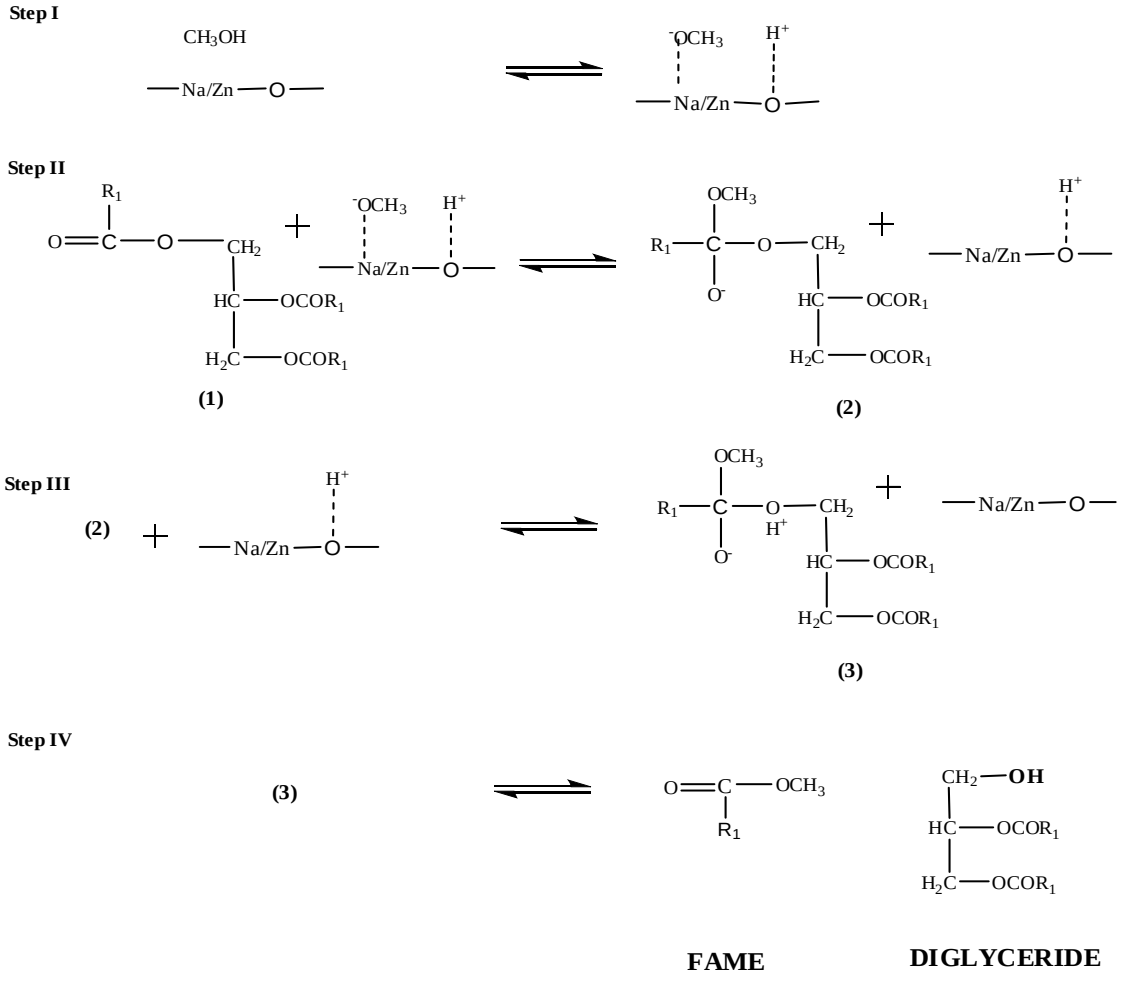

Fig. 4.8. Proposed mechanism of transesterification catalysed by 10-Na/ZnO/SBA-15.

4.3.4. Effect of added FFA content

In order to determine the efficacy of 10-Na/ZnO/SBA-15 catalyst towards the methanolysis of higher FFA containing VCO, reactions were carried out under optimised conditions with

12 wt% of catalyst at a temperature of 65 °C and employing methanol to oil molar ratio 24:1.To find the maximum FFA tolerance, methanolysis of VCO was performed by adding palmitic acid in to the reaction mixture. When externally added FFA concentration was increased (>1 wt%), catalytic efficiency was found to reduce and the catalyst could not perform the complete transesterification reaction even after a longer reaction time (as long as 20 h). 19% FAMEs yield was achieved when FFA content of VCO was 1.4 wt% (0.4 wt% already present + 1 wt% externally added). Hence, the present catalyst was found to be suitable for transesterification of the feedstock with very less FFA contents.

The deactivation of catalyst in response to higher FFA content can be explained through neutralisation or partial blockage of active basic sites of catalyst by the interaction with polar carboxyl group of FFA to explain the decline in the catalyst action in the presence of higher FFA content (Kaur and Ali, 2014).

4.3.5. Reusability and homogeneous contribution

Solid catalysts are profitable over their homogeneous counterparts owing to their easy separation from the reaction muddle. Thus, they reduce the requirement of product washing and thereby reducing the pollutants generated during the process. Separated catalyst could be reused to catalyze the next reaction cycles and thus may reduce the effective cost of the chemical transformation.

With an aim to determine the reusability of the present catalyst and decline in its activity, transesterification with 10-Na/ZnO/SBA-15 was performed under optimised conditions. The 10-Na/ZnO/SBA-15 catalyst was recovered *via* filtration method and subjected to several runs of washing with hexane as well as methanol to take away or eliminate polar as well as non-polar contaminants. The catalyst was dried at 110 °C and then calcined at 600 °C.

The regenerated catalyst was utilised to carry out transesterification for 5 successive cycles employing the similar experimental conditions and regeneration method. The reused catalyst was found to be capable of yielding complete conversion of VCO to FAMEs during 3 consecutive runs. However, during the 4^{th} and 5^{th} run, 93% and ~74% FAMEs yield, respectively, were obtained. It can be said that mesoporous SBA-15 support stabilises the active catalyst and helps in improving the recyclability which is a clear advantage of the catalyst under study. The TOF and FAMEs yield of the catalyst in every successive run have been compared in Fig. 4.9.

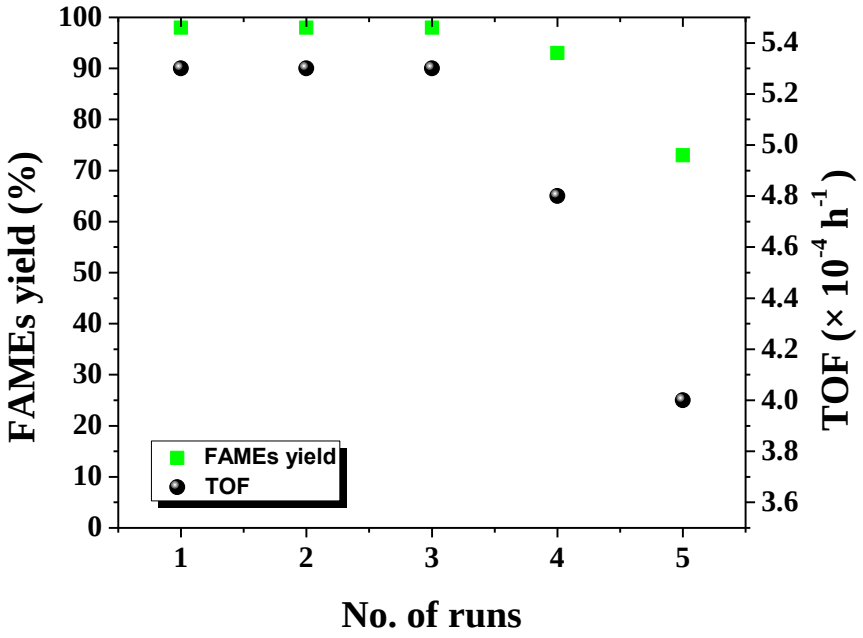

Fig. 4.9. Reusability of 10-Na/ZnO/SBA-15 catalyst (Reaction conditions: MeOH/oil molar ratio = 24:1; Catalyst amount = 12 wt%; Temperature = 65 °C, reaction time= 4 h).

In the present study 74% FAMEs yield was obtained during 5th run to signify the reduction in the catalyst efficacy. The gradual dissolution of the catalytically potent species in the reaction media may be the reason behind the loss of the catalyst activity. In case of alkali metal supported catalysts, the leaching of the alkali metals ions out of support material has been repeatedly reported in the literature (Sivasamy et al., 2009) and is associated with the loss in catalytic activity. In order to establish the extent of the leaching of active species from the prepared catalyst, the metal analysis in the reaction mixture was performed by using MP-AES technique and the results are shown in Table 4.3.

Table 4.3. Dissolved metal ion concentration (ppm) in reaction mixture after every catalytic cycle.

Catalytic run	Metal concentration (ppm)					
	Biodiesel layer			Glycerol layer		
	Si	Na	Zn	Si	Na	Zn
I	*NF*	*NF*	*NF*	*NF*	*NF*	*NF*
II	*NF*	*NF*	*NF*	*NF*	*NF*	*NF*
III	*NF*	*NF*	*NF*	*NF*	*NF*	*NF*
IV	*NF*	0.24	*NF*	*NF*	0.42	*NF*
V	4.50	0.44	0.60	0.34	0.56	*NF*

**NF= not found*

As could be seen from the MP-AES results, no significant metal leaching was observed during first three catalytic runs. However, the metal content in reaction mixture was found to increase during 4th and 5th cycle to support the partial dissolution of the catalyst. The loss of active metal from the catalyst could be ascribed to the partial loss of catalytic activity during 5th run.

As can be clearly seen from Table 4.3, even after 5th cycle, total concentration of metal present in BD layer was found to be within ASTM specified limitations (*i.e.* < 5ppm). From commercial aspect of biodiesel production, this is a very significant observation in the present study since the BD produced would not require the much complicated and tedious washing step thereby preventing the generation of harmful effluents which is unavoidable in case of homogeneous catalysts. This is an important result since it clearly enlightens the fact that present catalyst structure is fairly stable even after successive reuse during 4 cycles and can bear the washing and recalcination treatments.

For quantification of the contribution of dissolved catalyst in overall activity, and validate the heterogeneous manner of activity of the prepared catalyst, hot filtration test was performed under optimal reaction conditions. The VCO transesterification was carried out under the optimized conditions for 1 h, after that the catalyst was separated *via* filtration method and reaction was allowed to continue for more 3 h. As it could be clearly seen from the Fig. 4.10, that no increment in FAMEs yield was observed when the reaction was continued in absence

of catalyst to support that (i) the mode of action the prepared catalyst is heterogeneous and (ii) the leached metal ions have no significant contribution in catalytic activity.

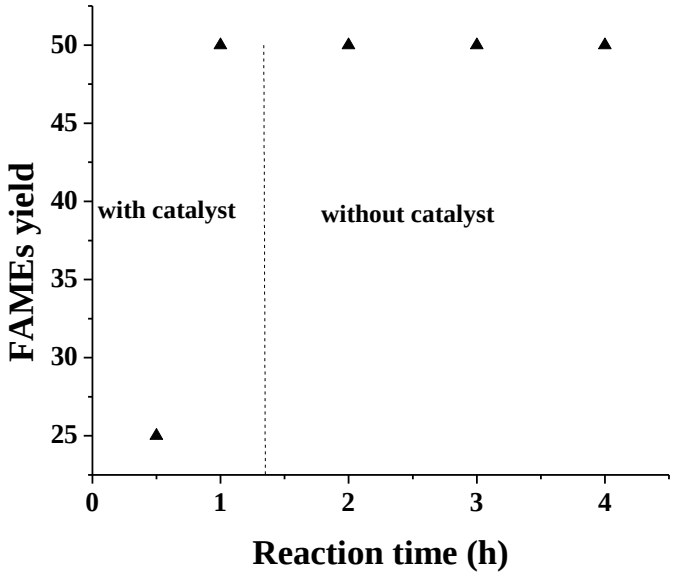

Fig. 4.10. Hot filtration test for 10-Na/ZnO/SBA-15 catalyzed transesterification.

In addition to MP-AES metal analysis, XRD study of reused catalyst was also carried out. Although, there was no structural difference observed in the XRD patterns of fresh and reused catalysts, (Fig. 4.11) but, crystallite size of reused catalyst was found to be almost twice of the fresh catalyst *i.e.*~ 34 nm. This could be due to the partial agglomeration of the catalyst to form the large particle size which may cause the reduction in the surface active sites causing decline in activity after 5^{th} cycle (Xie and Yang, 2012). Here, it is to be noted that, crystallite size of the reused catalyst (after 5 cycles) is almost doubled in comparison to the original one which is also accompanied with the partial loss of active sites as suggested by the metal analysis of the reaction mixture (Table 4.3). Consequently, basic sites available over catalyst surface decrease which reflects in lower FAMEs yield.

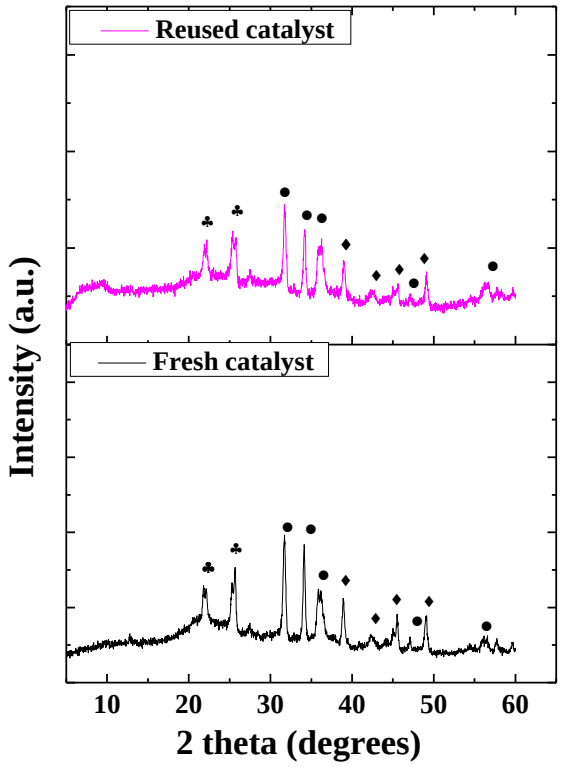

Fig. 4.11. Comparison of the XRD patterns of fresh and reused 10-Na/ZnO/SBA-15 (• = wurtzite ZnO, ♦ = Sodium silicate, ♣ = amorphous silica).

4.3.6. Kinetic study

With the intention to find out the rate constants at different temperatures, the transesterification of VCO was performed under the optimised reaction conditions by altering the temperature range from 35 to 65 °C. The plot of -ln (1-X_{me}) *versus* 't' showed that the plots were linear in nature similar to those obtained in Chapter 3. From the linear nature of the plot (R^2 = 0.93)., it could be deduced that the reaction has followed kinetics of first order (Zhang et al., 2010). The rate constant value at 65 °C was found to be 0.0167 min^{-1}.

To calculate energy of activation and (E_a), Arrhenius equation (2.3) was employed whereas the heat of reaction ($\Delta H^{\ddagger}$) and its entropy of activation ($\Delta S^{\ddagger}$) were determined using Eyring–Polanyi equation (2.4) discussed in chapter 2. These thermodynamic parameters, $\Delta H^{\ddagger}$ and $\Delta S^{\ddagger}$ were calculated from the slope {$-\Delta H^{\ddagger}/R$} and intercept {$\ln(k_B/h)+\Delta S^{\ddagger}/R$} of Eyring-Polanyi plot, respectively.

The activation energy of the reaction was found to be 77.3 kJ mol^{-1}. The R^2 value of Arrhenius plot (ln K *vs* 1/T) was found to be 0.99. The observed value of activation energy for the reaction was found within the range (33-84 kJ mol^{-1}) reported for transesterification of

vegetable oils by heterogeneous catalysts (Sun et al., 2008). Since, this value of E_a found was greater than 25 kJ mol^{-1}. It supports that reaction is chemically controlled and not by diffusion or mass transfer limitations (Patel and Brahmkhatri, 2013). Table 4.4 depicts the experimentally determined values of all thermodynamic parameters.

Table 4.4. Experimentally determined values of thermodynamic parameters.

Thermodynamic Parameter	**kJ mol^{-1}**
Activation Energy (E_a)	77.3
Enthalpy of Reaction ($\Delta H^{\ddagger}$)	74.2
Entropy of Reaction ($\Delta S^{\ddagger}$)	-0.064
Gibbs Free Energy ($\Delta G^{\ddagger}$)	93.2

The $\Delta G^{\ddagger}$ for the 10-Na/ZnO/SBA-15 catalysed transesterification reaction was found to be + 93.2 kJ mol^{-1}. The positive value of $\Delta G^{\ddagger}$, clearly shows that 10-Na/ZnO/SBA-15 catalysed transesterification of VCO is a non-spontaneous reaction and the energy level of transition state is greater than the energy level of reactants (Pogaku et al., 2012).

A negative value of $\Delta S^{\ddagger}$ depicts that there is more order in transition state than that of reactants when present in their ground or native state. Thus, the associative pathway has been followed by methanolysis reaction catalysed by 10-Na/ZnO/SBA-15 (Kaur and Ali, 2015). Further, from the positive value of $\Delta H^{\ddagger}$, it can be concluded that the reaction is endothermic by nature and needs heating from an external source in order to form the intermediate transition state and move in forward direction (Beall, 1994).

4.4. Conclusions

Present work depicts the synthesis and utilisation of 10-Na/ZnO/SBA-15 assolid and reusable catalyst for the production of biodiesel, from virgin cotton seed oil. 5-Na/ZnO was impregnated on SBA-15 by one-pot method. Under the optimized conditions of methanol to oil molar ratio of 24:1, catalyst amount of 12 wt%, and 65 °C temperature, > 98% FAME yield was obtained in 4 h of reaction duration. Under the mentioned reaction conditions, transesterification of virgin cotton seed oil followed (pseudo) first order kinetic equation. The catalyst exhibited good reusability for it maintained original activity (98% FAMEs yield) during 3 catalytic runs. 74% FAMEs yield was obtained during 5^{th} catalytic cycle. Metal

analysis study exhibited < 5 ppm leaching of metal contents into reaction media during consecutive catalytic runs. From, application point of view, least metal leaching due to siliceous support is significant observation in present chapter.

References

Andrews, L., 1969. Infrared Spectra and bonding in the sodium superoxide and Sodium peroxide molecules. J. Phys. Chem. 78, 3922-3928.

Babu, S., Reddy, A.R., Sujatha, C.H., Reddy, K.V., Mallika, A.N., 2013. Synthesis and optical characterization of porous ZnO. J. Adv. Ceramics 3, 260-265.

Barnwal, B.K., Sharma, M.P., 2004. Prospect of biodiesel production from vegetable oil in India. Renew. Sustain. Energy. Rev. 238-246.

Beall, H., 1994. Probing Student Misconceptions in Thermodynamics with In-Class Writing. J. Chem. Educ. 71, 1056-1057.

Berrichi, Z.E., Louis, B., J.P. Tessonnier, J.P., Ersen, O., Cherif, L., Ledoux, M.J., Huu, C.P.,2007. One-pot synthesis of Ga-SBA-15: Activity comparison with Ga-post-treated SBA-15 catalysts. Appl. Catal. A: Gen. 316, 219-225.

Bo, X., Guomin, X., Lingfeng, X., Ruiping, W., Lijing, G., 2007. Transesterification of palm oil with methanol to biodiesel over a KF/Al_2O_3 heterogeneous base catalyst. Energy Fuels 21, 3109-3112.

Bore, M.T., Pham, H.N., Switzer, E.E., Ward, T.L., Fukuoka, A., Datye A.K., 2005. The role of pore size and structure on the thermal stability of gold nanoparticles within mesoporous silica. J. Phys. Chem. B. 109, 2873-2880.

Brahmkhatri, V., Patel, A., 2011. 12-Tungstophosphoric acid anchored to SBA-15: An efficient, environmentally benign reusable catalysts for biodiesel production by esterification of free fatty acids. Appl. Catal. A: Gen. 403, 161-172.

Charan, P.H.K., Rangarao, G., 2015. Textural and morphological studies of transition metal doped SBA-15 by co-condensation method. J. Chem. Sci.5, 909–919.

Chen, S.Y., Mochizuki, T., Abe, Y., Toba, M., Yoshimura, Y., 2014. Ti-incorporated SBA-15 mesoporous silica as an efficient and robust Lewis solid acid catalyst for production of high quality diesel fuels. Appl. Catal. B: Environ. 148-149, 345-346.

Do Nascimento, A.R., De Figueredo, G.P., Da Costa, T.R., De F Melo, M.A., De A Melo, D.M., De Souza, M.J.B., 2017. Thermodynamics of CO_2 adsorption on mesoporous materials impregnated with nickel. Ceramica, 63, 524-529.

Eckey, E.W., 1956. Esterification and interesterification. J. Am. Chem. Soc. 33, 575-579.

Encinar, J.M., Gonzalez, J.F., Rodriguez, R. A., 2005. Biodiesel from used frying oil, variables affecting the yield and characteristics of biodiesel. Ind. Eng. Chem. Res. 44, 5491-5499.

Faungnawakij, K., Yoosuk, B., Namuangruk, S., Krasae, P., Empikul, N.V.,Puttasawat, B.,2012. Sr–Mg Mixed Oxides as Biodiesel Production Catalysts. Chem Cat Chem. 4, 209 – 216.

Jha, G.K., Pal, S., Mathur, V.C., Bisaria, G., Anbukkani, P., Burman, R.R., Dubey, S.K., 2012. Edible Oilseeds Supply and Demand Scenario in India: Implications for Policy. IARI 7-31.

Kaur, M., Malhotra, R., Ali, A., 2018. Tungsten supported titanosilicate nanoflowers as reusable heterogeneous catalyst for biodiesel production. Renew. Energy 116, 109-119.

Kaur, N., Ali, A., 2014. One –pot transesterification and esterification of waste cooking oil using Sr:Zr mixed oxide as solid catalyst. RSC Adv. 4, 43671-43681.

Kaur, N., Ali, A., 2015. Biodiesel production *via* ethanolysis of jatropha oil using molybdenum impregnated calcium oxide as solid catalyst. RSC Adv. 5, 13285-13295.

Kim, H. J., Kang, B. S., Kim, M. J., Park, Y. M., Kim, D. K., Lee, J. S., Lee, K. Y., 2004. Transesterification of vegetable oil to biodiesel using heterogeneous base catalyst.Catal. Today 93-95, 315-320.

Kulkarni, M.G., Gopinath, R., Meher, L.C., Dalai, A.K., 2006. Solid acid catalysed biodiesel production by simultaneous esterification and transesterification. Green Chem. 12, 1056-1062.

Lee, J., Cho, W., Shim, W., 2004. Application of MCM-48 and SBA-15 materials for the separation of biochemicals dissolved in aqueous solution. Korean J. Chem. Eng. 21, 246-251.

Li, E., Rudolph, V., 2008. Transesterification of Vegetable Oil to Biodiesel over MgO-Functionalized Mesoporous Catalysts. Energy Fuels 22, 145-149.

Lu, Q., Wang, Z., Li, J., Wang, P., Ye, X., 2009. Structure and Photoluminescent Properties of ZnO encapsulated in Mesoporous silica SBA-15 Fabricated by Two-solvent strategy. Nanoscale Res. Lett. 7, 646-654.

Ma, F., Hanna, M.A., 1999.Biodiesel production: a review. Bioresour. Technol. 70, 1-15.

Morales, V. H., Acosta-Silva, Y.J., Nava, R., Pawelec, B., 2012. Adsorption of lead (II) on SBA-15 mesoporous molecular sieve functionalized with $–NH_2$ groups. Microporous Mesoporous Mater. 160, 133-141.

Negrila., C.C., Cotirlan, C., Ungureanu, F., Logofatu, C., Ghita, R.V., Lazarescu, M.F., 2008. ARXPS analysis of silicon oxide films. J. Optoelectron. Adv. Mater. 6, 1379-1383.

Pal, N., Cho, E.B., Kim, D., 2014. Synthesis of Ordered Mesoporous Silica/Ceria-Silica Composites and their High Catalytic Performance for Solvent-Free Oxidation of Benzyl Alcohol at Room Temperature. RSC Adv. 4, 9213-9222.

Patel, A., Brahmkhatri, V., 2013. Kinetic study of oleic acid transesterification over 12-tungstophosphoric acid catalyst anchored to different mesoporous silica supports.Fuel Process. Technol. 113, 141-149.

Patil, P.D., Deng, S., 2009. Optimisation of biodiesel production from edible and non-edible vegetable oils. Fuel 7, 1302-1306.

Pogaku, R., Raman, J.K., Ravikumar, G.,2012. Evaluation of Activation Energy and Thermodynamic Properties of Enzyme-Catalysed Transesterification Reactions. Adv. Chem. Eng. Sci. 2, 150-154.

Precht, R., Stolz, S., Mankel, E., Mayer, T., Jaegermanna, W., Hausbranda, R., 2016. Investigation of sodium insertion into tetracyanoquinodimethane (TCNQ): results for a TCNQ thin film obtained by a surface science approach. Phys. Chem. Chem. Phys. 18, 3056-3064.

Qadri, S.B., Skelton, E.F., Hsu, D., Dinsmore, A.D., Yang, J., Gray, H.F., Ratna, B.R., 1999. Size –induced transition-temperature reduction in nanoparticles of ZnS. Phys. Rev. B. 60, 9191-9193.

Reddy, B.M., Bharali, P., Saikia, P., Park, S.E., Vanden Berg, M.W.E., Muhler, M., Gru¨nert, W., 2008. Structural Characterization and Catalytic Activity of Nanosized $Ce_xM_{1-x}O_2$ (M = Zr and Hf) Mixed Oxides. J. Phys. Chem. C. 112, 11729-11737.

Sankaranarayanan, S., Antonyraj, C.A., Kannan, S., 2012. Transesterification of edible, non-edible and waste cooking oils for biodiesel production using calcined layered double hydroxides as reusable base catalysts. Bioresour. Technol. 109, 57- 62.

Sareen, S., Mutreja, V., Singh, S., Pal, B., 2015. Highly dispersed Au, Ag and Cu nanoparticles in mesoporous SBA-15 for highly selective catalytic reduction of nitroaromatics. RSC Adv. 5, 184-190.

Shi, C.W., Wu, W.V., Li, S., Bian, X., Zhao, S.L., Pei, M.Y., 2016. Investigation of Y/SBA Composite Molecular sieves Morphology Control and Catalytic Performance for n-Pentane Aromatization. Sci. Rep.. 6, 23826-23833.

Sing, K.S.W., Everett, D.H., Haul, R.A.W., Moscou, L., Pierotti, R.A., Rouquerol, J., Siemieniewska, T., 1985.Reporting physisorption data for gas solid systems with Special Reference to the Determination of Surface Area and Porosity. Pure & Appl. Chem. 57, 603-619.

Sivasamy, A., Cheah, K. Y., Fornasiero, P., Kemausuor, F., Zinoviev, S., Miertus, S., 2009. Catalytic applications in the production of biodiesel from vegetable oils. Chem. Sus. Chem.2, 278-300.

Srivastava, A., Prasad, R., 2000. Triglycerides-based diesel fuels. Renew. Sustain. Energy. Rev. 4,111-133.

Sun, H., Hu, K., Lou, H., Zheng, X., 2008. Biodiesel production from transesterification of Rapeseed oil using KF/Eu_2O_3 as a Catalyst. Energy Fuels 22, 2756-2760.

Tu, C.H.,Wang, A.Q., Zheng, M.Y., Wang, X.D., Zhang, T., 2006. Factors influencing the catalytic activity of SBA-15-supported copper nanoparticles in CO oxidation. Appl. Catal. A: Gen. 297,40–47.

Vunain, E., Jalama, K., Enus, R.M., Meijboom, R., 2013. The effect of recrystallisation time on pore size and surface area of mesoporous SBA-15. J. Sol-Gel Sci. Technol. 68, 270-277.

Wagner, C.D., Passoja, D.E., Hillery, H.F., Kinsiky,T.G., Six, H.A., Jansen, W.T., 1982. Auger and photoelectron line energy relationships in aluminium-oxygen and silicon-oxygen compounds. J. Vac. Sci. Technol. 21, 933-944.

Wu, H., Zhang, J., Liu, Y., Zheng, J., Wei, Q., 2014. Biodiesel production from Jatropha oil using mesoporous molecular sieves supporting K_2SiO_3 as catalysts for transesterification. Fuel Process. Technol.19, 114-120.

Xie, W., Yang, D., 2012. Transesterification of soyabean oil over WO_3 supported on $AlPO_4$ as a solid acid catalyst. Bioresour. Technol.119, 60-65.

Yahya, N.Y., Ngadi, N., Jusoh, M., Amirah, N., Halim, A., 2016. Characterization and parametric study of mesoporous calcium titanate catalyst for transesterification of waste cooking oil into biodiesel. Energy Convers. Manag. 129, 275-283.

Zhang, L., Sheng, B., Xin, Z., Liu, Q., Sun, S., 2010. Kinetics of transesterification of palm oil and dimethyl carbonate for biodiesel production at the catalysis of heterogeneous base catalyst. Bioresour. Technol. 101, 8144-8150.

K-Na Couple Impregnated Mesoporous Silica as an Effective and Reusable Solid Catalyst for Biodiesel Synthesis from Cottonseed Oil

Abstract:

K-Na couple imbued SBA-15 (20-Na-K/SBA-15) has been prepared by wet-incipient method under normal atmospheric conditions (without employing hydrothermal treatment). The prepared catalyst was characterised by employing a number of techniques *viz.*, BET for calculation of surface area, SEM for morphological study, XPS to find the oxidation state of elements. The catalyst was exploited for transesterification of virgin cotton seed oil and its activity was found to rely on its basic strength. Under optimum reaction conditions, catalyst amount 8 wt%, MeOH to oil molar ratio of 24:1 and temperature of 65 °C, the prepared catalyst could acquiesce > 98 % fatty acid methyl ester in 2 h of reaction duration. The catalyst could even capitulate conversion of ~ 76 % even in 7^{th} successive cycle of regeneration. The thermodynamic and kinetic parameters for the 20-Na-K/SBA-15 reaction were found to E_a = 45.8, $\Delta H^{\ddagger}$ = 43.3, $\Delta S^{\ddagger}$ = -0.148 $\Delta G^{\ddagger}$ = 83.7 kJ/mol respectively. The reaction was found to trail pseudo-first order kinetic pathway and endothermic in nature.

Keywords: Transesterification, Methanolysis, Basicity, Reusability, Solid catalyst, Leaching

5.1. Introduction

In previous chapters, the prepared catalysts were although quite stable thermally and showed acceptable catalytic activity and required almost 4 h of reaction duration to achieve > 98% FAMEs yield. In this chapter, it is endeavoured to prepare the catalyst to achieve complete transesterification in comparatively lesser time by employing a combination of highly active alkali metals (Na and K) over thermally secure mesoporous silica to save time and energy consumption. Alkali metals tend to show maximum percolation into the reaction media (De Lima et al, 2016). By impregnation over stable matrix, the concern of leaching is decreased significantly, and simultaneously carrying out the reaction at a fast pace to make the process suitable in all aspects. Moreover, to our knowledge, prospects of coalescing two active alkali metals over thermally stable self-synthesised siliceous support have not been explored for transesterification. The typical procedure for mesoporous silica synthesis involves the synthesis under high pressure conditions inside a Teflon autoclave. The temperature inside the autoclave is raised to nearly 100 ºC and the slurry is kept in autoclave for 2-3 days. Such methodology becomes tedious and consumes lot of time (Sareen et al., 2015). However, mesoporous silica synthesis carried out in present work doesn't employ harsh reaction conditions and use of autoclave. The synthesis has been carried out in normal easy to attain conditions. Moreover, it is to be noted that the catalysts formed were of mesoporous nature which has been evidenced with XRD, BET and morphological analysis. The samples were able to retain their hexagonal order even after impregnation. Hence, synthesis of mesoporous silica without employing tedious hydrothermal method is an interesting and advantageous alternative.

In this chapter, the parameters for transesterification were investigated to acquire the absolute transesterification of VCO in lesser time by impregnating highly active metals (Na and K) over mesoporous silica to trim down the energy need for FAMEs production. Recyclability of the catalyst as well as kinetics of the reaction were also examined under optimised conditions.

5.2. Experimental Section

5.2.1. Synthesis of SBA-15

Mesoporous SBA-15 support was prepared by utilising Pluronic 123 as the surfactant. In the classic synthesis, 8 g of Pluronic 123 was suspended in 60 mL of distilled water and stirred for 1h. Further, to this, 240 ml of 2M hydrochloric acid was added and stirring was continued

for additional 2 h. In next step, 17 mL of TEOS was added and resulting solution was stirred at room temperature (38 ºC) for 24 h. The mixture was then aged at 90 ºC for 48 h without stirring and without employing hydrothermal conditions. The solid product so formed was recuperated by filtration, dried and finally calcined at 600 ºC for 5 h.

5.2.2. Catalyst preparation

Catalysts were prepared by introducing active metallic centres inside the SBA-15 by incipient wet impregnation method. 1 g of SBA-15 was suspended in 40 ml of distilled water. To this, 10 ml solution of KNO_3 (having 0.51 g of salt) was added to obtain 20 wt% of K metal loaded SBA-15. To this, 10 mL Na_2CO_3 solution of desired concentration to obtain (10-25 wt% Na metal) was added. The resulted slurry was stirred for 24 h at room temperature (35-38 ºC), dried at 110 ºC for 24 h and calcined in muffle furnace at 550 ºC for 5 h. The catalysts thus obtained were labelled as x-Na-K/SBA-15 where, x is the wt% of Na metal in catalyst.

5.2.3. Transesterification of triglycerides

All transesterification reactions were performed in 100 mL, 2-necked round bottom flask furnished with an oil bath, water-cooled reflux condenser, thermometer and magnetic protester. In a classic reaction, the flask was charged with 10 g of virgin cottonseed oil (VCO) and assorted with desired amount of catalyst and MeOH and whisked at definite temperature for fixed duration. The reaction mixture obtained was set aside in separatory funnel for 10 h in order to part the upper biodiesel layer from the lower lying glycerol layer. The FAMEs thus produced were quantified using ^{1}H-NMR analysis using equation (2.6).

5.3. Results and discussion

5.3.1. Catalyst characterisation

5.1.1.1 Powder XRD study

Fig. 5.1 demonstrates XRD patterns of SBA-15 and Na-K/SBA-15 catalysts. Low angle XRD patterns show diffraction peak of lofty intensity at $2\theta \sim 0.9°$ which is trait of *p6mm* hexagonal symmetry of SBA-15. This typical peak could be ascribed to (100) plane. This evidently points out that modification of SBA-15 with active metallic species does not perturb the regular hexagonal facets of SBA-15 host. Although, minute shifting of reflection of (100)

plane towards smaller angles (2θ ~0.63°) upon impregnation with Na and K species was detected. This can be credited to the minute changes in lattice framework due to unit cell parameters due to expansion in the lattice and development of tension in SBA-15 on inclusion of active metallic species. Furthermore, it is apparent from the XRD results that SBA-15 support is thermally very stable and elevated temperature exposures does not dislocate the structure of mesoporous silica (Charan and Rao, 2015).

High angle XRD patterns of Na-K/SBA-15 are shown in Fig. 1b. The peak appearing at 23.8° is due to amorphous silica. The peaks present at 17.02°, 25.2°, 29.6°, 37.5°, 39.05°, 46.8°, 52.3°, 54.5° are due to sodium silicate (JCPDS card no. 01-072-0079). The peaks at 32.5° 34.02°, 44.4° are for potassium oxide (JCPDS card no. 01-023-0493) and the peaks visible at 35.1°, 38.8°, 48.3° support the existence of sodium oxide during catalyst preparation (JCPDS card no. 00-003-1074).

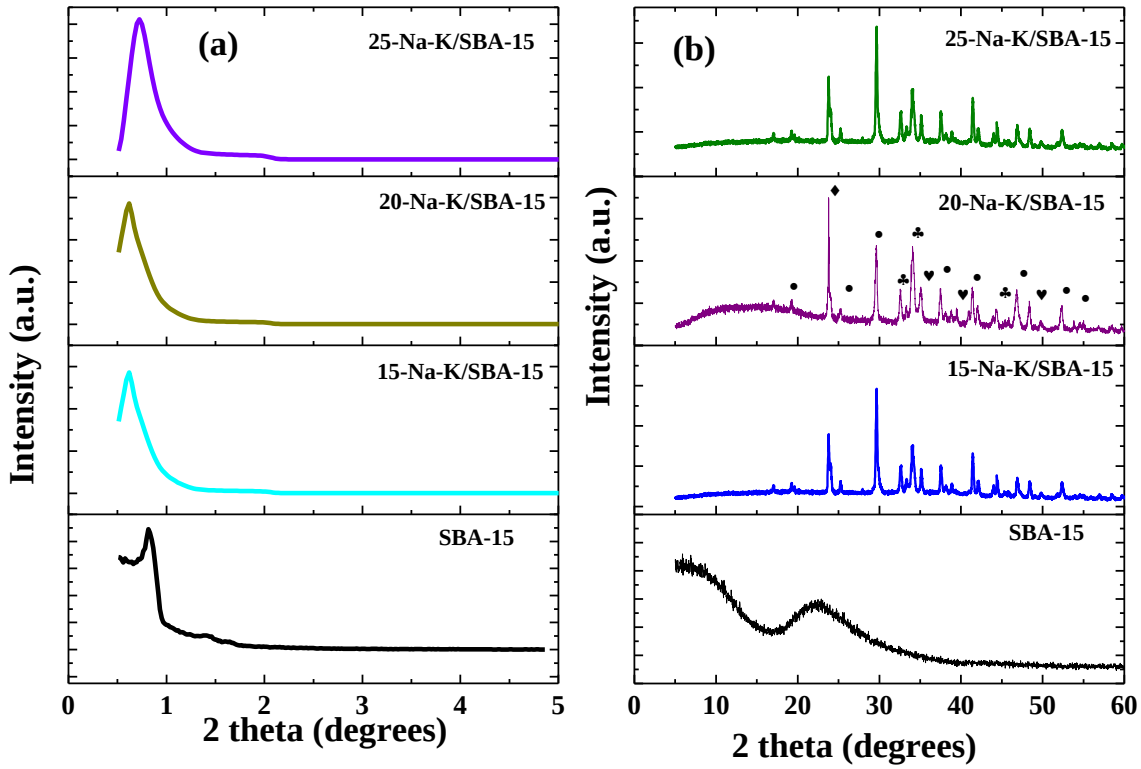

Fig. 5.1. (a) Low angle and (b) wide angle XRD patterns of SBA-15 and Na-K/SBA-15. catalysts (• = Na_2SiO_3, ♣ = K_2O, ♥= Na_2O).

5.3.1.2. Porosity and Surface area Study

To study the BET surface area of prepared catalysts, N_2-sorption isotherms were evaluated. Table 5.1 depicts textural properties of the prepared catalysts. The isotherms are type IV in nature having H_1 hysteresis loops, (Fig. 5.2a) that is a leading attribute of mesoporous nature of materials (Luo et al., 2008). The hysteresis loop is indication of porosity and arises due to capillary condensation inside mesopores. The initial component of the curve is ascribed to monolayer adsorption. The spiky nature of adsorption and desorption branches (at relative pressure ~ 0.4- 0.6) and its sustainance inspite of escalating the loading of active metallic species points towards the regularity and homogeny of pore channels and narrow pore size distribution of bare SBA and Na-K impregnated SBA-15 (Vunain et al., 2013). However, it is to be noted that the isotherm of 25-Na-K/SBA-15, although is type 1V, but the hysteresis changed from type H_1 to H_3. This can be credited to the decrease in the mesoporous order, partial blocking of mesoporous network and presence of aggregated or clustered particles which give rise to slit-shaped pores (Sing et al., 1985).

Table 5.1. Surface area, average pore size and average pore volume of the prepared catalysts.

Sample name	Surface area ($m^2 g^{-1}$)	Average pore volume ($cm^3 g^{-1}$)	Average pore diameter (nm)
SBA-15	441.8	0.56	5.09
15-Na-K/SBA-15	326.5	0.46	5.64
20-Na-K/SBA-15	246.6	0.55	9.05
25-Na-K/SBA-15	10.64	0.013	4.92

Barrett-Joyner-Halenda (BJH) method (Fig. 5.2b) was utilised to determine pore size from Nitrogen-sorption isotherms which depicts the gradual increase in pore diameter with increasing level of impregnation by active metallic species and narrow and broad pore-size distribution of bare mesoporous silica and x-Na-K/SBA-15 catalysts respectively as also observed in Chapter 4. Table 5.1 represents demur in surface area, and average pore volume with the rise in Na-K concentration SBA-15. This decrease can be endorsed to the spreading of Na-K particles into the pores of SBA-15. However, the pore volume of 20-Na-K/SBA-15 was found to be slightly higher inspite of lower surface area. This kind of observation has also been previously reported in literature and can be explained on the basis of slight

contraction of the pore walls due to metal agglomeration leading to pore stretching (Setiabudi et al., 2017). The decline in surface area was, much more in case of 25-Na-K/SBA-15, owing to excessive blocking of pores and aggregation or cluster formation due to high Na metal content. However, the decline in the pore size in case of 25-Na-K/SBA-15 can be accredited to distribution of Na-K species over the mesopore surface and, hence tenancy of some pore space (Sareen et al., 2015).

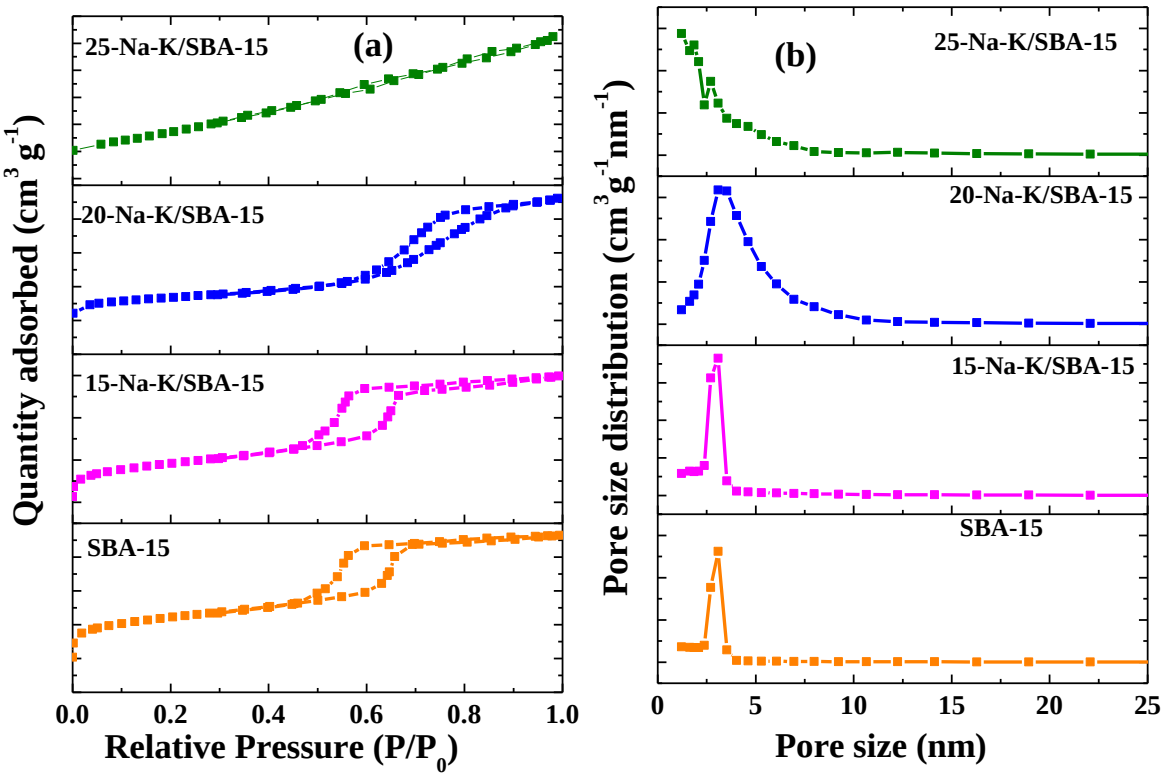

Fig. 5.2. (a) N_2 adsorption–desorption isotherms and (b) pore size distribution of x-Na-K/SBA-15 catalysts.

5.3.1.3. SEM-EDS analysis

SBA-15 material as well as 20-Na-K/SBA-15 catalyst were characterised by SEM technique to examine the morphological features. The SEM analysis (Fig. 5.3a) of SBA-15 depicted the aggregates of hexagonal and few irregular shaped particles. The morphological study showed 2-D hexagonal shape with an average length and width of 9 μm and 5 μm respectively. The particles are likely to reside in clustered manner. Fig. 5.3b depicts the SEM image of 20-Na-

K/SBA-15 which showed the rod-shaped catalyst particles of an average length of 12 μm. The EDS spectra of active catalyst demonstrates the presence of ~ 20.98 and 20.84 wt% Na and K metals respectively which is pretty close to theoretical loading of 20 wt%. The spectra also indicated the purity of catalyst and presence of no impurities. The elemental mapping (Fig.5.4) of the catalyst also confirmed the loading of Na and K in the matrix of SBA-15 and homogeneous distribution of Na and K metallic species in the siliceous framework. The presence of different elements in catalysts has been depicted with different colors in Fig. 5.4

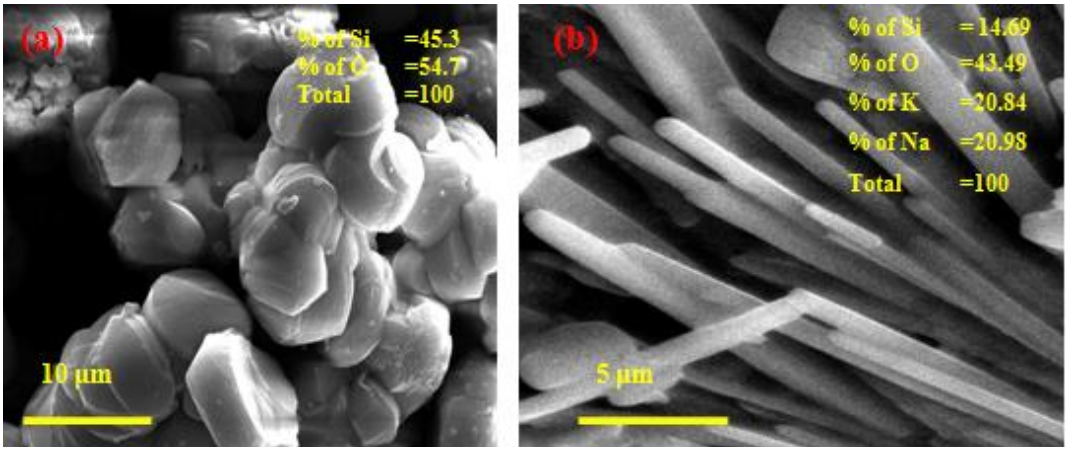

Fig. 5.3. FE-SEM images of (a) bare SBA-15 support (b) 20-Na-K/SBA-15 catalyst.

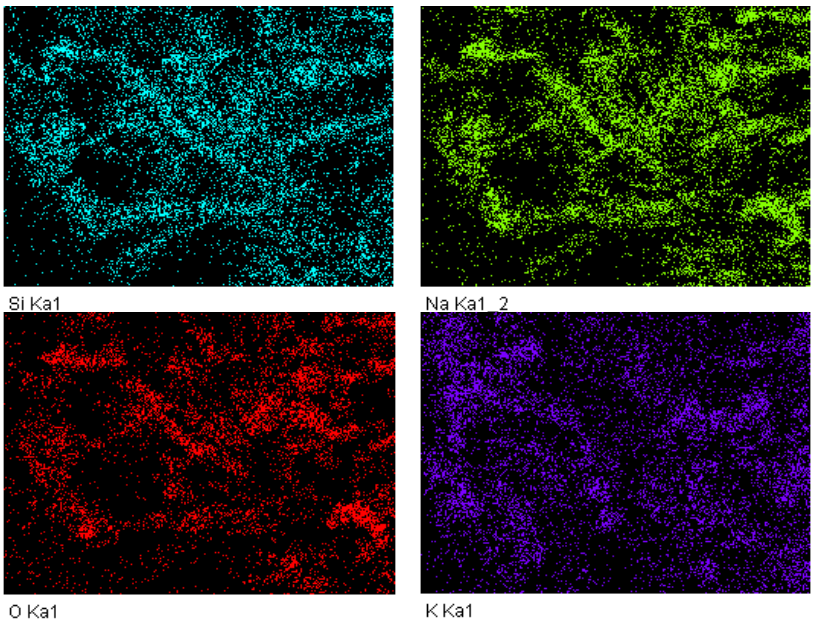

Fig. 5.4. Elemental mapping or compositional study of 20-Na-K/SBA-15.

5.3.1.4. HR-TEM study

HRTEM analysis of Na-K infused SBA-15 to observe the distribution of pores and is depicted in Fig 5.5. The micrographs revealed the well formed rods of catalyst species (Fig. 5.5a) with active metal species infused over silica. The arrays of mesoporous channels, typical feature of SBA-15 can also be seen in Fig. 5.5b. While the calcination treatment, is done, the metal particles budge inside the channels of SBA-15. Highly dispersed metal species are visible in the channels of SBA-15 (Fig. 5.5b and 5.5c). The darker spots evidence the incidence of mesopores and their impregnation and blocking with active metallic species
From the HRTEM analysis, it can be evidenced that the functionalisation and infusion of SBA-15 with Na-K metallic species didn't disturb or erupt its morphology and typical porous structure of SBA-15 was sustained after impregnation with metallic species. The presence of porous structure is the main catch in mesoporous catalysts which is chiefly favorable for eliminating mass transfer limitations and facilitates easy entry of reactants and provides good degree of exposure to active sites. The selected area electron diffraction (SAED) pattern (Fig.5.5d) revealed that the prepared catalyst possessed polycrystalline character ascribed to the incidence of multiple rings formed by small bright spots corresponding to the (200), (111), (310), (021) planes of sodium silicate species present in prepared catalyst.

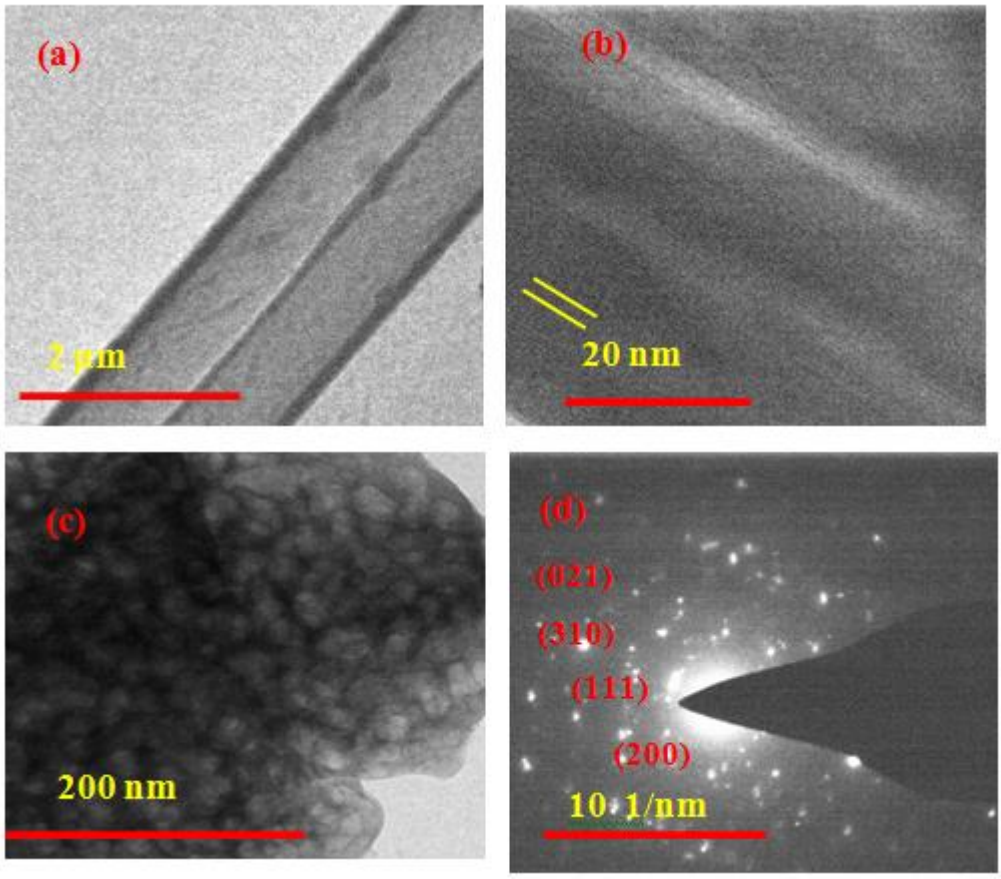

Fig. 5.5. HR-TEM images of (a) rods of catalyst, (b) dispersion of metal inside siliceous matrix (c) porous structure of SBA-15 and infusion of Na-K species and (d) SAED pattern of 20-Na-K/SBA-15.

5.3.1.5. XPS study

To ascertain the elemental state of the elements present in 20-Na-K/SBA-15, XPS study was carried out. As depicted in Fig. 5.6, the peak spotted at 103.5 eV supports the incidence of silicon in Si 2p state in SBA-15 matrix (Pal et al., 2014), while the peak perceived at 101.5 eV could be assigned to Si^{4+} present in Si-O surface bonds at the near interface, and the peak observed at 101.8 eV is assigned to the Si 2p in +4 oxidation state due to formation of Si-O-M (M= metal atom) species in the catalysts (Negrila et al., 2008). The peak ensuing to O 1s, could be deconvoluted into 3 peaks. The strong peak at 533 eV can be endorsed to oxygen in amorphous SBA-15. The other 2 peaks appearing at 530.9 eV and 531.7 eV can be correspondingly accredited to lattice oxygen and softly attached oxygen of physisorbed water (Reddy et al., 2008). The peak at 1071.3 eV consigns to Na 1s state (Precht et al., 2016). K

2p spectrum is a doublet K $2p_{3/2}$– K $2p_{1/2}$ with peaks at 292.6 and 295.7 respectively (Nili et al., 2013).

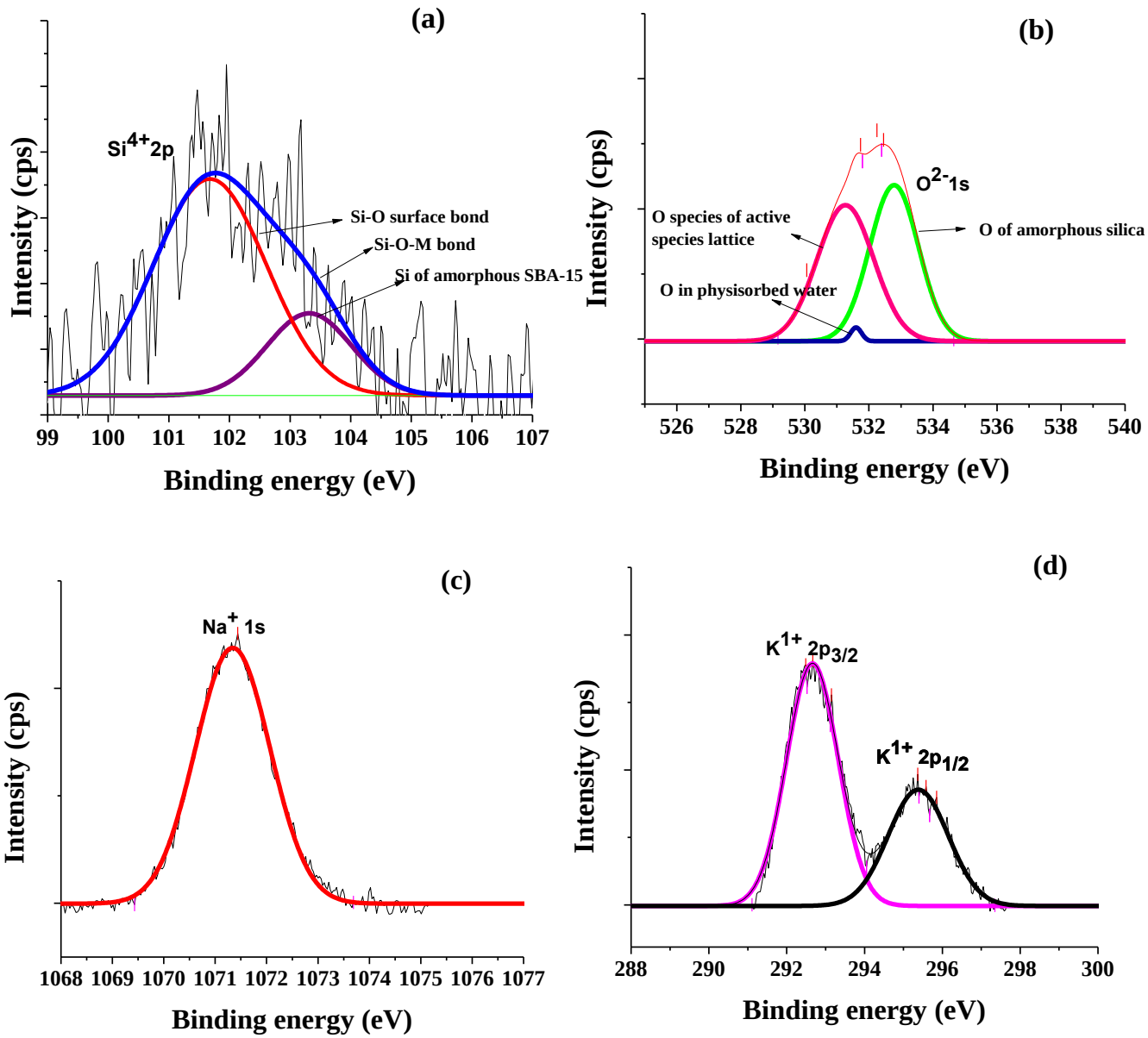

Fig. 5.6. XPS spectra of (a) Si (b) O (c) Na and (d) K present in 20-Na-K/SBA-15 catalyst.

5.3.1.6. Hammett indicator study

Hammett indicator benzene carboxylic acid titration method was utilised to enumerate the basic sites over the catalyst. It is visible from Table 5.2, that naked SBA-15 had weakly basic

sites that could not initiate the transesterification of VCO on their own. On escalating the loading of Na-K species over SBA-15 matrix, the basic sites were found to augment that consequently led to superior catalytic activity.

Table 5.2. Comparison of basic strengths, and TOFs for the Na-K//SBA-15 catalyzed transesterification.

Catalyst	Indicators used					Total basicity (mmol g^{-1})	TOF ($\times 10^{-4}$ h^{-1})
	Bromothymol blue ($H_0 \leq +7.2$)	Phenolphthalein ($H_0 \leq +9.3$)	Nile blue ($H_0 \leq 10.1$)	Trapeolin ($H_0 \leq +11.1$)	2,4-dinitroaniline ($H_0 \leq +15$)		
SBA-15	0.59	NCC	NCC	NCC	NCC	0.59	-
10-Na-K/SBA-15	2.1	2.3	2.9	3.2	3.8	14.3	26
15-Na-K/SBA-15	2.4	2.7	2.9	3.1	3.9	15	38
20-Na-K/SBA-15	2.6	2.9	3.3	3.4	4.2	16.4	45
25-Na-K/SBA-15	2.7	3.0	3.2	3.5	4.3	16.7	46

**NCC stands for no colour change*

**TOF is calculated at 50% level of conversion ; Reaction conditions = methanol to oil molar ratio of 24 :1 at a Temperature of 65 °C, in the presence of 8 wt% of catalyst with respect to oil at 600 rpm stirring speed.*

5.3.2. Catalytic activity of sodium impregnated K/SBA-15

There is existence of basic sites in the prepared catalyst due to which it is able to exhibit transesterification activity. With aim to settle on the optimum reaction conditions, the transesterification was performed in the attendance of catalyst with virgin cottonseed oil and methanol. Reaction parameters were investigated by changing one factor at a time out of (i) impregnated wt% of Na (weight ratio of Na:K), (ii) amount of catalyst, (iii) reaction temperature, and (iv) MeOH/oil molar ratio.

5.3.2.1. Influence of Na loading

To determine the optimal ratio of Na-K, for the best catalytic doings, a sequence of catalysts were synthesised by loading of set weight % of potassium metal and then impregnating 10-25 wt % of Na over SBA-15. Transesterification reactions were carried out at 65 °C and utilising the 24:1 methanol to oil molar ratio in the attendance of 8 wt % of catalyst.

With the increase in concentration of Na metal (from 10-25 wt%), catalyst activity improved and the rate of reaction was found to augment and complete conversion of VCO into BD was observed within 2 h (Fig.5.7a). Parallel trends have been shown by the TOF of the prepared catalyst, that were found to raise from 26 × 10^{-4} to 46 × 10^{-4} h^{-1} as the Na-loading was increased. Any more increase in Na concentration (from 20-25 wt %) did not affect the TOF to any considerable extent. The TOF of 20 and 25 wt% Na loaded K/SBA-15 were found to be nearly similar. Thus, 20-Na-K/SBA-15 was chosen for optimising other parameters.

5.3.2.2. Effect of concentration of catalyst

To determine the optimal catalyst concentration, transesterification reactions were carried out, using a 24:1 MeOH/oil molar ratio at 65 °C and altering the 20-Na-K/SBA-15 amount from 5 to 9 wt% (catalyst/oil). The results have been abridged in Fig. 5.7b, which depicts that a rise in catalyst amount up to 8 wt% raised the rate of reaction. This can be credited to the more number of active catalytic sites on rising the catalyst concentration. However, additional increase in amount of catalyst (9 wt%) didn't impinge on the reaction speed and yield and hence, further study was performed with 8 wt% catalyst.

5.3.2.3. Effect of reaction Temperature

To find the most favourable temperature for the reaction, transesterification reactions were carried out with 8 wt % of 20-Na-K/SBA-15, employing 24:1 methanol to oil molar ratio and altering the temperature from 35 °C to 65 °C. When temperature was augmented from 35°C to 65 °C, the reaction rate boosted significantly. With rise in temperature, the reaction went to completion within 2 h of time. However, any more increment in reaction temperature was not able to improve catalytic efficiency to any noteworthy extent (Fig.5.7c). Hence, 65 °C temperature was chosen to accomplish the complete transesterification in least probable time. Any elevated temperature > 65 °C will cause the methanol to evaporate from the reaction mixture. The methanol thus vaporized won't be in contact with the other reactants, and the catalyst activity won't improve as temperature is raised past 65 °C.

5.3.2.4. Effect of MeOH/oil molar ratio on FAMEs yield

MeOH/oil molar ratio is one of the vital factors having a substantial effect on the FAMEs yield in addition to production cost. The least molar ratio of MeOH to oil must be 3:1 to obtain 100% BD yield from vegetable oil. However, being a reversible procedure, transesterification is typically performed using an excess amount of methanol to swing the equilibrium to right side. Solid catalysts, because of phase difference, are able to catalyze the reaction with somewhat slower speed and hence, entail additional time to complete the reaction.

In the present chapter, the transesterification reactions were performed at 65 °C using 8 wt% of 20-Na-K/SBA-15, and altering the MeOH to oil molar ratios from 6:1 to 30:1 (Fig. 5.7d). The rate of reaction rate increased as MeOH/oil molar ratio was increased from 6:1 to 24:1. Any extra hoist in the MeOH/oil molar ratio from 24:1 to 30:1 was not found to affect the reaction rate to substantial level. Hence, 24:1 methanol to oil molar ratio was preferred as optimised fraction for the present catalyst

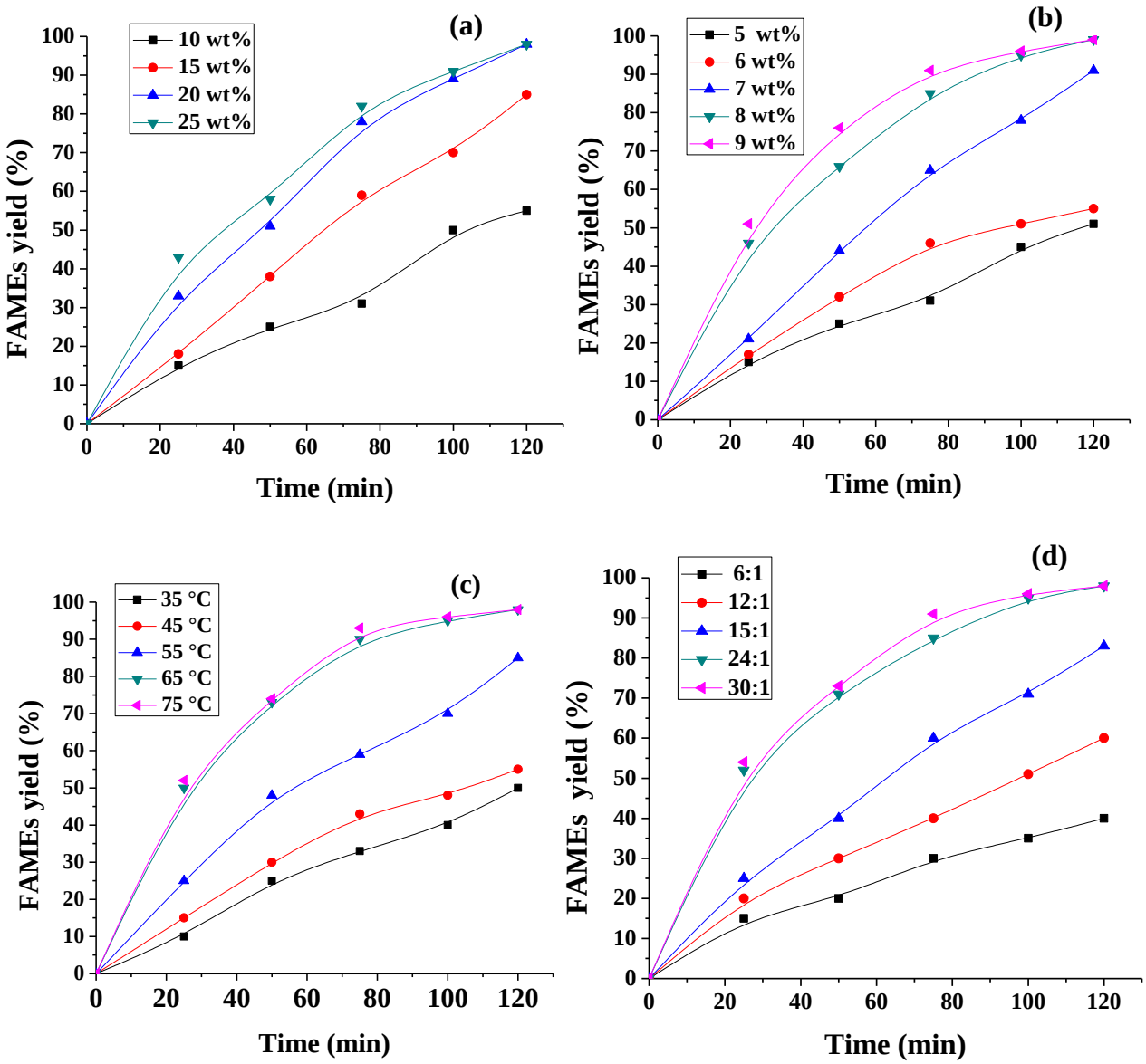

Fig. 5.7. Effect of (a) Na concentration, (b) catalyst concentration, (c) reaction temperature and (d) MeOH/oil molar ratio on methanolysis of VCO.

5.3.3. Effect of FFA content on catalyst activity

In case of homogeneous catalyst, existence of > 0.5 wt% FFA contents in oil was found to disengage the catalyst *via* saponification. In the present chapter, the prepared catalyst was employed for transesterification of VCO having FFA contents of 0.4 wt%. To discover the highest FFA acceptance of present catalyst, transesterification reactions of VCO were performed under optimised conditions by externally adding palmitic acid to reaction (upto 7

wt%). It was observed that upto addition of 6 wt% of palmitic acid, the catalyst was able to capitulate the absolute conversion of VCO into FAMEs, although reaction time was increased upto 6.5 h. An auxiliary increment in FFA content, (7 wt%), was found to trim down the catalyst activity since, 80% FAMEs yield was obtained even after 8 h of reaction time (Fig. 5.8). This decline in reaction rate and catalytic activity can be ascribed to partial neutralisation of active sites of catalyst due to tough interactions of polar carboxylic group ($-COO^-$) of FFA with catalyst active sites (Na^+, K^+) that consequently led to partial blockage of active sites of catalyst (Kaur and Ali, 2014).

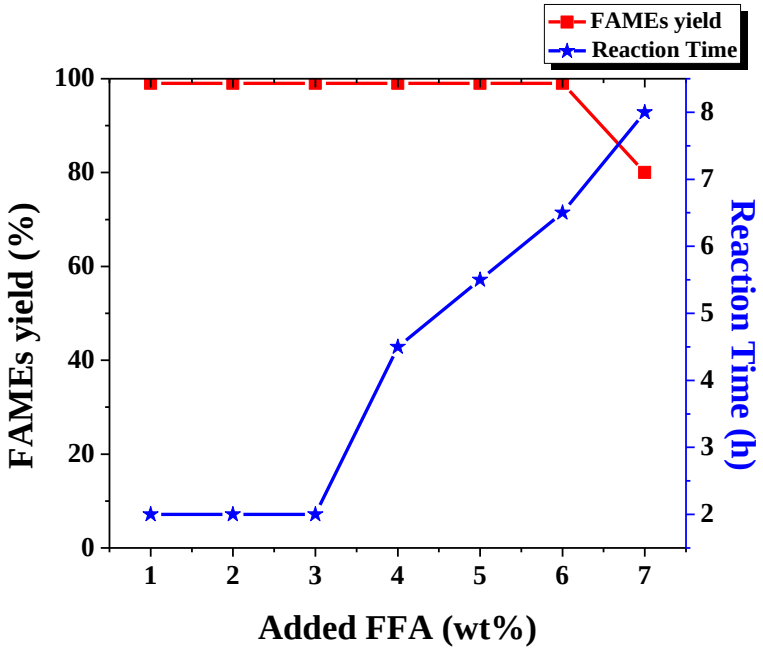

Fig. 5.8. Effect of added FFA content on the FAMEs on 20-Na-K/SBA-15 catalyzed transesterification of VCO (Reaction conditions: MeOH/oil molar ratio = 24:1; Catalyst amount = 8 wt% of oil; Temperature = 65 °C).

5.3.4. Reusability and homogeneous contribution

Reusability is a very significant and profitable attribute for heterogeneous catalysts since catalyst separation becomes trouble-free and also cuts the effective production cost. To assess the catalyst reusability transesterification reaction with 20-Na-K/SBA-15 was carried out under optimized reaction conditions. The used catalyst was recovered through filtration, sluiced with hexane and methanol several times to remove the contaminants, dried at 120 °C

and calcined at 600 °C. The revived catalyst was utilised for methanolysis of VCO for 7 consecutive runs under the like experimental conditions and regeneration method. The reused catalyst was able to yield complete conversion of feedstock into FAMEs for 6 repeated runs. Activity of the catalyst demurred as indicated in Fig. 5.9 in the 7th run yielding 76% biodiesel yield.

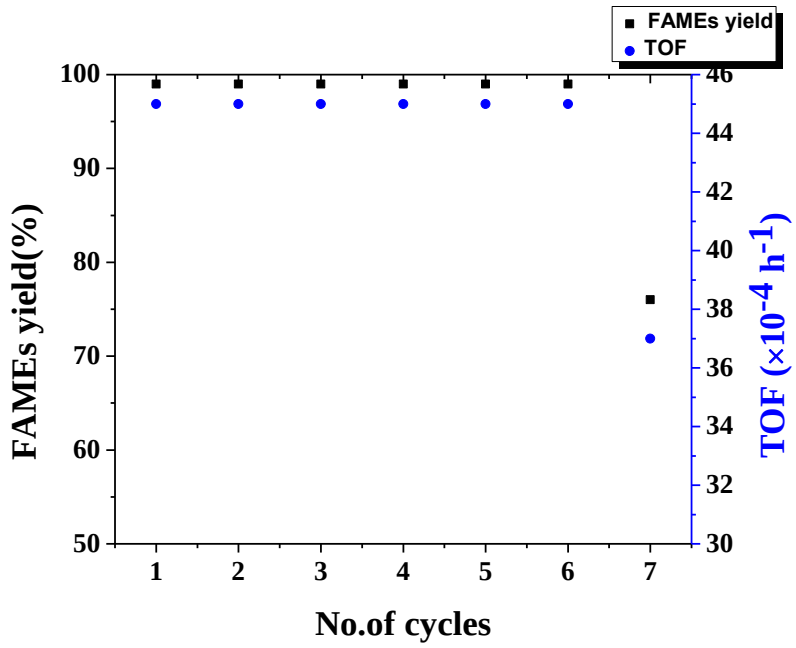

Fig. 5.9. Reusability of 20-Na-K/SBA-15 catalyst (Reaction conditions: MeOH/oil molar ratio = 24:1; Catalyst amount = 8 wt% of oil; Temperature = 65 °C).

Oozing out of the active species from the catalyst is a setback often faced in the heterogeneous catalytic systems, particularly in case of alkali and alkaline earth metals acting as dynamic catalytic centres (Sivasamy et al., 2009). The concentration of active Na and K metals was quantified in FAMEs and glycerol layer in the 7th cycle with Flame photometry when the activity of the catalyst demurred. During the 7th cycle, 267 ppm and 369 ppm of Na was detected in BD and glycerol layers whereas 603 ppm and 573 ppm of K was found in BD and glycerol layers respectively. This seeping may be accredited to partial breakdown of siliceous matrix of mesoporous silica during the 7th catalytic run to let the active moiety ooze out into the reaction media. During the primary 6 catalytic cycles, it can be established that no active metal would have leached out in the reaction mixture since the catalyst was able to sustain its action in the reaction mixture to yield the complete conversion of feedstock into BD. Thus, it can be deduced that SBA-15 support made the catalyst reasonably stable and

prevented the seeping out of prone to leaching Na and K metal into the reaction media. Thus, active species arrested over mesoporous silica is visibly a gainful selection over uncorroborated catalyst, since it could retain its deed over consecutive cycles with no probable leaching out of otherwise leachable alkali metals clearly presenting it as a superior counterpart.

The basicity test of regenerated catalyst was also performed to establish the rationale for reduced catalytic action. The basicity of regenerated catalyst was found to be 15.3 mmol g^{-1}, lower than that of fresh catalyst (16.4 mmol g^{-1}) to support the percolation of active metals into reaction medium and consequent decline in catalytic bustle.

To further launch the reason other than oozing out of active species, behind the trouncing in catalytic activity after 6 cycles, surface area analysis of recycled catalyst was performed. It was deduced that surface area of reused catalyst was found to be significantly lower (= 10.9 m^2 g^{-1}) than that of fresh catalyst (246.6 m^2 g^{-1}) to support the diminution in catalytic action. It can be deduced from above results that decline in surface area combined with percolation of active species in the 7^{th} reaction cycle led the catalyst to show less bustle in the reaction. Both the factors, surface area decline and percolation of active metals into reaction media worked synergistically to contribute to decline in catalytic activity.

Additionally, to certify the heterogeneous means of action of the present catalyst, hot filtration test was performed in optimized conditions. The catalyst was recuperated by filtration of reaction mixture after 45 minutes and the reactants (without catalyst) were further heated for 1.25 h. It is clear from Fig. 5.10, that no mount in FAMEs yield was observed as the reaction was proceeded in nonattendance of catalyst. This examination establishes (i) the heterogeneous means of catalytic activity and (ii) the leached metal ions had no role in catalyst action.

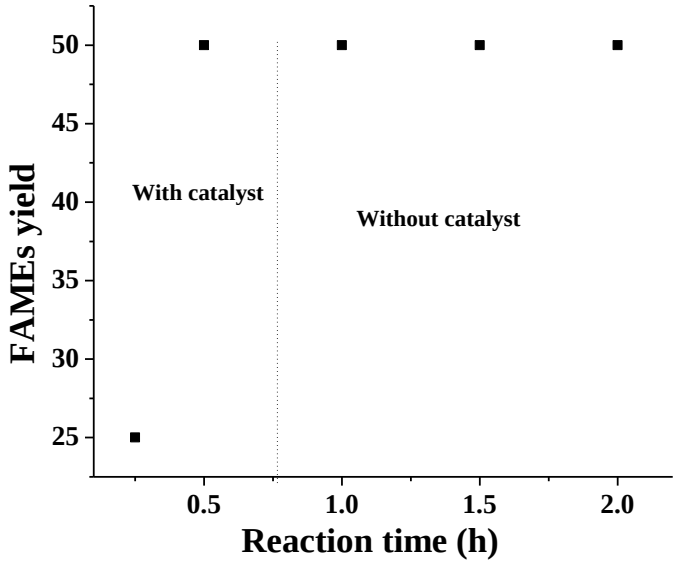

Fig. 5.10. Hot filtration test for 20-Na-K/SBA-15 catalyzed transesterification.

5.3.5. Kinetic Study

Kinetic study was carried out in the same way as carried out in chapter 3. To find the rate constants at different temperatures, the transesterification reactions were performed at 35 to 65 °C temperatures under optimized conditions. The conversion values at these temperatures were incorporated in the equation (2.2) to get individual rate constants. The plot of –ln (1-X_{me}) *versus* 't' was found to be linear in nature (R^2 value = 0.98 at 65 °C) to support that reaction has tracked 1st order kinetics (Zhang et al., 2010). The rate constant at 65 °C was found to be 0.039 min^{-1}. Energy of activation (E_a) was calculated from the slope of Arrhenius plot using Arrhenius equation (2.3) and Equation (2.4) was employed to compute the enthalpy ($\Delta H^{\ddagger}$) and entropy of activation ($\Delta S^{\ddagger}$) for the reaction.

E_a was found to be 45.8 kJ mol^{-1}. The R^2 value of Arrhenius plot (ln K *vs* 1/T) was found to be 0.86. The E_a was found to be inside the reported range (33-84 kJ mol^{-1}) for methanolysis of vegetable oils. (Sun et al., 2008). A value of Ea > 25 kJ mol^{-1}, further supports that reaction was controlled chemically and not by diffusion or mass transfer limitations (Patel and Brahmkhatri, 2013).

A linear plot was obtained between ln (k/T) and 1/T with R^2 value of 0.84. From the curve, $\Delta H^{\ddagger}$ and $\Delta S^{\ddagger}$ were found to be +43.3 kJ mol^{-1} and - 0.148 kJ mol^{-1} respectively.

The Gibb's free energy ($\Delta G^{\ddagger}$) was found to be + 83.7 kJ mol^{-1}.

Table 5.3. Experimentally determined values of thermodynamic parameters.

Thermodynamic Parameter	kJ mol^{-1}.
Activation Energy (E_a)	45.8
Enthalpy of Reaction ($\Delta H^{\ddagger}$)	43.3
Entropy of Reaction ($\Delta S^{\ddagger}$)	-0.148
Gibbs Free Energy ($\Delta G^{\ddagger}$)	83.7

Since the value of $\Delta G^{\ddagger}$ was found to be a positive value, it can be deduced that 20-Na-K/SBA-15, catalysed methanolysis of VCO was a non-spontaneous reaction and energy strata of transition state was elevated as compared to that of reactants (Pogaku et al., 2012)

Further to note that negative $\Delta S^{\ddagger}$ value shows that transition state acquires more order than the reactants in ground state. Thus, 20-Na-K/SBA-15 catalysed methanolysis has trailed an associative reaction pathway (Espenson, 2002). Positive $\Delta H^{\ddagger}$ depicted that reaction was endothermic and needed exterior heating to reach the transition state and move in forward direction (Beall, 1994).

5.4. Conclusions

Present chapter represents preparation and exploration of 20-Na-K/SBA-15 as heterogeneous and regenerable catalyst for the BD production from virgin cotton seed oil. Under optimised reaction conditions of 8 wt% catalyst/oil amount at 65 °C reaction temperature and MeOH/oil molar ratio of 24:1, more than 98% FAME yield was obtained within a duration of 2 h. The 20-Na-K/SBA-15 catalysed transesterification chased (pseudo) first order kinetics. The catalyst paraded very fine recyclability for it was able to uphold its activity (98% FAMEs yield) for 6 catalytic runs. However, during the seventh cycle, only 76% FAMEs yield was achieved. From commercial perspective, retention of activity, due to stable and locked siliceous matrix is considerable observation in present chapter. The catalyst followed heterogeneous mode of action and no homogeneous contribution was found.

References

Beall, H., 1994. Probing Student Misconceptions in Thermodynamics with In-Class Writing. J. Chem. Educ. 71, 1056-1057.

Charan, P.H.K., Rao, G.R., 2015. Textural and morphological studies of transition metal doped SBA-15 by co-condensation method. J. Chem. Sci. 5, 909–919.

De Lima, A., Ronconi Machado, C., Mota, C., 2016. Heterogeneous basic catalysts for biodiesel production. Catal. Sci. Technol. 6, 2877-2891.

Espenson, J.H., 2002. Chemical Kinetics and Reaction Mechanisms, second ed. McGraw-Hill, India.

Kaur, N., Ali, A., 2014. One –pot transesterification and esterification of waste cooking oil using Sr:Zr mixed oxide as solid catalyst RSC Adv. 4, 43671-43681.

Luo, Y., Hou, Z., Li, R., Zheng, X., 2008. Rapid synthesis of ordered mesoporous silica with the aid of heteropolyacids. Microporous Mesoporous Mater. 109, 585-590.

Negrila, C.C., Cotirlan, C., Ungureanu, F., Logofatu, C., Ghita, R.V., Lazarescu, M.F., 2008. ARXPS analysis of silicon oxide films. J.Optoelectron.Adv.Mater.6, 1379-1383.

Nili, H., Kandjani, A,E., Plessis, J.D., Bansal, V., Zadeh, K.K., Bhaskaran, M., 2013. Alkali ratio control for lead-free piezoelectric thin films utilising elemental diffusivities in plasma. Cryst. Eng. Comm. 15, 7222-7999.

Pal, N., Cho, E.B., Kim, D., 2014. Synthesis of Ordered Mesoporous Silica/Ceria-Silica Composites and their High Catalytic Performance for Solvent-Free Oxidation of Benzyl Alcohol at Room Temperature. RSC Adv. 4, 9213−9222

Patel, A., Brahmkhatri, V., 2013. Kinetic study of oleic acid transesterification over 12-tungstophosphoric acid catalyst anchored to different mesoporous silica supports. Fuel Process. Technol. 113, 141-149.

Pogaku, R., Raman, J.K., Ravikumar, G., 2012. Evaluation of Activation Energy and Thermodynamic Properties of Enzyme-Catalysed Transesterification Reactions. Adv. Chem. Eng. Sci. 2, 150-154.

Precht, R., Stolz, S., Mankel, E., Mayer, T., Jaegermanna, W., Hausbranda, R., 2016. Investigation of sodium insertion into tetracyanoquinodimethane (TCNQ): results for a TCNQ thin film obtained by a surface science approach. Phys. Chem. Chem. Phys. 18, 3056-3064.

Reddy, B.M., Bharali, P., Saikia, P., Park, S.E., Vanden Berg, M.W.E., Muhler, M., Gru¨nert, W., 2008. Structural characterization and catalytic activity of nanosized $Ce_xM_{1-x}O_2$ (M = Zr and Hf) mixed oxides. J. Phys. Chem. C. 112, 11729–11737.

Sareen, S., Mutreja, V., Singh, S., Pal, B., 2015. Highly dispersed Au, Ag and Cu nanoparticles in mesoporous SBA-15 for highly selective catalytic reduction of nitroaromatics. RSC Adv. 5, 184-190.

Setiabudi, H.D., Lim, K.H., Chin, S.Y., Kamarudin, N.H.N., 2017. CO_2 reforming of CH_4 over Ni/SBA-15: Influence of Ni loading on metal-support interaction and catalytic activity. J. Mat. Environ. Sci. 2, 573-581.

Sing, K.S.W., Everett, D.H., Haul, R.A.W., Moscou, L., Pierotti, R.A., Rouquerol, J., Siemieniewska, T., 1985. Reporting physisorption data for gas solid systems with Special Reference to the determination of surface area and porosity. Pure & Appl. Chem. 57, 603-619.

Sivasamy, A., Cheah, K. Y.,Fornasiero, P., Kemausuor, F., Zinoviev, S., Miertus, S., 2009. Catalytic applications in the production of biodiesel from vegetable oils. Chem. Sus. Chem.2, 278-300.

Sun, H., Hu, K., Lou, H., Zheng, X., 2008. Biodiesel production from transesterification of Rapeseed oil using KF/Eu_2O_3 as a Catalyst. Energy Fuels 22, 2756–2760.

Vunain, E., Jalama, K., Enus, R.M., Meijboom, R., 2013. The effect of recrystallization time on pore size and surface area of mesoporous SBA-15. J. Sol-Gel Sci. Technol. 68, 270–277

Zhang, L., Sheng, B., Xin, Z., Liu, Q., Sun, S., 2010. Kinetics of transesterification of palm oil and dimethyl carbonate for biodiesel production at the catalysis of heterogeneous base catalyst. Bioresour. Technol.101, 8144-8150.

Sodium/Zirconia Mixed Metals Drenched SBA-15 as a Reusable Solid Catalyst for Concurrent Esterification and Transesterification of Low Quality Oils

Abstract

Sodium/zirconia metals impregnated SBA-15 has been prepared without using hydrothermal treatment trailing the wet impregnation route. The prepared catalyst has been characterised by employing various techniques *viz.*, BET surface area analysis, SEM for morphological study, XPS for determination element oxidation state. It was found that catalyst seized both acidic and basic sites therefore, successfully employed for one-pot or concurrent esterification and transesterification of VCO and high FFA containing oils. Under most favourable reaction conditions, catalyst concentration 10 wt%, MeOH/oil molar ratio of 30:1 at 65 °C, the catalyst could confer > 98 % fatty acid methyl ester yield within 3 h of reaction duration.

Regeneration study advocated that the catalyst may well be recycled for 5 successive cycles without any significant trouncing of activity and even yielded 86% FAMEs during 6^{th} cycle. The activation energy (E_a) for the reaction was found to be 42.9 kJ mol^{-1}, while $\Delta H^{\ddagger}$, $\Delta G^{\ddagger}$ and $\Delta S^{\ddagger}$ were found to be 40.1 kJ mol^{-1}, + 84 kJ $mol^{-1}$and - 0.161 kJ mol^{-1}, respectively. On the grounds of thermodynamic parameters, the reaction is anticipated to be non-spontaneous, endothermic and tracking an associative pathway.

Keywords: Heterogeneous catalysts, mesoporous, basicity, acidity, transesterification, thermodynamic parameters

6.1. Introduction

In the present chapter, the catalyst was developed carrying both acidic as well as basic sites so as to facilitate concurrent esterification and transesterification of VO. Typically, biodiesel from VOs with high FFA content is produced by 2-step method involving acid- catalyzed esterification trailed by base-catalyzed transesterification. Extremely acerbic acid and base catalysts necessitate to be initially neutralized and salt thus formed then has to be rinsed out from the BD product which generates considerable amount of effluents (Gorgi and Ghanei, 2014).

In this context, relevance of stable solid catalyst would be surely profitable and gainful from commercial and environmental aspect for biodiesel production using cheap quality high FFA containing feedstock or inedible oils. Solid catalysts cut down the production expenses and detrimental effluent generation, making the BD production more eco-friendly process. Literature reports the use of $SnSO_4$ for concurrent esterification and transesterification of high FFA holding soyabean oil. The catalyst yielded 92% FAMEs at a temperature of 100 °C using 5 wt% of catalyst (Pereira et al., 2014). Another report presents the use of 20-CeO_2/Li_2O/SBA-15 as catalyst for concurrent esterification and transesterification of WCO (chapter 3).

In this chapter, Na/ZrO_2 species which carries both acidic as well as basic sites was impregnated over mesoporous silica and with a view to perform concurrent esterification and transesterification of VCO and high FFA carrying non-edible oils (Jatropha and waste soyabean oil). The reaction conditions were investigated and reusability, tolerance to FFA and kinetic study was also performed. Jatropha oil and WSO oils are inexpensive, inedible and readily available in India.

6.2. Experimental section

6.2.1. Synthesis of SBA-15

The SBA-15 was prepared by following the exactly same method as in chapter 5. In the characteristic synthesis, 8 g of Pluronic 123 was suspended in 60 mL of distilled water and stirred for 1h. Further, 240 ml of 2M hydrochloric acid was added and stirring was continued for additional 2 h. In next step, 17 mL of TEOS was added and resulting solution was stirred at normal room temperature (38 ºC) for 24 h. The mixture was then aged at 90 ºC for 48 h without stirring. The solid product so formed was recuperated by filtration, dried and finally calcined at 600 ºC for 5 h.

6.2.2. Synthesis of Na/ZrO_2

Sodium metal was impregnated over zirconia by wet impregnation method. 5 g of ZrO_2 was suspended in 20 ml of distilled water. To the suspension, 20 mL Na_2CO_3 sol containing 2.3 g of salt was added to obtain 20 wt% loading of Na over zirconia. The slurry was agitated for 20 h at room temperature (38 ºC), dried at 110 ºC for 24 h and finally calcined at 900 ºC for 5 h. The resulting product was designated as $20\text{-}Na/ZrO_2$.

6.2.3. Synthesis of sodium zirconate impregnated mesoporous silica

In order to impregnate above prepared active species over SBA-15, 1 g of SBA-15 was suspended in 40 ml of distilled water and 10 mL suspension of $20\text{-}Na/ZrO_2$ of desired concentration (15-35 wt%) was added. The resulted slurry was agitated for 22 h at room temperature (38 ºC), dried at 110 ºC for 24 h and calcined in muffle furnace at 600 ºC for 6 h. The catalysts so formed were designated as $x\text{-}Na/ZrO_2/SBA\text{-}15$, x is the wt% of Na/ZrO_2.

6.2.4. Transesterification of triglycerides

All reactions were carried out in a 100 mL, two-necked round bottom flask furnished with an oil bath, water-cooled reflux condenser, magnetic protester and a thermometer. In a typical reaction, the flask was indicted with 10 g of vegetable oil (VO) and desired molar concentration of methanol as well as catalyst. The flask contents were roused at a specific temperature for definite reaction duration. The reaction mixture so obtained was set aside in separatory funnel for 10 h in order to part the two layers, upper BD and the lower glycerol layer. The FAMEs thus produced were quantified with ^{1}H-NMR by applying equation (2.6) as stated in chapter 2.

6.3. Results and discussion

6.3.1 Catalyst characterisation

6.3.1.1 Powder XRD study

Small angle XRD patterns (Fig. 1a) of as synthesised SBA-15, shows distinctive peak at $2\theta \sim 0.90°$, which could be indexed to (100) plane. This peak is typical feature of *p6mm* hexagonal symmetry and 2D hexagonal structure of SBA-15. Small angle XRD patterns of Na/ZrO_2 impregnated SBA-15 shows the like kind of diffraction patterns. This demonstrates the preservation of long range mesoscopic order of SBA-15 even on functionalisation with active

species. Though, after doping with active metallic species, reflection consequent to (100) plane was found to reallocate to a little higher angle from 0.90 to 1.1°. This may be accredited to small change in the wall properties and contraction in the lattice framework of mesoporous silica due to partial jamming of mesopores by active metallic species (Li and Rudolph, 2008; Charan and Rao, 2015).

Fig. 1b depicts the XRD pattern of as synthesised Na/ZrO_2 material which depicts the formation of monoclinic sodium zirconate and monoclinic zirconia. The wide angle powder XRD patterns of Na/ZrO_2 impregnated mesoporous silica are depicted in the Fig. 6.1b. The patterns show peak at $2\theta = 23.5°$ which can be ascribed to the amorphous walls of siliceous SBA-15. The peaks at $2\theta =$ 17.1, 31.1°, 34.2°, 35.5°, 38.8°, 40.9°, 50.5° 55.4° are due to subsistence of crystalline monoclinic sodium zirconate (JCPDS file no. 35-0770). Diffraction peaks of monoclinic zirconia at $2\theta = 49.1°$, 54.2°, 28.2° were also observed (JCPDS file no. 88-2390). The observations clearly indicate that there was retention of crystalline phases of monoclinic sodium zirconate and monoclinic zirconia even after the impregnation of Na/ZrO_2 over mesoporous silica. Similar observation has been mentioned in literature while the native structure of phosphotungstic acid (HPW) and WO_3 were retained even after impregnating them over mesoporous siliceous support (Chen et al., 2016).

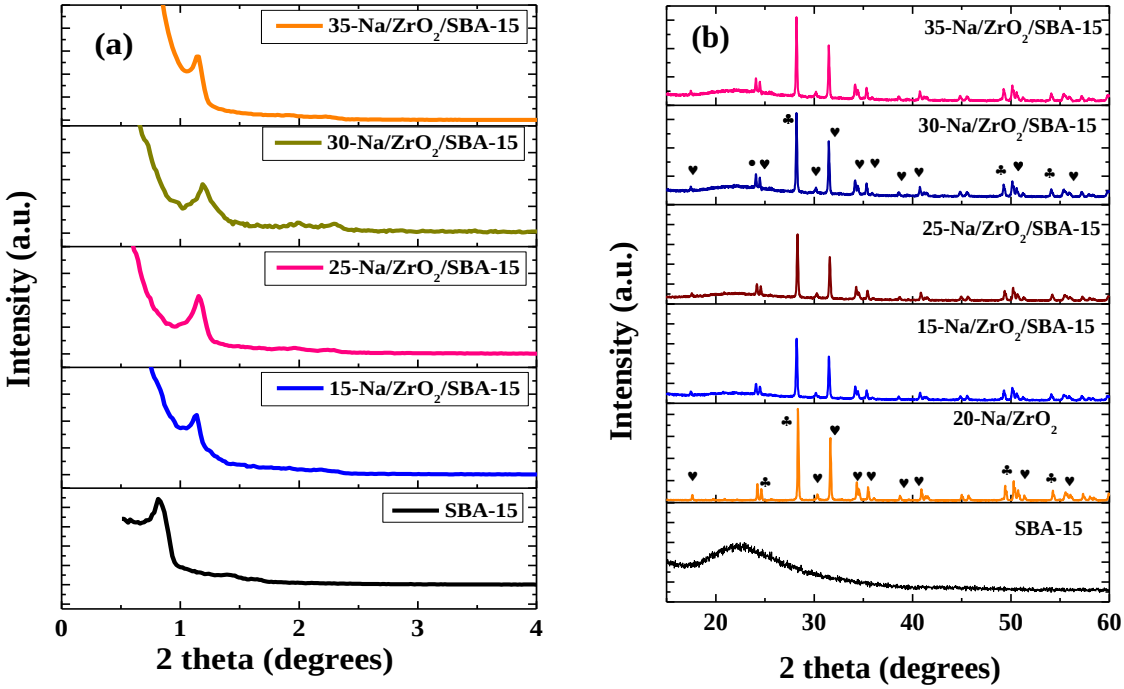

Fig. 6.1. (a) Low angle XRD patterns of SBA-15 and x-Na/ZrO_2/SBA-15 (b) wide angle XRD patterns of SBA-15 and x-Na/ZrO_2/SBA-15 catalysts (• =amorphous SBA-15, ♥ = monoclinic Na_2ZrO_3, ♣ = monoclinic ZrO_2).

6.3.1.2. Study of textural properties

To study the textural attributes of catalysts prepared, nitrogen sorption isotherms were assessed. Nitrogen adsorption-desorption isotherms for SBA-15 and Na/ZrO_2 loaded SBA-15 have been depicted in Fig. 6.2a. It is visible that all isotherms are type IV in nature with H1 hysterisis loop which is typical of mesoporous materials according to IUPAC categorization. This indicates that mesoporous nature is preserved even when active species is laden over SBA-15 template. As the impregnation was raised, the shift in P/P_o to higher relative pressure was seen owing to a raise in pore diameter However, in case of 35-Na/ZrO_2/SBA-15, the hysteresis, transformed from H_1 to H_4. This transformation in the hysteresis could be endorsed to tapering and tightening of pores of SBA-15 on impregnation with high amount of Na/ZrO_2 (Sing et al., 1985). Table 6.1 represents demur in surface area, and average pore volume with the rise in Na/ZrO_2 concentration SBA-15. This decline in surface area and pore volume upon incorporation of active species has also been reported earlier in literature where Au particles were incorporated over SBA-15 material and surface area declined from 664 m^2g^{-1} for bare SBA-15 to 292.6 m^2g^{-1} for Au loaded SBA-15 (Sareen et al., 2015). This decrease in surface area and pore volume can be backed to the dispersal of Na/ZrO_2 species into the pore channels of SBA-15. Inclusion of the active species over the support although led to the reduction in surface area, however, increase in number of active sites, at the same time, was found to enhance the catalyst activity.

Table 6.1. Surface area, average pore size and average pore volume of the synthesised catalysts.

Sample name	Surface area ($m^2 g^{-1}$)	Average pore volume ($cm^3 g^{-1}$)	Average pore diameter (nm)
SBA-15	441.8	0.56	5.09
15- Na/ZrO_2/SBA-15	255.8	0.39	6.14
30- Na/ZrO_2/SBA-15	78.3	0.15	7.95
35- Na/ZrO_2/SBA-15	23.9	0.10	16.9

Barrett-Joyner-Halenda (BJH) method was engaged to calculate pore size distribution (PSD) from adsorption branch of N_2- adsorption-desorption isotherms (Fig. 6.2b) which depicted narrow PSD of prepared materials confirmative of uniformity of pores. The increase in pore size can be credited to the anchorage of Na/ZrO_2 species to exterior silanol groups present on

the outer area of pore walls. Hence, pores of SBA-15 might have inflated, either owing to ingress of active species into the pores or the attachment of Na/ZrO_2 outside the walls causing a stretch. But the pore volume was found to reduce to support the jamming of mesochannels of siliceous support on permeation and infusion of Na/ZrO_2. Similar observations have been reported earlier elsewhere when Al metal was infused over SBA-15 and a rise in pore diameter from 8 nm (bare SBA-15) to 12.7 nm (Al-SBA-15) was observed with the rise in Al metal content (Grieken et al., 2009).

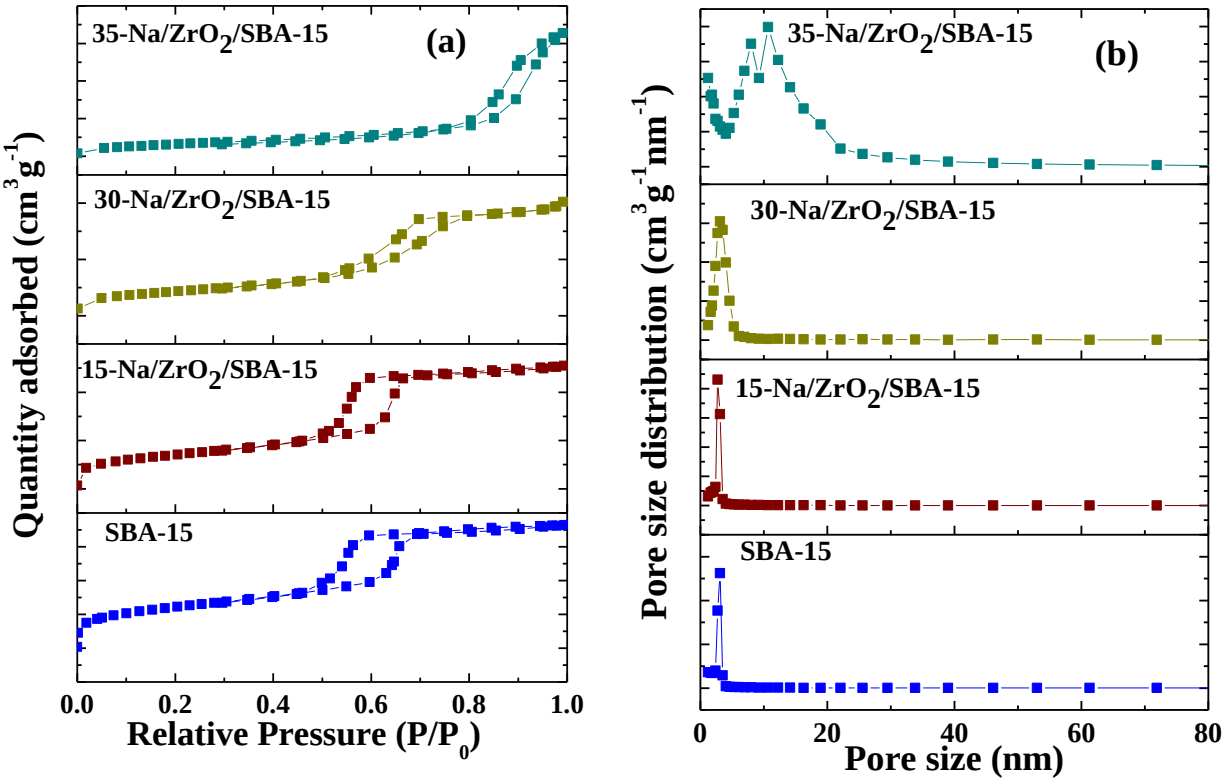

Fig. 6.2. (a) N_2 adsorption–desorption isotherms and (b) pore size distribution of SBA-15 and x-Na/ZrO_2/SBA-15 catalysts.

6.3.1.3. SEM-EDS study

Both SBA-15 support as well as 30-Na/ZrO_2/SBA-15 catalyst were typified by SEM technique to scrutinize the morphological facets. The SEM analysis (Fig. 6.3a) of SBA-15 portrayed the clusters of hexagonal and few irregular units or particles with smooth surface. The particles tend to dwell in aggregated manner. Fig. 6.3b depicts the SEM image of 30-Na/ZrO_2/SBA-15 which showed the almost rectangular shaped catalyst particles of an average length and width of 0.9 μm and 0.4 μm respectively. The SEM analysis clearly is indicative of transformation from hexagonal and irregular particles of stripped SBA-15 to

rectangular shaped catalyst particles after impregnation of active species. The EDS of SBA-15 confirms the presence of only Si and O species indicating the purity of prepared material while EDS spectra of active catalyst demonstrates the presence of Na, Zr, Si, O species again pointing towards no contamination in prepared catalyst. The elemental mapping or chemical map analysis (Fig. 6.4) of the catalyst also confirmed the loading of Na and Zr in the matrix of SBA-15 and uniform and consistent allocation of Na and Zr metallic species in the siliceous framework. The incidence of different elements in catalyst has been shown with different colours.

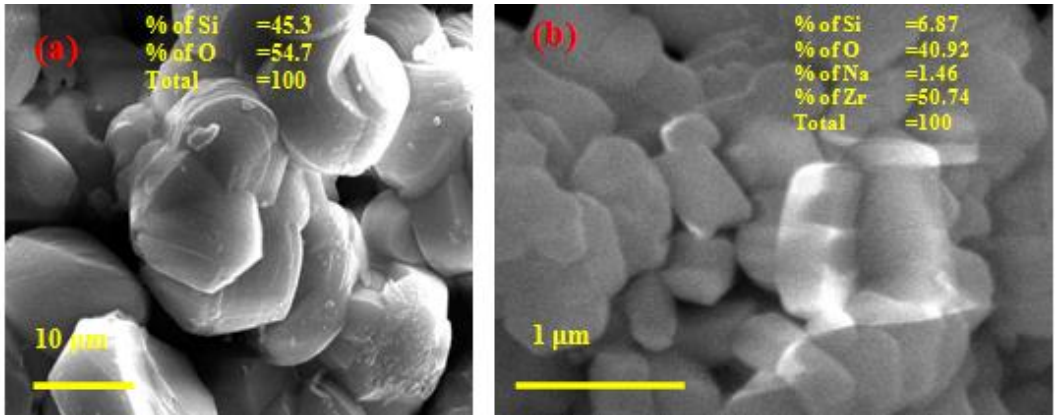

Fig. 6.3. SEM images of (a) bare SBA-15 support (b) 30-Na/ZrO_2/SBA-15.

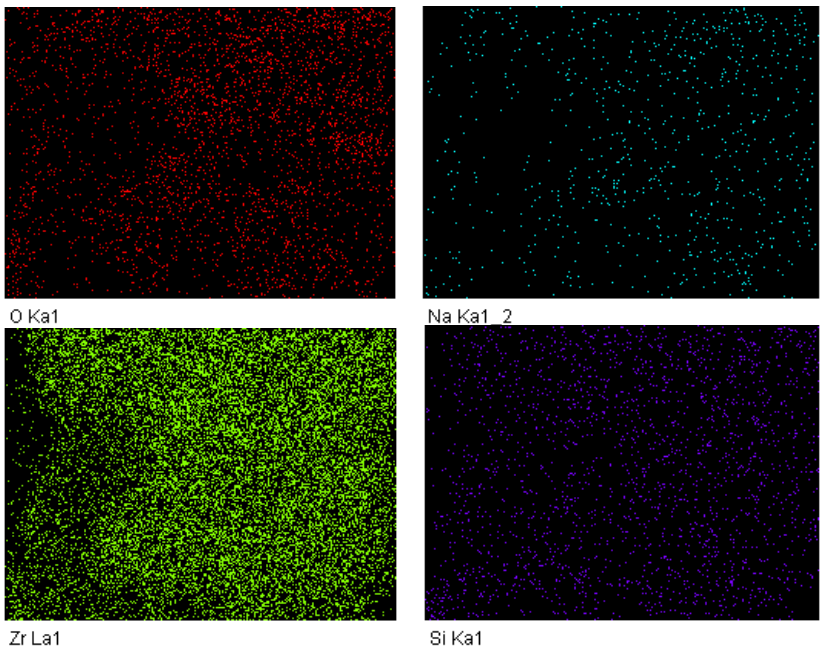

Fig. 6.4. Elemental mapping of 30-Na/ZrO_2/SBA-15 catalyst.

6.3.1.4. HRTEM study

HRTEM analysis of Na/ZrO_2 functionalised mesoporous silica is portrayed in Fig 6.5. The investigation of the prepared catalyst by HRTEM technique revealed that the smooth clusters of catalyst particles are made up of rhombus and rectangular shaped units (Fig. 5a). The micrographs also displayed the well defined channels arranged in 2D hexagonal fashion, a typical feature of SBA-15 (Fig. 6.5b) and highly dispersed Na/ZrO_2 particles are present in the mesopore channels of SBA-15. Presence of Na/ZrO_2 particles over SBA-15 surface are evidently visible against the lighter backdrop of SBA-15 matrix (Fig. 6.5b). Moreover, it is further evident from HRTEM study that functionalisation and inclusion of SBA-15 with Na/ZrO_2 *via* wet-chemical method didn't breakdown its morphology of SBA-15.

Presence of Na and Zr in the EDS analysis of prepared catalyst further sustain the Na/ZrO_2 inclusion over the SBA-15. The SAED pattern (Fig. 6.5c) of the catalyst depicts the polycrystalline nature of catalyst owing to the incidence of bright diffraction spots, arranged in multiple rings corresponding to planes of sodium zirconate crystal also consistent with aforementioned XRD analysis of the same catalyst. The minutely diffused character in the multiple rings is attributed to the non-crystalline nature of SBA-15 material present in the catalyst.

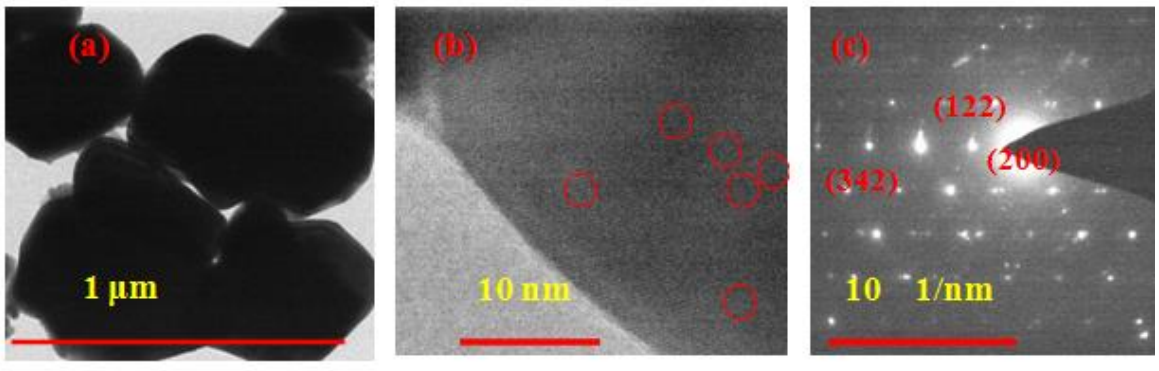

Fig. 6.5. HR-TEM images of a) rhombus and rectangular units of catalyst particles, b) dark spots signify the loading of Na/ZrO_2 over SBA-15, and c) SAED pattern of 30-Na/ZrO_2/SBA-15 catalyst.

6.3.1.5. XPS study

To establish the oxidation state of the elements present in 30-Na/ZrO_2/SBA-15, XPS study was utilized. As depicted in Fig. 6.6a, the peak detected at 105.1 eV supports the occurrence of Si 2p of amorphous silica in +4 oxidation state. A report observed similar value (103 eV) of binding energy (B.E.) for Si present in amorphous silica wherein ceria-silica composite was synthesised (Pal et al., 2014). The peak at 105.6 eV is due to the incidence of Si^{4+} in surface Si-O-Si bonds. In literature presence of surface Si-O-Si bonding with Si^{4+} state was reported at B.E. of 103.7 eV (Post et al., 2018). The peak consequent to the O 1s, could be deconvoluted into three peaks (Fig. 6.6b) *viz.*, at 535 eV, 531.5 eV and 533 eV. The strong peak appeared at 535 eV can be ascribed to oxygen of amorphous SBA-15 material while remaining two peaks at 531.5 eV and 533 eV can be respectively pointed to O^{2-} species of lattice oxygen of active species and feebly bonded oxygen of physisorbed water molecule. Similar spectra for O 1s was obtained with 3 convoluted Gaussian peaks in a report where Ca ans Mo metals were impregnated over SBA-15 with peaks appearing at 533.1 eV, 529.8 eV and 531eV (Xie and Zhao, 2014). The peak at 1073.5 eV (Fig. 6.6c) refers to Na 1s state also supported by recent report where Na 1s spectra was obtained at 1071.6 eV (Precht et al., 2016). Zr 3d spectrum (Fig. 6.6d) is a doublet corresponding to Zr^{4+} $3d_{5/2}$–Zr $3d_{3/2}$ spin–orbit splitting corresponding to the B.E. positioned at 183.6 and 186.7 eV, respectively. Similar spectra and peak positions was obtained in another report in which Zr was present in Zr^{4+} $3d_{5/2}$–Zr $3d_{3/2}$ spin states show the B.E. positions at 182.2 eV and 184.6 eV, respectively (Bulavchenko et al., 2015). It is to be noted that spectral lines of all elements in present catalyst show a general shift ~ 2 eV with regard to the reference lines (O 1s of SBA ~ 532.9 eV and Zr $3d_{5/2}$ at 182 eV). This slight reallocation is due to accumulation of excessive electrical charge on sample surface while irradiation of photons. Similar observation has been reported in literature where a similar shift in XPS spectral lines has been observed (Singh et al., 2012).

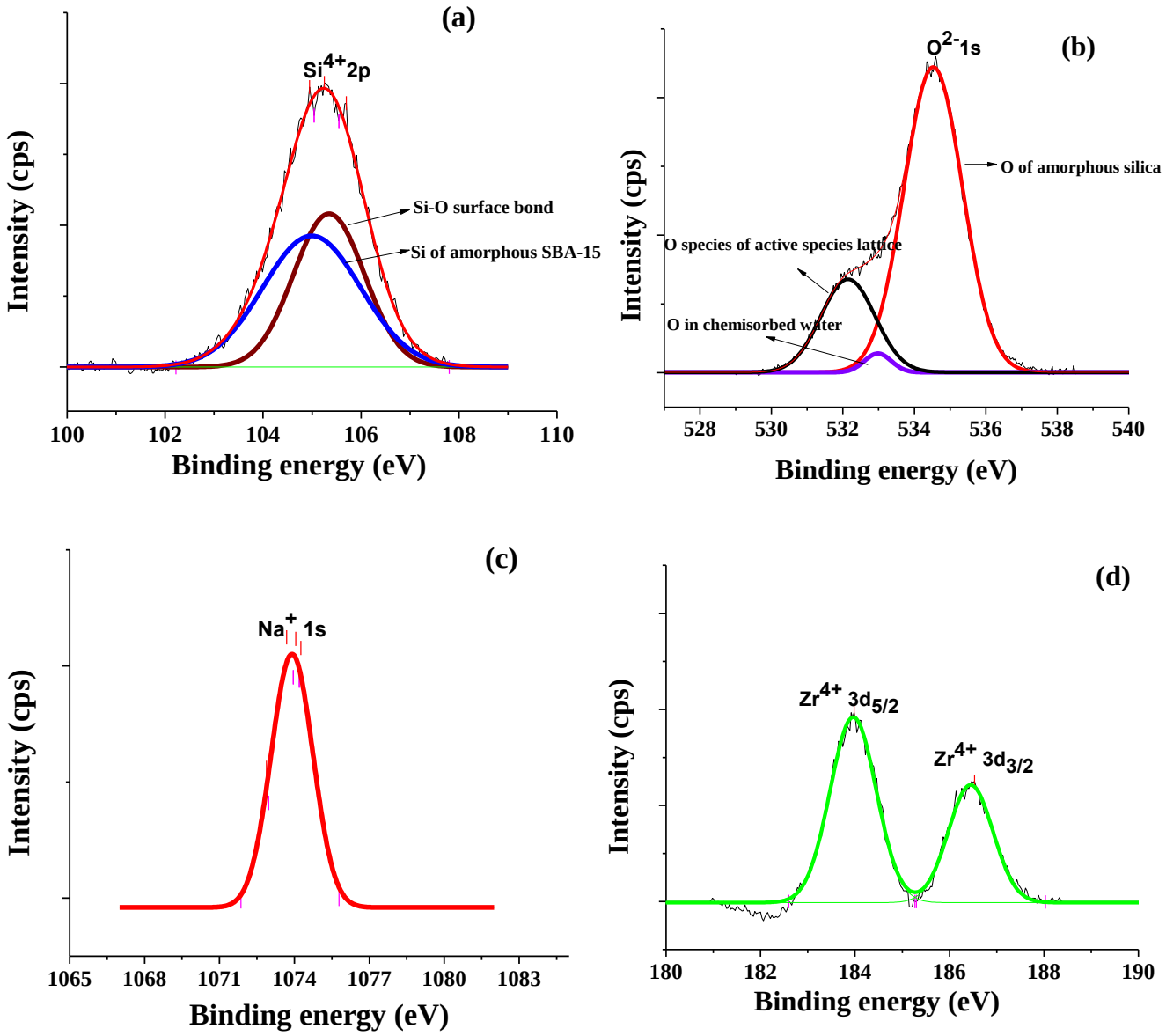

Fig. 6.6. XPS spectra of (a) Si (b) O (c) Na and (d) Zr present in 30-Na/ZrO_2/SBA-15.

6.3.1.6. Hammett indicator study

In order to compute the amount of basic and acidic sites, Hammett indicator test was executed. Trichloroacetic acid and n-butylamine were employed as titrants to enumerate the basic and acidic sites of the synthesised catalysts. Na/ZrO_2 impregnation boosted the Lewis basic and acidic sites that are liable to commence transesterification of the triglyceride (Table 6.2). Literature reports that presence of Lewis acid sites promotes esterification whereas existence of Lewis basic sites in the catalyst is responsible for transesterification (Pereira et al., 2014). A catalyst which seizes both type of sites can bring about esterification and

transesterification concurrently. The bare SBA-15 template, even though acquires some intrinsic acidity as well as basicity, but, not sturdy enough to commence and kick off the transesterification or esterification reactions under ambient conditions. As the impregnation amount amplified, the basicity and therefore activity of catalyst too simultaneously augmented up (from 4.19 mmol/g to 4.65 mmol/g). However, utmost catalytic action and highest catalyst bustle was observed with 30 wt% impregnation of Na/ZrO_2 over SBA-15 and therefore, it became the choice as most favourable catalyst for the further studies.

Table 6.2. Comparison of acidic and basic strengths, and TOFs for the x-Na/ZrO_2/SBA-15 catalyzed transesterification.

Catalyst	Acidity			Basicity					Total acidity (mmol g^{-1})	Total basicity (mmol g^{-1})	TOF ($\times 10^{-3}$ h^{-1})
	($H_0 \leq +4.8$)	($H_0 \leq +6.8$)	($H_0 \leq +7.2$)	($H_0 \leq +7.2$)	($H_0 \leq +9.3$)	($H_0 \leq +10.1$)	($H_0 \leq +11.1$)	($H_0 \leq +15$)			
SBA-15	NCC	0.16	NCC	0.59	NCC	NCC	NCC	NCC	0.16	0.59	-
15- Na/ZrO_2 /SBA-15	0.12	0.18	0.22	0.63	0.69	0.74	0.72	1.41	0.52	4.19	3.9
20- Na/ZrO_2 /SBA-15	0.25	0.25	0.28	0.63	0.68	0.75	0.81	1.45	0.78	4.32	5
25- Na/ZrO_2 /SBA-15	0.28	0.31	0.31	0.64	0.70	0.73	0.80	1.48	0.9	4.35	9.9
30- Na/ZrO_2 /SBA-15	0.34	0.37	0.39	0.65	0.69	0.73	0.81	1.67	1.1	4.55	16.6
35-Na/ZrO_2 /SBA-15	0.33	0.37	0.40	0.64	0.69	0.74	0.82	1.76	1.1	4.65	16.3

**NCC stands for No colour change.*

**TOF is calculated at 50% conversion level on the basis of basic sites; Reaction conditions = methanol to oil molar ratio of 30 : 1 at 65 °C reaction temperature, in the presence of 10 wt% of catalyst with respect to oil at 600 rpm stirring speed.*

**Indicators used:* methyl red ($H_0 \leq 4.8$), neutral red ($H_0 \leq 6.8$), bromothymol blue ($H_0 \leq 7.2$), phenolphthalein ($H_0 \leq 9.3$), Nile blue ($H_0 \leq 10.1$), tropaeolin ($H_0 \leq 11.1$), 2, 4-dinitroaniline ($H_0 \leq 15.0$)

6.3.2. Catalytic activity

The catalytic bustle of the prepared catalysts was tested for methanolysis of virgin cottonseed oil (VCO). The reaction parameters were investigated for transesterification activity with a goal to accomplish highest yield of FAMEs in minimum possible time. One factor at a time of the following was altered to attain the optimised reaction conditions: (i) impregnated Na/ZrO_2 concentration, (ii) catalyst amount (iii) molar ratio of MeOH/oil and (iv) reaction temperature.

6.3.2.1. Effect of Na/ZrO_2 concentration on catalytic action

To conclude the most favourable amount of Na/ZrO_2 over SBA-15, a sequence of catalysts were synthesised by varying Na/ZrO_2 concentration from 15-35 wt%. At 65 °C, using a 30:1 MeOH/oil molar ratio and 10 wt% (catalyst/oil) of catalyst, the reactions were performed. Entire transesterification of VCO into BD was achieved in 3 h when Na/ZrO_2 impregnation was increased from 15 to 35 wt% (Fig. 6.7a). This boost in rate of reaction with mounting Na/ZrO_2 amount is expected as there will be consequential rise in number of active sites in the catalyst as depicted in Table 6.2. An auxiliary increase in Na/ZrO_2 amount (from 30 to 35 wt %) could not reduce the duration of reaction significantly. Hence, 30 wt% of Na/ZrO_2 on SBA-15 was elected as the finest amount of active catalytic species. In the present study, maximum amount of active basic sites observed were with 35 wt% loading of active moiety. However, catalysts with highest Na/ZrO_2 loading amounts (30 and 35 wt%) depicted almost similar TOFs. Hence, 30 wt% of Na/ZrO_2 loading was optimised for loading on mesoporous silica.

6.3.2.2. Effect of amount of the catalyst

For any chemical procedure, the amount of catalyst is vital and has noteworthy effect on the production cost. To assess the optimal catalyst concentration, transesterification reactions were carried out with 30-Na/ZrO_2/SBA-15 using 30:1 MeOH/oil molar ratio at 65 °C. Amount of catalyst was stippled from 6 to 11 wt% (catalyst/oil). The FAMEs yield showed an augmentation as the catalyst amount was raised from 6 to 10 wt% as shown in Fig.6.7b. Any more addition to catalyst amount (10 to 11 wt %) was not found to sway the reaction rate to any remarkable level. Therefore, all reactions were carried out using 10 wt% of catalyst at 65 °C.

6.3.2.3. Effect of methanol to oil molar ratio

As discussed in previous chapters also, idyllically, for the transesterification to reach completion, the stoichiometric molar ratio compulsory, is 3:1 (methanol/triglyceride). However, as the reaction is reversible, it is often performed by utilising superfluous amount of alcohol with an intension to smooth the progress of forward reaction and avert the back reaction.

To settle on the most advantageous methanol/oil molar ratio, a succession of methanolysis reactions were carried out with 30-Na/ZrO_2/SBA-15 at 65 °C and altering the MeOH/oil molar ratio from 10:1 to 30:1. The reaction rate amplified as the MeOH/oil molar ratio was raised from 10:1 to 30:1. The reaction went to completion within 3 h when 30:1 MeOH/oil ratio was employed. Any more addition in the MeOH/oil molar ratio did not influence the reaction rate to any momentous extent (Fig. 6.7c). Therefore, 30:1 MeOH/oil molar ratio was chosen to be optimum to achieve complete transesterification of VCO.

6.3.2.4. Effect of reaction temperature

30-Na/ZrO_2/SBA-15 catalyzed transesterification was executed at different temperatures with a view to assess the effect of reaction temperature on pace of reaction by employing 30:1 MeOH/oil molar ratio and 10 wt% of catalyst.

The rate of methanolyis was found to boost up as the reaction temperature was raised from 35 to 65 ºC as shown in Fig. 6.7d. Further raise in reaction temperature was not found to affect the FAMEs yield or reaction rate significantly. This observation can be attributed to the formation of vapours of methanol and its consequent loss from the reaction mixture.

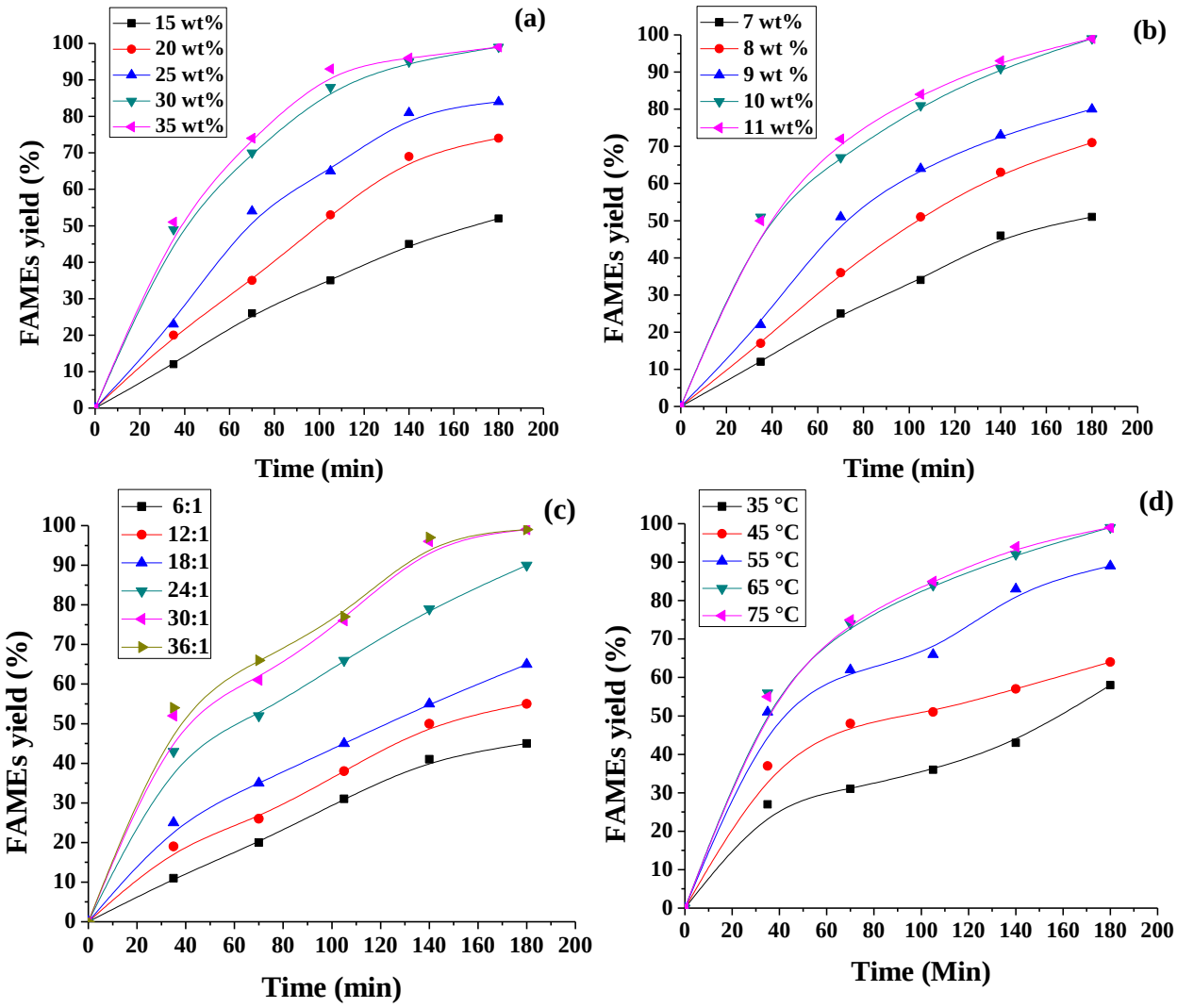

Fig. 6.7. Effect of (a) Na/ZrO_2 concentration on SBA-15, (b) catalyst concentration, (c) methanol/oil molar ratio on methanolysis of VCO and (d) reaction temperature.

6.3.3. Effect of FFA on catalytic activity

Non-edible or ravaged cooking oils generally contain usually FFA contents in fairly elevated amount. Traditionally, the transesterification of such elevated levels of FFA-holding oils is executed in two-steps involving firstly, acid-catalyzed pre-esterification with an acid catalyst and subsequent transesterification using an alkali catalyst. The 30-Na/ZrO_2/SBA-15 catalyst was found exhibit both esterification plus transesterification action. To express the simultaneous esterification and transesterification action of the catalyst in one-pot, system, transesterification reactions of waste soyabean oil (WSO) and jatropha oil (JO) (containing 3.9 and 9.7 wt% FFA respectively) were carried out with methanol. It was concluded that although the present catalyst was efficient for the transesterification of FFA rich feedstock,

dwindle in TOF was observed as the levels rose. The duration of reaction entailed to achieve absolute conversion raised to 5.5 h and 8.5 h for WSO and JO respectively (Fig. 6.8). This drop in TOF of catalyst can be endorsed to partial blocking of the active sites of catalyst due to the interaction of basic sites with free fatty acids in the feedstock to consequent the partial trouncing of catalyst action.

To establish the esterification activity of 30-Na/ZrO_2/SBA-15 catalyst, in a different reaction oleic acid was reacted with MeOH under the optimised conditions. Within 3 h of reaction duration 68% yield of methyl oleate was achieved to validate that the catalyst could catalyze esterification of fatty acids as well.

This is a clear advantage of present catalyst since cumbersome 2-step procedure first get rid of high FFA content in low-quality feedstock and then carrying out transesterification can be evaded to successfully bring about both esterification and transesterification in one-pot system.

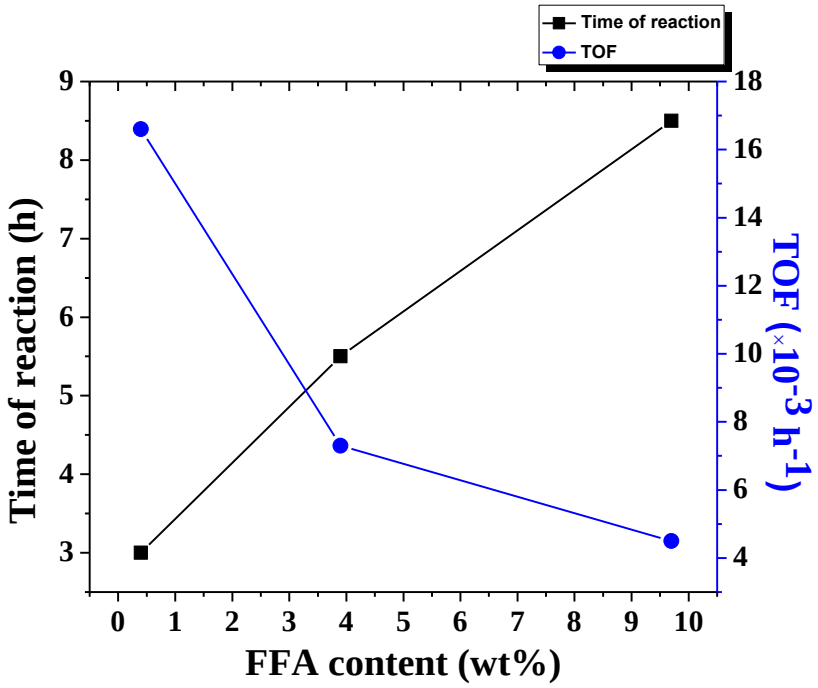

Fig. 6.8. Effect of added FFA content on 30-Na/ZrO_2/SBA-15 catalyzed methanolysis (Reaction conditions: MeOH/oil molar ratio = 30:1; Catalyst amount = 10 wt% of oil; Temperature = 65 °C).

6.3.4. Reusability and homogeneous contribution

Reusability and recycling of heterogeneous catalyst is a very imperative and gainful characteristic. Recycling of solid catalyst helps in their simpler separation procedure and simultaneously cutting down the cost and labour required during post production process. To assess the reusability and crumble in activity of present catalyst, transesterification reaction with 30-Na/ZrO_2/SBA-15 was executed under optimised conditions. The worn catalyst was then convalesced through filtration, subjected to washing with hexane and methanol to remove both polar as well as non polar contaminants, dried at 120 °C and then calcined at 600 °C. The revived catalyst was utilised for transesterification for 6 succeeding runs using parallel experimental clauses and revival method. It was found that the revived catalyst yielded complete conversion of feedstock into FAMEs for 5 subsequent runs. The action of the catalyst was found to show a demur in the 6th run when it yielded 86% FAMEs yield. The TOF of catalyst decreased following the 5th cycle (Fig. 6.9).

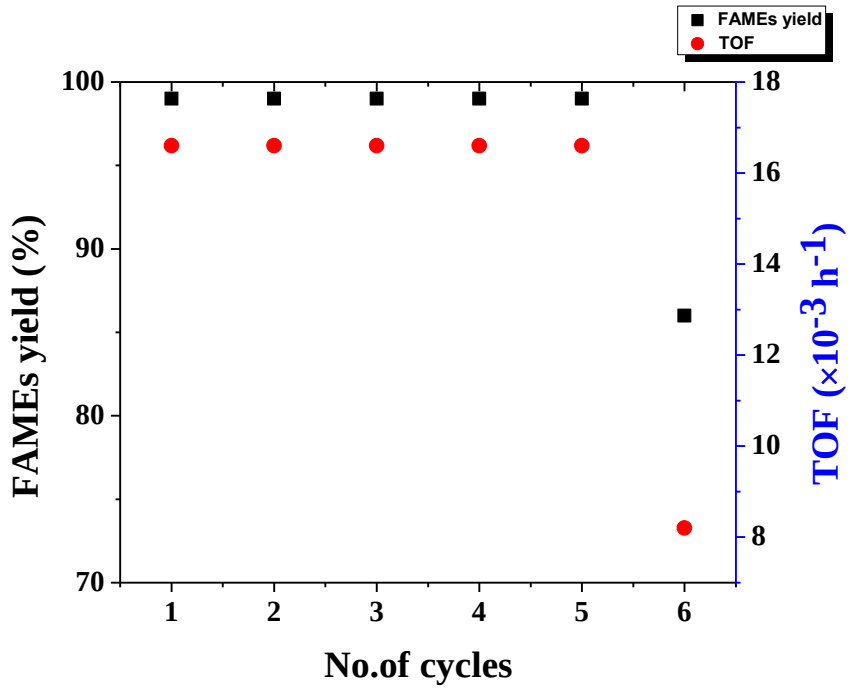

Fig. 6.9. Reusability of 30-Na/ZrO_2/SBA-15 catalyst (Reaction conditions: MeOH/oil molar ratio = 30:1; Catalyst amount = 10 wt% of oil; Temperature = 65 °C).

Percolation of the active catalytic species in the catalyst is a recurrently faced issue in case of heterogeneous catalysts. The amount of Na metal was quantified in FAMEs layers in 6th cycle with Flame photometry technique and was determined to be 485 ppm. All through early runs,

it can be supposed that no active metal would have oozed out into the reaction concoction since 30-Na/ZrO_2/SBA-15 was proficient of upholding its action and yielded complete conversion of VCO into BD. Hence, it can be construed that SBA-15 support was able to craft the catalyst into a sensibly and convincingly stable one simultaneously averting the leaking out of any active metal into reaction medium. Active species when seized over mesoporous silica evidently becomes a lucrative selection over unsupported catalyst, in view of the fact that it may well hang on to its venture over following cycles with no credible leaching of otherwise seepable alkali metals.

Additionally, surface area of reused catalyst were also calculated and was found to be 5.14 m^2 g^{-1} which was significantly lesser than the surface area of fresh catalyst (78.3 m^2 g^{-1}). Thus, decline in activity can be clarified by combined percolation and reduction in surface area of reused catalyst showing the way to lower catalytic activity. Moreover, the basicity test of reused catalyst was also carried out to ascertain the basis for reduced catalytic action. The basicity of regenerated catalyst was found to be 4.27 mmol g^{-1} (basicity of fresh catalyst = 4.55 mmol g^{-1}) to support the oozing of active metals into reaction mixture and consequential decline in catalytic flurry.

Percolation of active metallic species causes the fall in activity of catalyst and it is possible that leached species may catalyse the reaction like homogeneous catalysts. Hence, it becomes imperative to find the homogeneous contribution of the catalyst, if any. For quantification of the contribution of dissolved catalyst in overall activity, and validate the heterogeneous manner of activity of the prepared catalyst, hot filtration test was performed under optimal reaction conditions. The VCO transesterification was carried out under the optimized conditions for 1 h, after that catalyst was separated *via* filtration method and reaction was allowed to continue for more 2 h. As it could be clearly seen from the Fig. 6.10, that no increment in FAMEs yield was observed when the reaction was continued in absence of catalyst to support that (i) the mode of action of the prepared catalyst is heterogeneous and (ii) the leached metal ions have no significant contribution in catalytic activity.

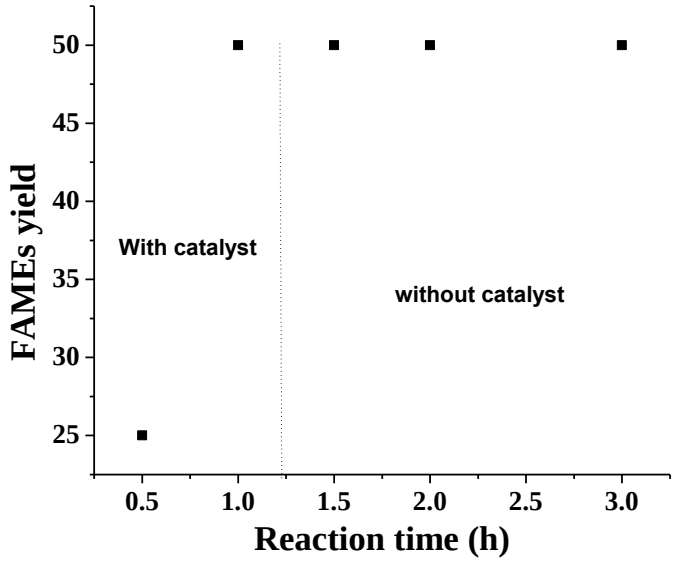

Fig. 6.10. Hot filtration test for 30-Na/ZrO_2/SBA-15 catalysed transesterification.

6.3.5. Kinetic study

Kinetic study was performed using the equivalent approach as followed in previous chapters. To get the rate constant values, the tranesterification reactions were executed at 35 to 65 °C temperatures. The plot of –ln (1-X_{me}) *versus* 't' was found to subsist as linear in nature (R^2 value = 0.97 at 65 °C) to maintain the first order kinetic route by the reaction (Zhang et al., 2010). The value of rate constant at 65 °C was found to be 0.026 min^{-1}.

Activation energy (E_a) for 30-Na/ZrO_2/SBA-15 was estimated from Arrhenius equation (2.3) and Equation (2.4) was utilized to determine the enthalpy ($\Delta H^{\ddagger}$) and entropy of activation ($\Delta S^{\ddagger}$) for 30-Na/ZrO_2/SBA-15 catalysed methanolysis. E_a was found to be 42.9 kJ mol^{-1} with R^2 value of the Arrhenius plot (ln K *vs* 1/T) being 0.87. The E_a lied in the range reported (33-84 kJ mol^{-1}) for transesterification of VOs (Sun et al., 2008). Since the Ea observed was > 25 kJ mol^{-1}, it evidenced that reaction was ruled and controlled chemically, not by diffusion or mass transfer limitations (Patel and Brahmkhatri, 2013).

A linear plot was observed between ln (k/T) and 1/T with R^2 value of 0.86.

From the Eyring Polanyi plot, $\Delta H^{\ddagger}$ and $\Delta S^{\ddagger}$ were found to be +40.1 kJ mol^{-1} and -0.161 kJ mol^{-1} respectively.

The Gibb's free energy ($\Delta G^{\ddagger}$) for the reaction was found to be +84 kJ mol^{-1}.

Table 6.3. Experimentally determined values of thermodynamic parameters.

Thermodynamic Parameter	**kJ mol^{-1}.**
Activation Energy (E_a)	42.9
Enthalpy of Reaction ($\Delta H^{\ddagger}$)	40.1
Entropy of Reaction ($\Delta S^{\ddagger}$)	-0.161
Gibbs Free Energy ($\Delta G^{\ddagger}$)	84

Because of positive value of $\Delta G^{\ddagger}$, it may be construed that 30-Na/ZrO_2/SBA-15, catalysed transesterification of VCO was non-spontaneous in nature. The energy strata of transition state was at higher level when compared to reactants (Pogaku et al., 2012)

The negative $\Delta S^{\ddagger}$ depicted that transition state was more ordered than reactants in ground state. Thus, the reaction has tracked an associative pathway (Espenson, 2002). Positive $\Delta H^{\ddagger}$ portrayed that reaction was endothermic and required heating from external source to arrive at transition state and shift in forward direction (Beall, 1994).

6.4. Conclusions

Present chapter embodies the synthesis and investigation of 30-Na/ZrO_2/SBA-15 as solid and revivable catalyst for BD production from virgin cotton seed oil. Under optimised reaction conditions of 10 wt% catalyst, 65 °C reaction temperature and MeOH/oil molar ratio of 30:1, > 98% FAMEs yield was attained within 3 h. The catalyst confiscated both acidic and basic sites and hence victoriously employed for concurrent esterification and transesterification. The transesterification by the present catalyst hounded (pseudo) first order kinetic pathway. The catalyst paraded very fine recyclability for it was able to uphold its activity (98% FAMEs yield) for 6 catalytic runs. 86% FAMEs yield was achieve in 6th cycle. From commercial perspective, retention of activity, due to stable and locked siliceous matrix is considerable observation in present chapter. The catalyst followed heterogeneous mode of action and no homogeneous contribution was found.

References

Beall, H., 1994. Probing Student Misconceptions in Thermodynamics with In-Class Writing. J. Chem. Educ. 71, 1056-1057.

Bulavchenko, O.A., Vinokurov, Z.S., Afonasenko, T.N., Saraev, A.A., Kaichev, V.V., 2015. Redcution of mixed Mn-Zr oxides: In situ XPS and XRD studies. Dalton Trans. 44, 15499-15507.

Charan, P.H.K., Rao, G.R., 2015. Textural and morphological studies of transition metal doped SBA-15 by co-condensation method. J. Chem. Sci. 5, 909–919.

Chen, G., Qiao, H., Cao, J., Wang, Z., Ye, M., Guo, C.Y., Wen, X., 2016. Well-dispersed sulfated mesoporous WO_3/SiO_2 hybrid colloidal spheres: High-efficiency catalysts for the synthesis of fatty acid alkyl esters. Fuel 163, 41-48.

Espenson, J.H., 2002. Chemical Kinetics and Reaction Mechanisms, second ed. McGraw-Hill, India.

Gorji, A., Ghanei, R., 2014. A review on catalytic biodiesel production. J.Bio & Env. Sci. 5, 48-59.

Grieken, R.V., Escola, J.M., Rodriguez, J.M.R., 2009. Direct synthesis of mesoporous M-SBA-15 (M= Al, Fe, B, Cr) and application to 1-hexene oligomerization. Chemical Engineering Journal 155, 442-450

Li, E., Rudolph, V., 2008. Transesterification of Vegetable Oil to Biodiesel over MgO-Functionalized Mesoporous Catalysts. Energy Fuels 22, 145-149.

Pal, N., Cho, E.B., Kim, D., 2014. Synthesis of Ordered Mesoporous Silica/Ceria-Silica Composites and their High Catalytic Performance for Solvent-Free Oxidation of Benzyl Alcohol at Room Temperature. RSC Adv. 4, 9213−9222.

Patel, A., Brahmkhatri, V., 2013. Kinetic study of oleic acid transesterification over 12-tungstophosphoric acid catalyst anchored to different mesoporous silica supports. Fuel Process. Technol. 113, 141-149.

Pereira, C.O., Portilho, M.F., Henriques, C.A., Zotin, F.M.Z., 2014. $SnSO_4$ as catalyst for simultaneous esterification and transesterification of acid soyabean oil. J. Braz. Chem. Soc. 25, 2409-2416.

Pogaku, R., Raman, J.K., Ravikumar, G., 2012. Evaluation of Activation Energy and Thermodynamic Properties of Enzyme-Catalysed Transesterification Reactions. Adv. Chem. Eng. Sci. 2, 150-154.

Post, P., Wurlitzer, L., Weber, A.P., 2018. Characterisation and applications of nanomaterials modified in-flight with silica or silica-organic coatings. Nanomaterials 8, 530-549.

Precht, R., Stolz, S., Mankel, E., Mayer, T., Jaegermanna, W., Hausbranda, R., 2016. Investigation of sodium insertion into tetracyanoquinodimethane (TCNQ): results for a TCNQ thin film obtained by a surface science approach. Phys. Chem. Chem. Phys. 18, 3056-3064.

Sareen, S., Mutreja, V., Singh, S., Pal, B., 2015. Highly dispersed Au, Ag and Cu nanoparticles in mesoporous SBA-15 for highly selective catalytic reduction of nitroaromatics. RSC Adv. 5, 184-190.

Sing, K.S.W., Everett, D.H., Haul, R.A.W., Moscou, L., Pierotti, R.A., Rouquerol, J., Siemieniewska, T., 1985. Reporting physisorption data for gas solid systems with Special Reference to the Determination of Surface Area and Porosity. Pure & Appl. Chem. 57, 603-619.

Singh, A.V., Ferri, M., Tamplenizza, M., Borghi, F., Divitini, G., Ducati, C., Lenardi, C., Piazzoni, C., Podesta, A., Milani, P., 2012. Bottom-up engineering of surface roughness of nanostructured cubic zirconia. Nanotechnology 23, 475101-475110.

Sun, H., Hu, K., Lou, H., Zheng, X., 2008. Biodiesel production from transesterification of Rapeseed oil using KF/Eu_2O_3 as a Catalyst. Energy Fuels 22, 2756–2760.

Xie, W., Zhao, L., 2014. Heterogeneous $CaO\text{-}MoO_3$-SBA-15 catalysts for biodiesel production from soyabean oil. Energy Convers. Manage. 79, 34-42.

Zhang, L., Sheng, B., Xin, Z., Liu, Q., Sun, S., 2010. Kinetics of transesterification of palm oil and dimethyl carbonate for biodiesel production at the catalysis of heterogeneous base catalyst. Bioresour. Technol.101, 8144-8150.

Summary and Futuristic aspects

Abstract

In this chapter, the work discussed in chapters 3-6 has been concluded, and with sketching a comparison and correlation. Along with this, the aspects of biodiesel production in future have also been mentioned.

7.1. Introduction

In the present thesis, work was performed to carry out the synthesis of biodiesel by employing the series of mesoporous silica based solid catalysts. The catalysts were synthesised using without hydrothermal treatment and tested for their activity for transesterification. Few catalysts were even able to catalyse concurrent esterification and transesterification.

7.2. Summary from present thesis

Li^+ and Ce^{4+} loaded SBA-15, 5-Na/ZnO incorporated SBA-15, duo of active K-Na metals imbued over mesoporous silica and Na/ZrO_2 drenched SBA-15 were prepared under normal conditions and used to catalyse transesterification of variety of feedstocks. 20-CeO_2/Li_2O/SBA-15 and Na/ZrO_2 drenched SBA-15 catalysts were found to seize both acidic plus basic sites and hence were able to show concurrent esterification and transesterification. The former catalyst employed WCO as feedstock and showed good recyclability, could be reused for 5 consecutive runs without significant loss of activity plus fairly good tolerance to FFA withstanding a total of 9.8 wt% FFA presence. The FE-SEM analysis depicted smooth spherical SBA-15 particles and EDS confirmed the presence of ~22% Ce loading over SBA-15 which was close to the theoretical loading. The fluorite structure of ceria was confirmed by HRTEM and XRD studies. The self-synthesised silica maintained its mesoporosity even after metal impregnation indicating the stable network which is immensely required for any material to act as support for active species. The latter catalyst Sodium/zirconia metals impregnated SBA-15, employed catalyst concentration 10 wt%, MeOH/oil molar ratio of 30:1 at 65 °C as its most favourable reaction conditions, to confer > 98 % fatty acid methyl ester yield within 3 h of reaction duration. Recyclability study suggested that the catalyst could well be reused for 5 successive runs without any noteworthy demur of activity and yielded 86% FAMEs during 6^{th} cycle. The time of reaction required to achieve absolute conversion was however found to heave to 5.5 h and 8.5 h when WSO and JO were employed as feedstocks respectively The activation energy (E_a) for the reaction was found to be 42.9 kJ mol^{-1}, while $\Delta H^{\ddagger}$, $\Delta G^{\ddagger}$ and $\Delta S^{\ddagger}$ were found to be 40.1 kJ mol^{-1}, + 84 kJ $mol^{-1}$and -0.161 kJ mol^{-1}, respectively.

The other 2 catalysts, 5-Na/ZnO incorporated SBA-15 and K-Na metals imbued over mesoporous silica were synthesised by one-pot method without employing hydrothermal treatment and the wet impregnation course respectively. Both seized the basic sites and

successfully employed for transesterification of VCO. The former catalyst could be rejuvenated for 5 runs giving away yield as good as 74% in 5th run. During catalyst preparation, synthesis of silica network along with impregnation of active catalytic species was performed in single step, cutting down the time and energy for catalyst preparation. It is to be mentioned that, even in the single step synthesis method, mesoporous siliceous network was completely developed, thus, making the catalyst generously stable. In case of K-Na metals imbued over mesoporous silica, the catalyst demonstrated very good recyclability. The catalyst could cede the conversion of ~ 76 % even in 7th cycle of regeneration in a row. The catalyst even depicted very good tolerance levels to externally added FFA which is a noticeable observation for this catalyst. The thermodynamic parameters for the 20-Na-K/SBA-15 catalysed transesterification reaction were established and the values were determined as, E_a = 45.8, $\Delta H^{\ddagger}$ = 43.3, $\Delta S^{\ddagger}$ = -0.148 $\Delta G^{\ddagger}$ = 83.7 kJ/mol respectively. All the reactions were found to trail pseudo-first order kinetic pathway and endothermic in natureTable 7.1 draws the comparison of activity and reaction conditions for transesterification by the catalysts synthesized in the present work.

Table 7.1. Assessment of the activity and reaction conditions for transesterification by the catalysts prepared in present thesis.

Catalyst	TG	FFA (wt%)	Reaction conditions							
			Temp (°C)	Time (h)	MeOH/ oil molar ratio	Catalyst (wt%)	Resue (cycles)	Yield (%)	TOF	E_a (kJ/mol)
20-CeO_2/Li_2O/SBA-15	WCO	4.8	65	4	40:1	10	5	> 98	1.7×10^{-3} h^{-1}	57.7
10-Na/ZnO/SBA-15	VCO	0.4	65	4	24:1	12	5	> 98	11×10^{-4} h^{-1}	77.3
20-Na-K/SBA-15	VCO	0.4	65	2	24:1	8	6	> 98	45×10^{-4} h^{-1}	45.8
30-Na/ZrO_2/SBA-15	VCO WSO, JO	0.4, 3.9, 9.7	65	3	30:1	10	***5***	> 98	16.6×10^{-3} h^{-1}	42.9

Thus, it can be concluded that all the catalysts showed excellent activity under easily attainable reaction conditions. The reactions needed moderate MeOH/oil molar ratios and catalyst amount unlike many of literature reported catalysts. Moreover, 2 catalysts also depicted concurrent esterification and transesterification. The fine recyclability was also the major feature of the prepared catalysts which is an extremely important factor for any catalyst

to be put for commercial usage. Moreover, the catalysts also depicted good FFA tolerance levels which again is an important perspective

7.3. Futuristic aspects

Few suggestions for future work are listed here.

1) In future, attempts can be made to prepare the mesoporous silica based catalysts which are stable and utilise them for biodiesel synthesis using methods other than conventional heating such as microwave synthesis. Other than the rewards of rapid heating, striking raise in the yield is achieved at milder reaction conditions. Active catalysts such as $ZnO/La_2O_2CO_3$ can be supported over siliceous matrix and can be explored for transesterification.

2) The FAMEs can be further renovated to epoxidized fatty acid esters,that participate significantly in large-scale industrial production of chemicals, plasticizers and stabilizers in PVC or constituents for lubricants or cosmetics. Presently, the commercial-scale epoxidation of unsaturated fatty acids is usually performed using the Prileshajew reaction. However, the route endures various drawbacks: (i) the selectivity of epoxides is comparatively less due to breaching of oxirane ring in the acidic media, (ii) the usage of percarbonic acids and concentrated H_2O_2 solutions is extremely hazardous, and (iii) aqueous solutions of C1–C3 carboxylic acids generated as byproducts are highly corrosive. Biodiesel can be transformed without any further refinement with up to 80% epoxide selectivity by employing mesoporous based catalysts such as mesoporous titanium silicalite which has been reported to overcome mass transfer limitations by improving the accessibility of active sites for bulkier FAMEs into the catalytic sites. Different mesoporous epoxidating agents can thus be employed to convert biodiesel into epoxide esters.

3) Different silica precursors can be explored to prepare mesoporous siliceous support such as sodium metasilicate to obtain the silica framework with pore walls of variable thickness. Moreover, the effect of salt addition can be utilised over the synthesis of SBA-15 which reduces the synthesis temperature to as low as 10 °C.

4) The magnetic catalysts supported with Fe_3O_4 core and impregnated with active metals having basic and acidic sites can be prepared and framed into a mesoporous framework to facilitate easier separation, increase recyclability, drop off the percolation of otherwise leachable metals into the reaction medium and raise the overall biodiesel yields.